

# **A COMPREHENSIVE STABILITY INVESTIGATION OF THE ATHABASCA-POINTS NORTH POWER SYSTEM**

**A Thesis**

**Submitted to the College of Graduate Studies and Research**

**in Partial Fulfillment of the Requirements**

**for the Degree of**

**Master of Science**

**in the**

**Department of Electrical Engineering**

**University of Saskatchewan**

**by**

**Zefeng Ao**

**Saskatoon, Saskatchewan**

**September 1993**

**Copyright® 1993 Zefeng Ao**

**To my eldest brother — Wufeng Ao**

## **COPYRIGHT**

The author has agreed that the library, University of Saskatchewan, may make this thesis freely available for inspection. Moreover, the author has agreed that permission for extensive copying of this thesis for scholarly purposes may be granted by the Professors who supervised the thesis work recorded herein or, in their absence, by the Head of the Department or the Dean of the College in which the thesis work was done. It is understood that due recognition will be given to the author of this thesis and to the University of Saskatchewan in any use of the material in this thesis. Copying and publication or any other use of this thesis for financial gain without approval by the University of Saskatchewan and the author's written permission is prohibited.

Request for permission to copy or to make any other use of the material in this thesis in whole or in part should be addressed to:

Head of the Department of Electrical Engineering  
University of Saskatchewan  
Saskatoon, Canada  
S7N 0W0

## ACKNOWLEDGMENTS

The author would like to thank the author's supervisors, Associate Professor T. S. Sidhu and Professor Emeritus Ronald J. Fleming for their guidance in the work reported in this thesis.

Special gratitude is given to the following from SaskPower: Messrs. Bill Kennedy, J. A. Martin, W. G. Stangl, Lorry A. Wilson, S. S. Sachdev, Paul Baerg and J. W. Purdle for their support during the research of the project. Generous assistance was received from Mr. Len Yee and Mr. Gary Belanger of SaskPower.

The financial assistance provided by the Natural Science and Engineering Research Council of Canada is acknowledged.

UNIVERSITY OF SASKATCHEWAN  
Electrical Engineering Abstract 93A384

# **A COMPREHENSIVE STABILITY INVESTIGATION OF THE ATHABASCA-POINTS NORTH POWER SYSTEM**

Student: Zefeng Ao, Supervisors: T. S. Sidhu  
R. J. Fleming

M. Sc. Thesis Presented to the  
College of Graduate Studies and Research

September 1993

## **ABSTRACT**

This thesis presents the principal results of an investigation of the Athabasca-Points North power system (APNS) that is of longitudinal structure. Its stability and stabilization by coordinated power system stabilizers (PSSs) were studied. The effects of the existing controllers on system stability are reported. If PSSs are not in service, the various modes of the system are either negatively or poorly damped and low frequency oscillations are present. Eigenvalue analysis shows that speed governors have little influence on damping while additional excitation control can considerably depress the sustained oscillations. In order to realize this control and to enhance the overall system stability, a coordinated design procedure for power system stabilizers has been developed based on generator coherency, total coupling factor and non-linear simulation. A PSS designed using this procedure is robust to different operating conditions and is very effective for damping out oscillations following both small and large disturbances. Comprehensive simulation studies were conducted and the results obtained are presented.

## TABLE OF CONTENTS

COPYRIGHT	i
ACKNOWLEDGMENTS	ii
ABSTRACT	iii
TABLE OF CONTENTS	iv
LIST OF TABLES	vii
LIST OF FIGURES	viii
LIST OF PRINCIPAL SYMBOLS	xi
1. INTRODUCTION	1
1.1 Power System Stability	1
1.2 Methods of Solution	3
1.3 Statement of Objectives	4
1.4 Overview of the Thesis	5
1.5 Summary	7
2. MODELING OF A POWER SYSTEM FOR STABILITY STUDIES	8
2.1 Introduction	8
2.2 Synchronous Machine Models	9
2.3 Controller Modeling	13
2.3.1 Excitation Systems	14
2.3.2 Speed Governing and Turbine Systems	15
2.3.3 Supplementary Excitation Controllers	16
2.4 Modeling of SVC	19
2.5 Modeling of Disturbances	20
2.6 Load Modeling	21
2.7 Modeling of Network and Transformers	23
2.8 Summary	23
3. A TRANSIENT STABILITY SIMULATION PACKAGE	
3.1 Introduction	25
3.2 Description of Modules within the TSSP	26
3.2.1 Machine Modules	27
3.2.2 Modules for Excitation Systems	28
3.2.3 Modules for Speed Governing and Turbine Systems	29
3.2.4 Modules for Power System Stabilizers	30
3.2.5 Disturbances	31
3.2.6 Load Representations, Network Model and Their Interface with Machine Models	32

3.2.7 User-Defined Modules	33
3.3 Data Files and Program Structure	33
3.4 Summary	35
4. STEADY STATE STABILITY STUDIES OF THE ATHABASCA-POINTS NORTH POWER SYSTEM	36
4.1 Low Frequency Oscillation and Damping	36
4.2 System Description	37
4.3 Load Flow Study in Steady State	40
4.4 Eigenvalue Analysis	41
4.4.1 Computation of Swing Modes	42
4.4.2 Factors that Affect Damping	43
4.5 Functional Sensitivity Studies	44
4.6 Time Domain Simulation	47
4.7 Summary	48
5. TRANSIENT STABILITY STUDIES OF THE ATHABASCA-POINTS NORTH POWER SYSTEM	50
5.1 Introduction	50
5.2 Operating Procedure of APNS	52
5.3 Parameters of Power Components and Controllers	53
5.3.1 Machine Data	54
5.3.2 Excitation System Data	55
5.3.3 Speed Governing and Turbine System Data	55
5.3.4 Power System Stabilizer Data	56
5.4 Transient Stability Studies	56
5.4.1 Disturbances in Different Geographic Areas	57
5.4.2 The Largest Load Area Is Lost	65
5.4.3 Symmetrical and Asymmetrical Disturbances	66
5.5 Summary	69
6. STABILIZATION OF THE APNS BY COORDINATED POWER SYSTEM STABILIZERS	71
6.1 Introduction	71
6.2 Effects of Existing Primary Controls	73
6.2.1 AVR Effect	73
6.2.2 Speed Governor Effect	75
6.2.3 PSS Effect	76
6.3 Coordinated PSS Design	78
6.3.1 Design Procedure	78
6.3.2 PSS Tuning	80
6.3.3 Communication of PSS Inputs	81
6.4 Improvement of System Stability by New PSSs	83
6.4.1 New Eigenvalues	83
6.4.2 Time Simulation of the Small Disturbance	83

6.4.3 Time Simulation of a Large Disturbance	84
6.5 Transient Simulation Studies	86
6.5.1 Existing PSSs	86
6.5.2 New PSS on #1-#9	86
6.5.3 New PSS on All Machines	89
6.5.4 Other Tests	90
6.6 Summary	92
7. CONCLUSIONS	93
REFERENCES	97
APPENDIX A. DATA FILE <i>pqlf.inp</i> AND LOAD FLOW RESULTS	101
A.1 Data File <i>pqlf.inp</i>	101
A.2 Load Flow Results	104
APPENDIX B. DATA FILE <i>ntwk.inp</i>	106
APPENDIX C. DATA FILE <i>mach.inp</i>	110
APPENDIX D. A FIFTH ORDER MACHINE MODEL	117
D.1 Generator Model	117
D.2 Saturated Reactances	119
D.3 Time Constants	120
APPENDIX E. SATURATION REPRESENTATION	123
E.1 Generation Saturation	123
E.2 Excitation Saturation	124

## LIST OF TABLES

<b>Table 2.1:</b>	PSS settings in APNS.	18
<b>Table 3.1:</b>	Module identifying numbers in TSSP.	32
<b>Table 4.1:</b>	Load and generation distribution(MW).	38
<b>Table 4.2:</b>	Eigenvalues of APNS.	42
<b>Table 4.3:</b>	Swing mode sensitivity to AVR transfer function.	47
<b>Table 4.4:</b>	Swing mode sensitivity to PSS transfer function.	47
<b>Table 6.1:</b>	PSS settings of the 4 generation groups.	81
<b>Table 6.2:</b>	Total coupling factors.	82
<b>Table 6.3:</b>	Eigenvalues after installation of new PSSs on #1-#7.	84

## LIST OF FIGURES

<b>Figure 2.1:</b>	Block diagram of the E" synchronous generator model.	11
<b>Figure 2.2:</b>	Block diagram for computation of speed and rotor angle.	11
<b>Figure 2.3:</b>	Modified IEEE DC type 2 excitation system as used by SaskPower.	14
<b>Figure 2.4:</b>	SCRX excitation system as used by SaskPower.	15
<b>Figure 2.5:</b>	Detailed representation of hydrogovernor turbine system.	16
<b>Figure 2.6:</b>	Simplified representation of hydrogovernor turbine system.	16
<b>Figure 2.7:</b>	IEEE SN PSS using generator electrical power as input.	17
<b>Figure 2.8:</b>	IEEE ST PSS using net accelerating power as input.	18
<b>Figure 2.9:</b>	IEEE standard PSS model.	19
<b>Figure 2.10:</b>	Transient study model of SVC.	19
<b>Figure 3.1:</b>	Overall structure of the TSSP.	34
<b>Figure 4.1:</b>	Geographic depiction of the Athabasca-Points North Power System.	38
<b>Figure 4.2:</b>	Single line diagram of the APNS.	39
<b>Figure 4.3:</b>	Damping versus AVR gain.	44
<b>Figure 4.4:</b>	Damping Affected by Speed Governor.	45
<b>Figure 4.5:</b>	Rotor angle response to 1% load increase at Rabbit Lake.	48
<b>Figure 5.1:</b>	Simplified single line diagram of the APNS.	52
<b>Figure 5.2:</b>	Machine shaft speed versus time. 3LG fault near Points North. Generators in Area N pull out of synchronism.	58

<b>Figure 5.3:</b> Machine shaft speed versus time. 3LG fault near Island Falls. Generators in Area N pull out of synchronism.	59
<b>Figure 5.4:</b> Rotor angle swings of generators #1 and #10 under the SLG fault. Reclosure in 10s of dead line.	61
<b>Figure 5.5:</b> PSS output voltages of generators #1 and #8 under the SLG fault. Reclosure in 10s of dead line.	61
<b>Figure 5.6:</b> Field voltage versus time. SLG fault on the double circuit line.	62
<b>Figure 5.7:</b> Terminal voltage versus time. SLG fault on the double circuit line.	62
<b>Figure 5.8:</b> Mechanical and electrical power responses of generator #5 to the SLG fault.	63
<b>Figure 5.9:</b> Rotor angle swings of generators #1 and #10 under the 3LG fault. Reclosure in 10s of dead line.	64
<b>Figure 5.10:</b> Transferred real power from Manitoba Hydro to this system. 3LG fault at bus 37 for 2.3s.	65
<b>Figure 5.11:</b> Rotor angle of generator #8. 3LG fault at bus 21 for 0.1s with and without autoreclosure.	67
<b>Figure 5.12:</b> Rotor angle of generator #8. SLG fault at bus 37 for 2s with and without reclosure.	68
<b>Figure 5.13:</b> Rotor angle swing of generator #8. SLG fault at bus 21 with and without reclosure.	69
<b>Figure 6.1:</b> Rotor angle plotting of generator #8 under 3 $\phi$ fault at bus 30.	74
<b>Figure 6.2:</b> Terminal voltage plotting of generator #8 under 3 $\phi$ fault at bus 30.	75

<b>Figure 6.3:</b> Mechanical power of generator #1 under 3 $\phi$ fault at bus 30.	76
<b>Figure 6.4:</b> Rotor angle swing of generators #1 and #8 under 3 $\phi$ fault at bus 30. Effects of PSSs.	77
<b>Figure 6.5:</b> Realization of PSS coordination.	81
<b>Figure 6.6:</b> Rotor angle swing responding to a load increase of 1% the system capacity at Rabbit Lake.	85
<b>Figure 6.7:</b> Rotor angle plotting of generator #1 versus time. Single phase fault near bus 61 for 6 cycles.	85
<b>Figure 6.8:</b> Time domain simulation of the SLG fault with and without the existing PSSs in service.	87
<b>Figure 6.9:</b> Time domain simulation of the SLG fault with new PSSs on generators #1 - #9 in service.	88
<b>Figure 6.10:</b> Time domain simulations of the SLG fault with new PSSs on all machines in service.	89
<b>Figure 6.11:</b> Responses of speed difference of generator #1 to 3LG fault for 6 cycles at bus 18.	91
<b>Figure 6.12:</b> Rotor angle swing of generator #1. SLG fault for 6 cycles under different system loading.	92

## LIST OF PRINCIPAL SYMBOLS

All angles are with reference to the infinite busbar synchronous frame. All voltages, currents, power quantities and line parameters are in per unit (p.u.) based on the 100 MVA system base. Machine impedance is in per unit based on its own rated capacity. All time constants and machine inertia constant  $H$  are in seconds.

### Abbreviations:

APNS = Athabasca-Points North Power System

AVR = Automatic Voltage Regulator

deg. = degree

PSS = Power System Stabilizer

r = radian

s = second

SGTS = Speed Governing and Turbine System

TSSP = Transient Stability Simulation Package

### Symbols:

$\delta$  = machine rotor angle (deg.)

$\delta$  = transient speed droop coefficient

$D$  = machine damping coefficient

$E$  = voltage

$E'$  = voltage behind transient reactance

$E''$  = subtransient voltage

$G$  = gate

$\phi$	= flux linkage
H	= machine inertia constant (s)
i	= current
k	= saturation factor
K	= gain of transfer function
P	= active power
p.u. or	
pu	= per unit
Q	= reactive power
R	= resistance
$\sigma$	= permanent speed droop coefficient
$\tau, T$	= time constant
T	= transformation of coordinate systems
T	= torque
v, V	= voltage
VEL	= velocity
$\omega$	= angular speed
$\omega_s$	= synchronous speed (r/s)
X	= reactance

### Subscripts:

a	= armature
ad, aq	= mutual
D, Q or	
d, q	= direct and quadrature axes
e	= electrical
E	= excitation

err	= error
f, fd	= field
G	= generator
G	= gate servomotor
i, j	= index
$\ell$	= leakage
l	= loss
L	= load
m	= mechanical
max	= maximum
min	= minimum
o	= open circuit
p	= pilot valve
R	= dashpot
ref	= reference
s	= extra signal
T, t	= terminal
w	= washout
x, y	= x and y coordinates

#### **Superscripts:**

'	= transient
"	= subtransient
(0)	= unsaturated value

#### **Mathematical operators:**

$\Delta$	= small change
----------	----------------

$\Sigma$  = summation

$s$  = Laplace operator

$\times$  = multiply

$\parallel$  = parallel

# 1. INTRODUCTION

## 1.1 Power System Stability

As the interconnections of power systems have increased, they have been able to provide more reliable power supply to the loads in the interconnected systems. However, new stability problems such as low-frequency electromechanical oscillations have also emerged.

Power system stability has been an area of study for several decades. As the stability of a power system is dependent on the size and type of a disturbance, a steady state operating condition may be stable for one disturbance but not for another. This leads to the classification of stability [1]: steady state or small disturbance stability; and transient or large disturbance stability. It is recommended that the terms *static* and *dynamic stability*, which are sometimes used for the steady state stability without and with automatic controls, respectively, be avoided [2].

A small disturbance is a disturbance for which the equations that describe the dynamics of the power system can be linearized for the purpose of analysis. The steady state stability of a power system is the stability following any small disturbance. A system is said to be steady state stable for a particular operating condition, following such a disturbance, if the system can reach another steady state condition that may or may not be identical or close to the pre-disturbance operating condition of the power system.

A large disturbance is a disturbance for which the equations that describe the dynamics of the power system can not be linearized for the purpose of analysis. The transient stability of a power system is the stability following a large disturbance. A system is said to be transient stable for a particular operating condition and for a specified disturbance if, following that disturbance, it can reach an acceptable steady state operating condition.

The principal task following a disturbance is to attempt to reestablish stable operating conditions in the system. As the cause of instability is the unbalanced energy in the system, it is important at first to decide whether this unbalanced energy is positive or negative. If positive, the unbalanced energy will accelerate generators while if negative, it will decelerate them. If the system is not capable of settling down to the original equilibrium point, or to a new one, by redistributing the energy in the network automatically, then corrective measures will have to be taken to resolve this unbalanced energy, either by tripping generators or by shedding some loads according to a pre-determined plan.

As our society's demand for and consumption of electrical energy has increased steadily, power systems over large geographic areas have been interconnected to meet this demand and to provide a reliable electrical power service. At the same time, sophisticated control equipment and protection schemes have been added to power systems to enhance their stability. As a result, the analysis of power system stability has become more difficult. Fortunately, enriched mathematical modeling and better computation facilities have made it possible to investigate the complicated problem of stability.

## 1.2 Methods of Solution

The mathematical representation of the problem of power system stability is based on the modeling of various power system components. The number of such components included in a study and the complexity of their mathematical descriptions will depend on the type of the problem and the nature of the system to be investigated. Appropriate modeling is essential to ensure that the results obtained are correct and reliable. Accurate modeling may be difficult to achieve due to:

- a) lack of actual parameters
- b) discrepancies between available data and the actual state of equipment, because of modification, deterioration, etc., after years of operation
- c) impracticality of obtaining useful data through field tests
- d) inappropriate choices of component models.

For a large power system with its numerous machines, lines, loads, and other components, the mathematical representation of the system for conducting stability studies can be immense, depending on the complexity of the models to be used in the study. The analysis of the consequences of a disturbance can also be very complicated.

Differential equations are utilized to describe the dynamic behavior of power system components. On the other hand, algebraic equations are sufficient to represent the relationship of electrical quantities in the network of the transmission lines. The key part of a stability study is to solve these differential and algebraic equations simultaneously.

According to the nature of the study, techniques for analysis of power system stability fall into two categories. Those for steady state stability studies are based on linear system analysis. For example, eigenvalue analysis has been the most commonly used technique for this purpose. Other methods, such as root-locus plots, frequency domain analysis, and Routh's criterion, have also been widely used. Methods for transient stability studies are based on numerical integration such as trapezoidal rule or modified Euler approach.

In the study reported in this thesis, eigenvalue analysis and sensitivity study techniques are utilized for steady state stability studies. The implicit integration technique for numerical solution of differential equations is employed for transient stability studies.

### **1.3 Statement of Objectives**

The objectives of this thesis are (i) to fully investigate the steady state and transient stability of a realistic power system, i.e., the Athabasca-Points North Power System (APNS) in northern Saskatchewan, Canada and (ii) to design more effective power system stabilizers to improve both steady state and transient stability of the APNS. Specifically, the following tasks were carried out to achieve the stated objectives.

#### **1. A Simulation Tool**

To solve a large number of nonlinear mathematical equations describing a stability problem, a numerical simulation tool is compulsory. A number of

commercial packages serving this purpose are available in the market. As the author of this thesis has no access to them due to financial restrictions, the development of a simulation package was the first objective of this thesis. This task was accomplished by developing a transient stability simulation package (TSSP) [3].

## 2. Stability Investigation of APNS

As the purpose of the project reported in this thesis was to investigate the stability of the APNS, analysis of its steady state stability was the first step taken to tackle the problem. This analysis was conducted with eigenvalue analysis and sensitivity study techniques. The investigation of the transient stability was conducted by utilizing the newly developed package (TSSP).

## 3. Stabilization of APNS

The final objective of the study was to improve the overall system stability of the APNS by introducing newly designed controllers, such as PSSs. A coordinated PSS design and application algorithm were introduced and new PSSs were designed. A comprehensive simulation study was carried out to verify the effectiveness of the newly designed PSSs.

## 1.4 Overview of the Thesis

This thesis consists of seven chapters and five appendixes. In Chapter 2, mathematical or block diagram representations of various power system components, i.e., generators, AVRs, PSSs, and SVC, used in the studies

reported in this thesis, are presented. The modeling of disturbances that cause system contingencies is discussed. Different load representations are also presented. The modeling of network and transformers is briefly covered.

In Chapter 3, a simulation tool, i.e., a transient stability simulation package, for power system stability studies is presented. The structure, database and modeling foundation of the package are discussed. The package consists of four parts: a fast decoupled load flow program (FDLF), a short circuit calculation program (STCC), the transient simulation main body (TSSP) including a coordinator, and a plotting program (WPLOT). It is implemented on an IBM PC in the FORTRAN language. A minimum of 410K conventional memory is required to do a stability study of a system of 100 buses, and a CGA, EGA or VGA graphics card is needed to run the WPLOT program.

Chapter 4 deals with steady state stability studies of the APNS. Eigenvalue analysis and sensitivity study techniques were used to investigate the factors that affect the damping of the various system swings. The best PSS installation sites were determined based on the magnitude of functional sensitivities of the swing modes with respect to PSS transfer functions.

Chapter 5 deals with transient stability studies of the APNS. An introduction to the purposes of transient stability studies of a power system is given. In order to facilitate the analysis and presentation of simulated results, generators in the system were divided into coherent groups. The system was also divided into three geographic areas. The system stability under different disturbances at various areas was studied.

A coordinated design procedure for power system stabilizers (PSSs) is discussed in Chapter 6, after carrying out a parametric sensitivity study of the primary controls by time simulation. The design procedure is based on generation coherency, lead/lag time constant spread and the total coupling factors among strongly coupled generators. New eigenvalues were computed with the newly designed PSSs in service. A comprehensive simulation study and comparison of the results obtained is also presented in this chapter.

In Chapter 7, conclusions are presented which have been drawn from the studies reported in this thesis.

Appendices A, B, and C contain the three data files required for the stability studies of the Athabasca-Points North system (APNS). Part of the results of a load flow study of the system is also given in Appendix A. Appendix D presents detailed mathematical derivation of a two-axis model of a generator with subtransient effects. Appendix E discusses the procedure for inclusion of the saturation of both the generator and its excitation system in simulation studies.

## **1.5 Summary**

An introduction to the basic concepts of power system stability has been presented at the beginning of this chapter. It is recognized that the source of power system instability is the unbalanced energy and its redistributing process. Then, a review of the methods of solving the stability problem is presented. In the last two sections, the objectives of the thesis and its structure are outlined.

## **2. MODELING OF A POWER SYSTEM FOR STABILITY STUDIES**

### **2.1 Introduction**

In order to study the steady state and transient stability of a power system, it is essential that the power system components included in a study be properly modeled. As power systems have expanded and modern excitation systems introduced into large synchronous machines, it may be inappropriate to utilize simplified machine models in investigating the transient stability beyond the first swing. Adequate machine modeling, including that of the AVR and the speed governing and turbine system, is essential in carrying out a stability study.

A synchronous machine can be modeled with varying complexity. It has been justified that a fifth order representation of the synchronous machine under disturbances can satisfy the requirement that the subtransient phenomena of the machine be properly modeled while its mathematical representation is still fairly simple [4]. Further detailed modeling is not worthwhile as the computation effort increases rapidly while the gains in terms of accuracy are very little. Three machine representations used in this study are discussed in this chapter. Symbols used in this chapter and hereafter are defined in the List of Principal Symbols at the beginning of this thesis.

Generally, an excitation system includes two major parts: a voltage regulator and an exciter. According to the type of power source utilized by the exciter, excitation systems can be classified as [5]:

1. type DC system which utilizes a DC generator with a commutator as the power source of the excitation system;
2. type AC system which utilizes an alternator and either stationary or rotating rectifiers to produce the direct current for the exciter; and
3. type ST system which utilizes transformers and rectifiers to provide the direct current.

Modeling details of the excitation systems used in this project are presented in this chapter.

The speed governing and turbine system for hydro power generators can be modeled either by a detailed or by a simplified representation [6]. Both the detailed and the simplified equivalent models are discussed here. Then the modeling of two specific power system stabilizers (PSSs) utilized in the studies reported in this thesis, and one IEEE standard PSS model utilized in designing the new PSSs are discussed. Lastly, the modeling of disturbances, load representations, and the modeling of transformers and the network are briefly presented.

## **2.2 Synchronous Machine Models**

The coordinate system utilized for synchronous machine modeling in this thesis is the original coordinate system employed by Park [7].

## 1. Two - Axis Model with Subtransient

With the effects of rotor damping being represented by two short circuited damper windings on the rotor in this model, the following derived differential equations are utilized to describe the subtransient behavior of a synchronous machine (see Appendix D for detailed derivation):

$$\dot{E}_q = \frac{1}{\tau_{do}} \left\{ kE_{fd} - E_q' - (x_d - x_d')i_d \right\} \quad (2.1)$$

$$\dot{E}_{sum} = \frac{1}{\tau_{do}} \left\{ -E_{sum} - (x_d' - x_d'')i_d \right\} \quad (2.2)$$

$$\dot{E}_d'' = \frac{1}{\tau_{qo}} \left\{ -E_d'' + (x_q - x_q'')i_q \right\} \quad (2.3)$$

where

$$E_{sum} = E_q'' - E_q'.$$

A block diagram of this model is shown in Figure 2.1.

The differential equation describing machine motion is given by

$$\Delta \ddot{\delta} = (P_m - P_e - P_l - D \Delta \omega) / 2H \quad (2.4)$$

$$\Delta \dot{\delta} = \omega_o (\Delta \omega) \quad (2.5)$$

where  $H$  is the machine inertia constant in seconds and  $\omega_o$  is the synchronous speed of the machine in radians per second.

The block diagram shown in Figure 2.2 depicts the relationship of the various variables in Equations (2.4) and (2.5).

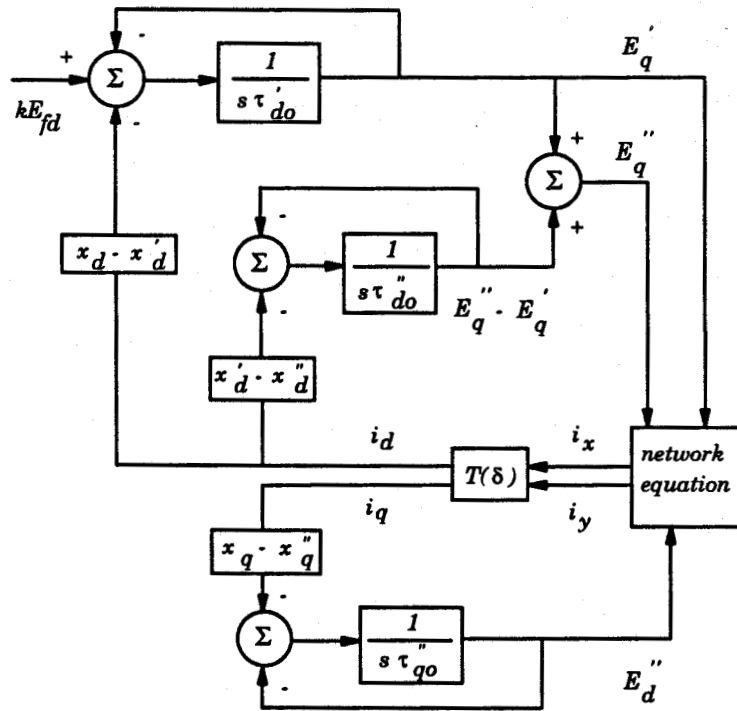


**Figure 2.1:** Block diagram of the  $E''$  synchronous generator model.

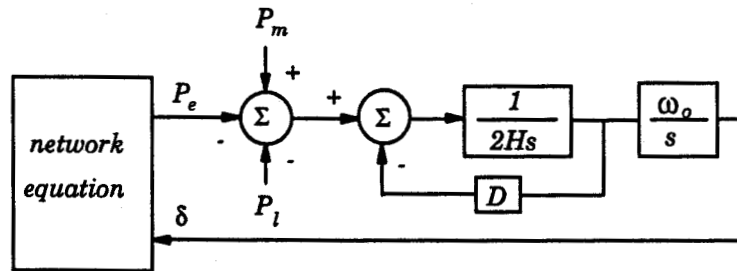


**Figure 2.2:** Block diagram for computation of speed and rotor angle.

Generation saturation can be taken into account by modifying the reactances  $x_{ad}$  and  $x_{aq}$  according to machine saturation at 1.0 pu and 1.2 pu terminal voltage that usually are known from the manufacturer. There are several algorithms to realize this modification [4,8]. An iterative procedure

was employed in the studies reported in this thesis. At the same time, the corresponding time constants must also be modified. Detailed derivation of their expressions is given in Appendix D of the thesis. They are quoted here as part of the mathematical model of the synchronous machine modeled by the two-axis representation with subtransient.

Saturated time constants are

$$\tau'_{do} = \tau_{do}^{(0)} \left\{ k + (1-k) \frac{x'_d - x_l}{x_d^{(0)} - x_l} \right\} \quad (2.6)$$

$$\tau''_{do} = \tau_{do}^{(0)} \left\{ k + (1-k) \frac{x''_d - x_l}{x_d^{(0)} - x_l} \right\} \quad (2.7)$$

$$\tau''_{qo} = \tau_{qo}^{(0)} \left\{ k + (1-k) \frac{x''_q - x_l}{x_q^{(0)} - x_l} \right\} \quad (2.8)$$

where the superscript (0) indicates unsaturated values, and  $k$  is the saturation factor. Other symbols are conventional.

## 2. Two-Axis Model with Transient

This model is similar to the one presented previously. The subtransient effects are totally ignored; however, the transient effects are taken into account. There are two rotor windings, one is the field winding in the d-axis and the other is the equivalent damper winding in the q-axis formed by the solid rotor.

The basic equations of this model are given by:

$$v_q = E'_q - x'_d i_d - r_a i_q \quad (2.9)$$

$$v_d = E'_d + x'_q i_q - r_a i_d \quad (2.10)$$

$$\dot{E}_q = \frac{1}{\tau_{do}} \left\{ kE_{fd} - E_q - (x_d - x'_d)i_d \right\} \quad (2.11)$$

$$\dot{E}_d = \frac{1}{\tau_{qo}} \left\{ -E_d + (x_q - x'_q)i_q \right\} \quad (2.12)$$

where  $\tau'_{do}$  is modified according to (2.6); and

$$\tau'_{qo} = \tau_{qo}^{(0)} \left\{ k + (1-k) \frac{x_q - x_\ell}{x_q^{(0)} - x_\ell} \right\}. \quad (2.13)$$

### 3. One-Axis Model with Transient

In this model, the amortisser effects are totally neglected. There is only one rotor winding present in the model, i.e., the field winding. Its differential equation is the same as (2.11). Saturation is treated in the same manner as explained previously. The difference between this model and the two-axis transient model is that as no damper windings are modeled, the differential equation for  $E'_d$  is, therefore, eliminated.

A voltage behind transient reactance model can be achieved by assuming that the time constant  $\tau'_{do}$  is very large.

## 2.3 Controller Modeling

There are three kinds of controllers that directly affect the operation of a synchronous generator, and thus the stability of a power system. They are the excitation system, the speed governing and turbine system, and the power system stabilizer. One of the most influential of the three is the

excitation system. This section presents the modeling of these three controllers in the form of block diagrams.

### 2.3.1 Excitation Systems

Throughout this thesis, the IEEE standard excitation representation has been adopted and the universally accepted convention is used. As power components and controllers are simulated by programming their block diagrams, mathematical expressions for their modeling may not be necessary. Therefore, only the block diagrams are presented.

Two solid state excitation systems, i.e., SCR<sub>X</sub> and SCR<sub>XIL</sub>, the latter having a maximum field current limit, and one modified DC type 2 excitation system are used in the research reported in this thesis. As these three models are non-standard IEEE models, they are discussed here in more detail.

#### 1. Modified DC type 2 excitation system — EXDC2B

A modified version of the DC type 2 excitation system, as shown in Figure 2.3, is utilized to model the rotating DC excitation system in this thesis.

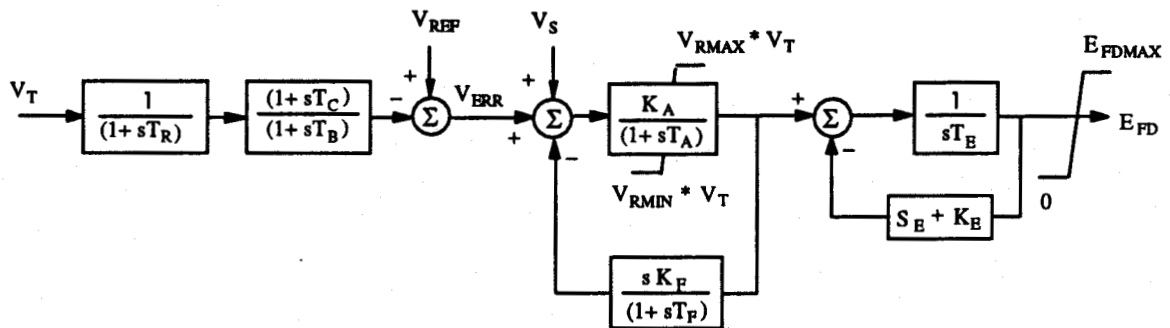


**Figure 2.3:** Modified IEEE DC type 2 excitation system as used by SaskPower

## 2. Solid state excitation systems — SCR<sub>X</sub>, and SCR<sub>XIL</sub>

The SCR<sub>X</sub> exciter is a solid state exciter fed by either the bus terminal voltage or an independent supply. The block diagram of the system is shown in Figure 2.4. The switch SW is set to terminal voltage  $V_T$  if the exciter is fed by bus. Otherwise it is set to 1.0. If the exciter accepts negative current, the negative current logic is bypassed. However, if  $I_{fd}$  is negative, the output voltage  $E_{fd}$  of the excitation system is reversed.

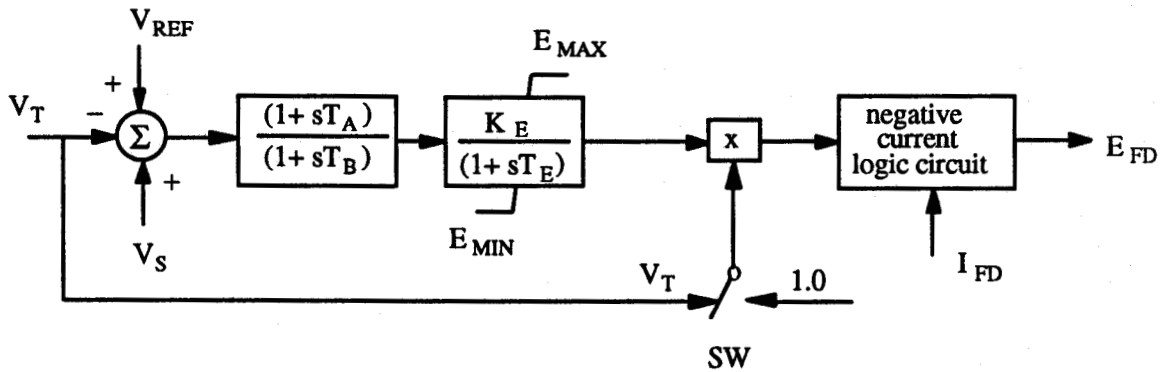


**Figure 2.4:** SCR<sub>X</sub> excitation system as used by SaskPower.

A variant of the SCR<sub>X</sub> type exciter is SCR<sub>XIL</sub> and is used in this project. The structure is the same as that of SCR<sub>X</sub> as shown in Figure 2.4, except that a maximum field current limitation is introduced. This maximum current limit protects the exciter and the generator rotor.

### 2.3.2 Speed Governing and Turbine Systems

The modeling of speed governing and turbine systems (SGTS) for both steam and hydro generators is quite standard [6]. As steam generators are not present in the system studied in this thesis, the modeling of their speed

governing and turbine system is not discussed here. The detailed model of a hydro generator's speed governing and turbine system is given in Figure 2.5. Its simplified representation, in which the time constant  $T_p$  and the gate servomotor limits are neglected, is also shown in Figure 2.6.

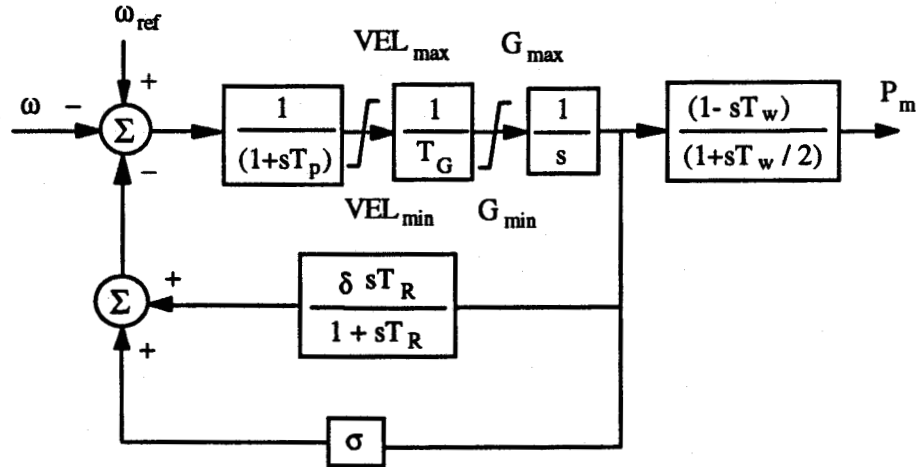


**Figure 2.5:** Detailed representation of hydrogovernor turbine system [6].

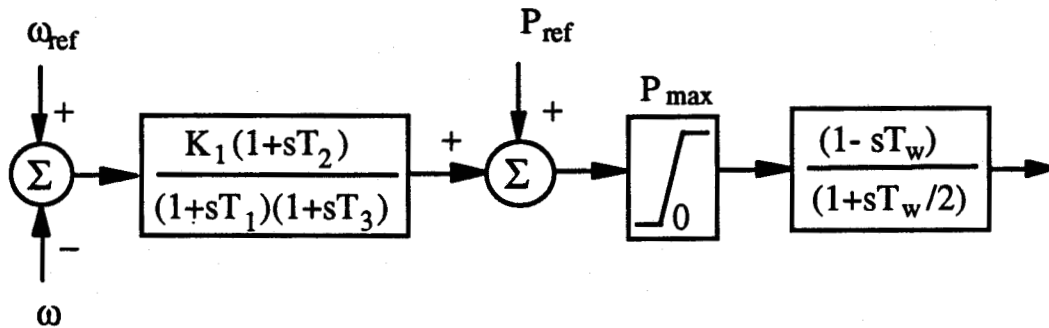


**Figure 2.6:** Simplified representation of hydrogovernor turbine system [6].

### 2.3.3 Supplementary Excitation Controllers

In order to suppress the low frequency electromechanical oscillations in a power system, supplementary excitation controllers well known as power system stabilizers (PSSs) are often installed to provide positive damping [9].

The PSS output ( $V_s$ ) feeds into the excitation system as shown in Figures 2.3 and 2.4.

The input signal to a PSS can be arbitrary [9]. Generally, any one or a combination of the following can be utilized as input signal:

- (a) deviation of machine shaft speed
- (b) deviation of terminal frequency
- (c) net accelerating power
- (d) deviation of terminal voltage

The input signals must be in per unit. A PSS with a different input signal will have a different transfer function.

Two PSS models are used in the studies reported in this thesis. Their input signals are generator electrical power and net accelerating power, respectively. The former is identified as IEEEESN and the latter as IEEEEST. Their block diagrams are shown in Figure 2.7 and Figure 2.8, respectively.

Note that only a single time constant  $A_1$  is present in the filter transfer function, this is because of the inherently low level of torsional interaction when net accelerating power is used as stabilizer input.

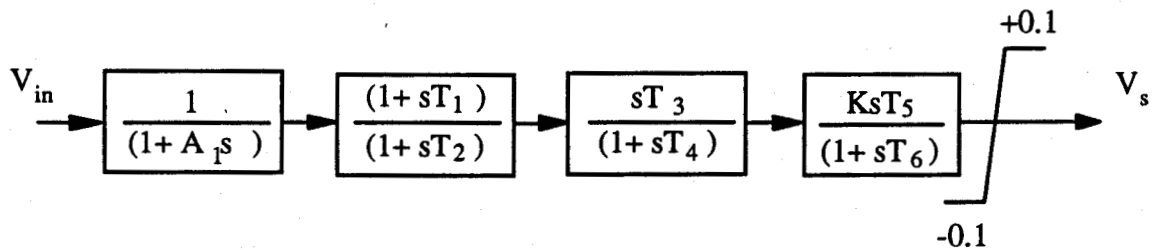


**Figure 2.7:** IEEEESN PSS using generator electrical power as input.

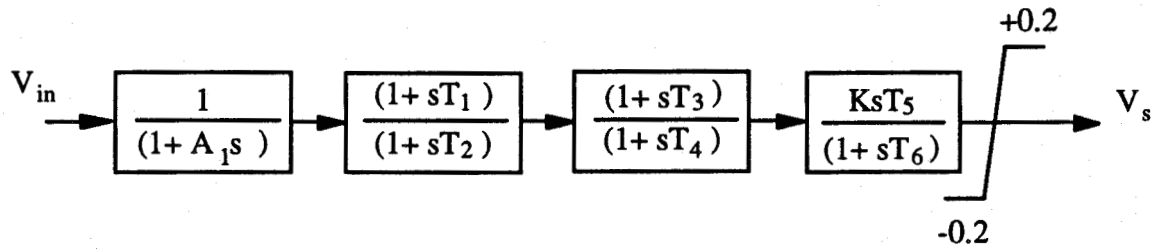


**Figure 2.8:** IEEE ST PSS using net accelerating power as input.

As an example, the settings of the two PSSs used in this project are listed in Table 2.1. Their effects on the system stability are discussed in subsequent chapters.

**Table 2.1:** PSS settings in APNS.

PSS	Input	K	A <sub>1</sub>	T <sub>1</sub>	T <sub>2</sub>	T <sub>3</sub>	T <sub>4</sub>	T <sub>5</sub>	T <sub>6</sub>	Limits
IEEE SN	g.e.p.	-.05	.014	.000	.025	4.4	4.4	5.0	5.0	±0.1
IEEE ST	n.a.p.	10.	.000	.400	1.00	.08	.50	2.0	2.0	±0.2

where g.e.p. is generator electrical power; and n.a.p. is net accelerating power.

The IEEE standard PSS model [5] is utilized to design new PSSs described in Chapter 6. The block diagram of the model is shown in Figure 2.9. The transfer function of the filter in the diagram can be expressed by:

$$\frac{(1 + A_5 s + A_6 s^2)}{(1 + A_1 s + A_2 s^2)(1 + A_3 s + A_4 s^2)} \quad (2.13)$$

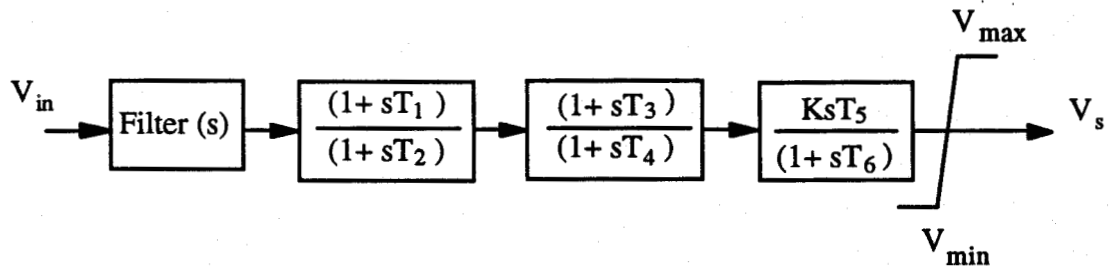


**Figure 2.9:** IEEE standard PSS model.

## 2.4 Modeling of SVC

A static var compensator (SVC) may function to meet any or all of the following objectives by fast and continuous control of reactive power flow in the system:

- (a) voltage regulation
- (b) enhancement of steady state and transient stability
- (c) compensation of reactive power flow, minimizing losses
- (d) damping of subsynchronous oscillations

A transient model of the SVC can be modeled by the block diagram as shown in Figure 2.10.

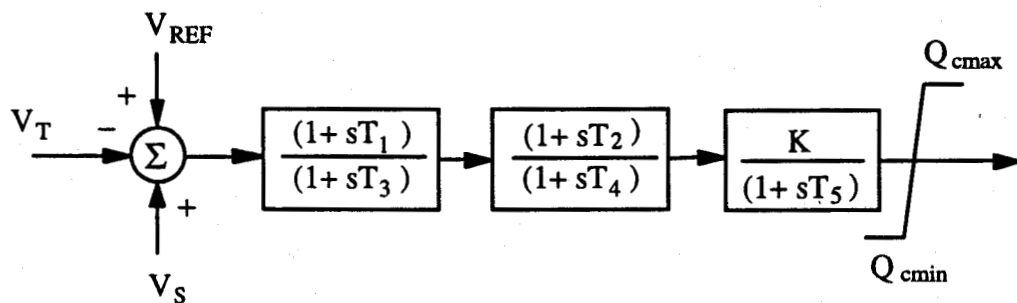


**Figure 2.10:** Transient study model of SVC[38].

In Figure 2.10,  $K$  is the gain setting,  $T_1 \sim T_5$  are time constants,  $Q_{cmin}$  and  $Q_{cmax}$  is minimum and maximum generated reactive power (in Mvar), respectively, injected into the network.

## 2.5 Modeling of Disturbances

The modeling of disturbances is an important aspect in simulating the dynamic behavior of a power system with acceptable accuracy. Both symmetrical and asymmetrical disturbances should be modeled. A symmetrical disturbance can be easily modeled as the system will remain symmetrical under such a disturbance. Under asymmetrical disturbance, the solution of a stability problem of the disturbed three-phase network can be carried out by a three-phase stability program, where the symmetrical component method is employed to resolve the system into three symmetrical three-phase systems. Thus the total computations will increase up to three times. On the other hand, it has been found [10] that the average braking torque produced by the reaction of the two magnetic fields, one produced by the negative sequence current and the other by the rotor winding current, is approximately zero, and that zero sequence currents yield a zero component torque as the three-phase zero sequence currents are electrically in phase and have 120 degree displacement in space. Hence, only the positive sequence quantities are needed to be taken into account during a transient process. However, the negative and zero sequence networks have to be incorporated into the positive sequence network at the fault point.

Each disturbance can be described and modeled as a sequence of four events. They are pre-fault, fault, post-fault and line restoration, i.e.,

autoreclosure if any. The admittance matrix of the network is modified each time there is a change in the configuration of the network during the disturbance.

As most faults in a practical power system are asymmetrical in nature, it is important that engineers know what behavior a system would exhibit under such disturbances and what measures should be taken to maintain system stability while maximizing the availability of power supply to customers.

## **2.6 Load Modeling**

Loads can be modeled by any characteristics as long as their representations are known. Specifically, a large induction motor can be simulated by its transient model [11]. Other load representations are [12]:

1. Constant impedance model

In this model, the power varies directly with the square of the voltage magnitude.

2. Constant current model

The power varies directly with the voltage magnitude in this model.

3. Constant power (MVA) model

In this model, the power does not vary with the changes in voltage magnitude.

4. Polynomial load model

This model expresses the relationship between power and voltage magnitude as:

$$P = P_0 \left\{ a_1 \left( \frac{V}{V_0} \right)^2 + a_2 \left( \frac{V}{V_0} \right) + a_3 \right\} \quad (2.14)$$

$$Q = Q_0 \left\{ a_4 \left( \frac{V}{V_0} \right)^2 + a_5 \left( \frac{V}{V_0} \right) + a_6 \right\} \quad (2.15)$$

where  $V_0$  should be the rated voltage, and  $P_0$  and  $Q_0$  should be the power consumed at rated voltage. However, they are normally taken as the values at the initial system operating condition for the study. The coefficients in the model satisfy the following equations:

$$a_1 + a_2 + a_3 = 1 \quad (2.16)$$

$$a_4 + a_5 + a_6 = 1 \quad (2.17)$$

Exact simulation of loads requires that at each time step, a load flow study be carried out to obtain the accurate bus voltage. This will increase the computation effort to an unacceptable extent. However, an alternative is to calculate the new operating point by the fast decoupled load flow program only at every instant following a disturbance till the system voltage is recovered. At other times, the bus voltage is held constant at the value computed in the latest load flow study. Load modeling itself is a very difficult task as meaningful data are simply unavailable and collecting and processing load data is expensive. Therefore, the constant impedance model was employed in the studies reported in this thesis.

## 2.7 Modeling of Network and Transformers

Transmission lines of a power system are represented by lumped parameters, as used in a load flow program. Positive, negative and zero sequence impedances of power apparatus are needed to assemble the three sequence admittance matrices. Algebraic equations are utilized to describe the relationship of the electrical quantities in the network during both steady state and transient process.

Transformers are modeled by their steady state equivalent circuits that consist of branches that are treated similar to transmission lines. The sequence impedances of transformers are also needed in assembling the admittance matrices of the network.

## 2.8 Summary

This chapter outlines the basic models used in the studies reported in this thesis.

Firstly, the modeling of synchronous machines and their three controllers are presented. Several synchronous generator models are discussed. However, more attention is given to the two-axis model in which the subtransient voltages of the two axes ( $d$ ,  $q$ ) are defined and, thereafter, the mathematical representation is given. Three excitation system models, which are not IEEE standard models, are presented. The detailed and simplified models of the speed governing and turbine system for hydro generators are given. PSS models and the modeling of a SVC are also introduced.

Then, the modeling of balanced and unbalanced disturbances, which plays an important role in stability simulation studies, is discussed. Finally, various load models are given and the modeling of transformers by their steady state equivalent circuits is presented.

### **3. A TRANSIENT STABILITY SIMULATION PACKAGE**

#### **3.1 Introduction**

Time domain simulation of power systems has been a classical tool for various purposes of stability studies for decades [13,14,15]. Various digital simulation packages [16,17] are in wide use as complementary tools in research. Many other computer softwares are also reported in the literature [18,19,20].

It is felt that every simulation package has its own advantages and shortcomings. A package available to one may not have all the features and flexibility that one needs. The possibility of changing the capability of the package is often limited if not impossible. With the increased power of micro computers in recent years, there has been a need of a new package that has the capacity of fulfilling most requirements in transient simulation studies of power systems. In answering this call, a transient stability simulation package (TSSP) implemented on an IBM PC has been developed at the University of Saskatchewan. It is written in the FORTRAN language. A minimum of 410K conventional memory is required to perform a stability study for a system of 100 buses and a CGA, EGA or VGA graphics card is needed to run the plotting utility. This package has been tested on the WSCC system [8] and the New England Test system. It has been also used to conduct the stability investigations reported in this thesis.

The following is a list of tasks that can be performed with the TSSP:

- a) Machine modeling of varying complexity
- b) Transients of induction motors
- c) Modeling of symmetrical and asymmetrical disturbances
- d) Various load representations
- e) Modeling of AVR, SGTS and PSS
- f) Interfacing of user-defined modules
- e) Load flow studies
- g) Short circuit calculations

### **3.2 Description of Modules within the TSSP**

The transient behavior of a power component or a controller is modeled by a set of first order differential equations. On the basis of the implicit integration method [10], this set of differential equations is simulated by building a block of integrators. Each such block forms an independent module to be called upon by a coordinator in the TSSP.

The TSSP has modules for four different synchronous machine models, one induction motor model, all current IEEE recommended excitation system models [5], speed governing and turbine system models [6] and the standard model for a power system stabilizer. Different load models can also be included. For most of the studies, these modules are sufficient. In cases where the module of a component is not available in the TSSP, a user-defined module can be written and easily interfaced to the simulation package. Descriptions of the modules provided in the TSSP are given in this section.

### 3.2.1 Machine Modules

As discussed in Chapter 2, a synchronous machine can be modeled with varying complexity. Each machine model is programmed into a module that is designated by a one-digit identifying number as illustrated in Table 3.1. Specifically, modules for the following machine representations are available:

- a) Two-axis subtransient model
- b) Two-axis transient model
- c) One-axis transient model
- d) Constant voltage behind  $x_d'$  model
- e) Infinite-bus
- f) Induction motor

The differential equations describing the two-axis subtransient model of a synchronous generator are given by (2.1) ~ (2.5) in Chapter 2. Detailed derivation of these equations is given in Appendix D. A block diagram for this model is also given in Chapter 2. Generation saturation has been taken into account by approximating the open circuit curve of the generator terminal voltage as an exponential function [8] and by modifying the reactances,  $x_{ad}$  and  $x_{aq}$ , and the three time constants according to (D.33) ~ (D.42), respectively, as illustrated in Appendix D.

A large induction motor is modeled by its transient models.

### 3.2.2 Modules for Excitation Systems

Any excitation system including its nonlinearities can be simulated in the TSSP. Modules for all current IEEE recommended excitation systems [5] and three other excitation systems given in Chapter 2 are included. Each system is designated by a two-digit model identifying number as shown in Table 3.1. Specifically, the following models are available in the package:

1. The following excitation systems use direct current generators as the source of power supply to the exciters:
  - a) DC type 1
  - b) DC type 2
  - c) DC type 3
  - d) DC type 2 modified
  
2. The following excitation systems use an alternator and either stationary or rotating rectifiers to produce the direct current for the exciters:
  - e) AC type 1
  - f) AC type 2
  - g) AC type 3
  - h) AC type 4
  
3. The following excitation systems use transformers and rectifiers to provide the direct current for the exciters:
  - i) ST type 1
  - j) ST type 2
  - k) ST type 3

4. The following excitation systems are solid state types:
  - l) SCR<sub>X</sub>, Figure 2.4 of Chapter 2
  - m) SCR<sub>XIL</sub> (SCR<sub>X</sub> with maximum field current limitation)
5. User - defined modules for excitation systems not listed above with the identifying numbers from 51 to 55 can be interfaced into the package.

### 3.2.3 Modules for Speed Governing and Turbine Systems

Modules of the speed governing and turbine systems (SGTS) for all steam and hydro generator models recommended by IEEE [6] are available in the TSSP. Each module is designated by a three-digit identifying number, as per Table 3.1:

1. For steam turbine systems, they are:
  - A) speed governing and turbine system for Non-Reheat configuration (NR)
  - B) speed governing and turbine system for Tandem-Compound, Single-Reheat configuration (TCSR)
  - C) speed governing and turbine system for Tandem-Compound, Double-Reheat configuration (TC<sub>DR</sub>)
  - D) speed governing and turbine system for Cross-Compound, Single-Reheat configuration A (CCSR-A)
  - E) speed governing and turbine system for Cross-Compound, Single-Reheat configuration B (CCSR-B)
  - F) speed governing and turbine system for Cross-Compound, Double-Reheat configuration (CC<sub>DR</sub>)

2. For hydro turbine systems, they are:

- A) Speed governing and hydro turbine system with a detailed representation
- B) Speed governing and hydro turbine system with a simplified representation

3. User - defined modules for speed governing and turbine systems not listed above with the identifying numbers from 231 to 235 can be interfaced into the package.

### **3.2.4 Modules for Power System Stabilizers**

Modules for the two specific PSS models, i.e., IEEEESN and IEEEEST, utilized in the studies reported in this thesis and one IEEE standard model [5] utilized to design new PSSs are incorporated in the TSSP. The block diagrams of these models are given in Chapter 2. For each PSS module, different input signals can be chosen by specifying the corresponding identifying numbers as listed in Table 3.1.

1. Available modules are:

- A) IEEEESN
- B) IEEEEST
- C) IEEE standard

2. User - defined modules for PSSs not listed above with the identifying numbers from 51 to 55 can be interfaced into the package.

### 3.2.5 Disturbances

Special attention is given to the modeling of various disturbances, as they are significant in influencing the stability of a system. To conduct a stability study, a disturbance, small or large, symmetrical or not, must be created and applied to the system under study. The common practice is that a balanced disturbance such as three phase fault is used as the most severe disturbance under certain operating conditions. The stability margin obtained under such a fault is quite conservative and pessimistic. Moreover, the frequency of occurrence of such disturbances is much lower than that of asymmetrical ones such as single phase faults. Therefore, it is desirable to conduct transient stability investigations under unbalanced disturbances at planning and operation stages.

As has been explained in Chapter 2, balanced disturbances can be modeled by using only the positive sequence network as the disturbed system remains symmetrical. Unbalanced disturbances can be modeled by incorporating the negative and zero sequence networks into the positive sequence network at the fault point. The following disturbances can be modeled in the TSSP. Provision is made to allow the use of fault and/or grounding impedance.

- A) Three phase to ground
- B) One phase to ground
- C) Two phases to ground
- D) Phase to phase
- E) One phase open

F) Two phases open

**Table 3.1: Module identifying numbers in the TSSP.**

Generator	AVR	SGTS	PSS
0 - Infinite-bus	11 - DC 1 12 - DC 2	211 - NR 212 - TCSR	311 - IEEEEST 312 - IEEESEN
1 - Classic	13 - DC 3 14 - EXDC2B	213 - TCDR 214 - CCSR-A	313 - IEEE standard
2 - Eq'		215 - CCSR-B 216 - CCCR	Input Identifier: 1 - Deviation of speed
3 - Ed', Eq'	21 - AC 1 22 - AC 2		2 - Deviation of terminal frequency
4 - Ed'', Eq''	23 - AC 3 24 - AC 4	221 - Hydro A 222 - Hydro B	3 - Electrical power
-1 - Induction motor	31 - ST 1 32 - ST 2 33 - ST 3 41 - SCRX 42 - SCRXIL		4 - Accelerating power 5 - Deviation of terminal voltage
	51 - 55 User - Defined	231 - 235 User - Defined	321 - 325 User - Defined

### 3.2.6 Load Representations, Network Model and Their

#### Interface with Machine Models

The simulation of various load models in the TSSP is accomplished as has been explained in Chapter 2. In order to maintain the accuracy at an acceptable level without making the computations excessive, a mechanism is designed to calculate new operating points by the fast decoupled load flow program only at instants when the configuration of the network changes. The network represented by lumped parameters is described by algebraic equations. The interface between network and machine models is accomplished by utilizing the iterative procedure of subtransient and transient saliency [14].

### 3.2.7 User-Defined Modules

If the module of a power component or a controller is not available in the TSSP, it is required to derive its transfer function. A block diagram can be built with integrators according to the transfer function. Then the block diagram can be programmed into a module. The name of the module is the name of the component, (for instance, AVR), plus the identifying number corresponding to it as given in Table 3.1. A dummy variable is required to identify the machine on which the component is installed. Other parameters for the module are passed through the input data file *mach.inp*. The detailed programming procedure is given in [3].

### 3.3 Data Files and Program Structure

Three input data files are created by copying and modifying the sample data files provided in the TSSP. Each data file consists of a number of blocks of data. In each block, data items are entered as a record in free format with a comma between items. A slash (/) signifies the end of a record. Preceding each block, there are comments and definitions specifying what data are to be entered and how. Any number of comments can be added into the files as long as a (!) precedes each comment line.

Data file *pqlf.inp* contains all the information required to perform a load flow study. Provision has been made to allow the use of different system base MVA, per unit or nominal unit system. Data file *ntwk.inp* contains fault information, sequence network parameters and branch incidence of the zero sequence network. Data file *mach.inp* contains parameters for machine,

excitation system (AVR), speed governor and turbine system (SGTS) and power system stabilizer (PSS) in four blocks. Each controller is identified in the corresponding block by its machine number. If a controller is absent from a machine, a record 888/ is entered to signify this fact.

The overall structure of the package is shown in Figure 3.1. To initialize the TSSP, the fast decoupled load flow (FDLF) is run first. Then, the short circuit calculation (STCC) program is executed. The results of the two runs are passed onto the TSSP coordinator internally. Finally, the TSSP is run. The end result of a simulation is stored in the file *simu.out*. A data sorting and plotting program (WPLOT) can be employed to plot a maximum of five curves on one screen and up to fifteen variables can be sorted out at a time. The sorted data is stored in a file specified by the user and can be further utilized by other applications.

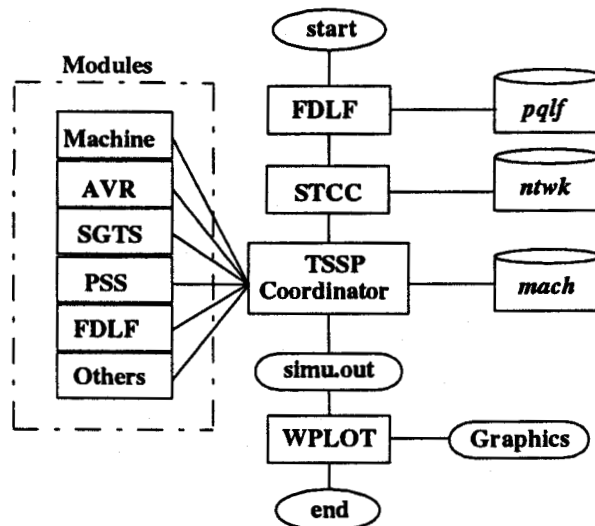


**Figure 3.1:** Overall structure of the TSSP.

### 3.4 Summary

This chapter presents a transient stability simulation package (TSSP) implemented on an IBM PC in the FORTRAN language. The structure, database and modeling aspect of the package are described.

The package consists of four parts: a fast decoupled load flow program (FDLF), a short circuit calculation program (STCC), the transient simulation main body (TSSP) including a coordinator, and a plotting program (WPLOT). Three data files are required for a complete stability study. A minimum of 410K conventional memory is required to perform a stability study for a system of 100 buses and a CGA, EGA or VGA graphics card is needed to run the WPLOT program.

A power component or a controller is simulated by its written module. Modules for commonly used power components and controllers are available in the TSSP. User-defined modules can also be incorporated into the package. The TSSP was used to perform the stability studies reported in subsequent chapters.

## **4. STEADY STATE STABILITY STUDIES OF THE ATHABASCA- POINTS NORTH POWER SYSTEM**

### **4.1 Low Frequency Oscillation and Damping**

Electromechanical oscillations of low frequency, in the order of several cycles per minute, are inherent characteristics of power systems with either longitudinal structure or weak tie-lines. The presence of such oscillations has been reported all over the world [21,22,23,24]. Of interest is that the longitudinal type of power systems seems to be more susceptible to poor damping.

Low frequency oscillations are also called system modes. Principally, there are two categories of modes: one is intertie modes associated with one group of generators or plants at one end of a tie-line oscillating against another group at the other end; the other is local modes associated with each individual generator oscillating against the rest of the system, particularly significant with weakly connected power systems or remote generating units weakly connected to a large power system. Different system modes can occur simultaneously. This coupling among modes makes it difficult to define "cause and effect" relationships in analyzing the dynamic behavior of a multimachine system, especially for intertie-line oscillations [9,25,26,27].

It is recognized that the low frequency oscillations are due to the lack of damping of the system modes. The common remedy for inadequate damping is to utilize additional excitation control by means of power system stabilizers (PSSs) [9,28]. The effectiveness of the PSSs applied to a system depends on their design and on-site tuning. Low frequency oscillations may still occur if the installed PSSs are inappropriately designed and/or tuned. This is specially true in the case that the PSSs are designed according to one-machine infinite-bus system models.

Coordinated PSSs can overcome the drawbacks that exist in PSSs designed based on the one-machine system model. Furthermore, coordinated PSSs are more efficient in providing the desired damping to suppress the low frequency oscillations. This subject is discussed in Chapter 6.

## 4.2 System Description

The system under consideration is the Athabasca - Points North power system located in northern Saskatchewan, Canada, reaching from the north-western Charlot River plant to the eastern Island Falls station along an 850 kilometer overhead line operating at 110 KV and 138 KV. A simplified geographic depiction of the system is shown in Figure 4.1 and a single-line diagram of the system showing the main generation and load buses is given in Figure 4.2. Table 4.1 shows a typical load and generation distribution according to geographic area.

There are twelve utility owned hydro generators connected at both ends of the transmission line while loads are distributed along the line. At the eastern end, the system is connected to the Manitoba Hydro system through

a rather weak tie-line. The connecting point to Manitoba Hydro system is modeled as an infinite bus. The Island Falls plant mainly feeds Flin Flon through a double circuit 95 kilometers long. At normal operation, the power transfer over the double circuit line is about 80% of the total generation of the Island Falls plant.

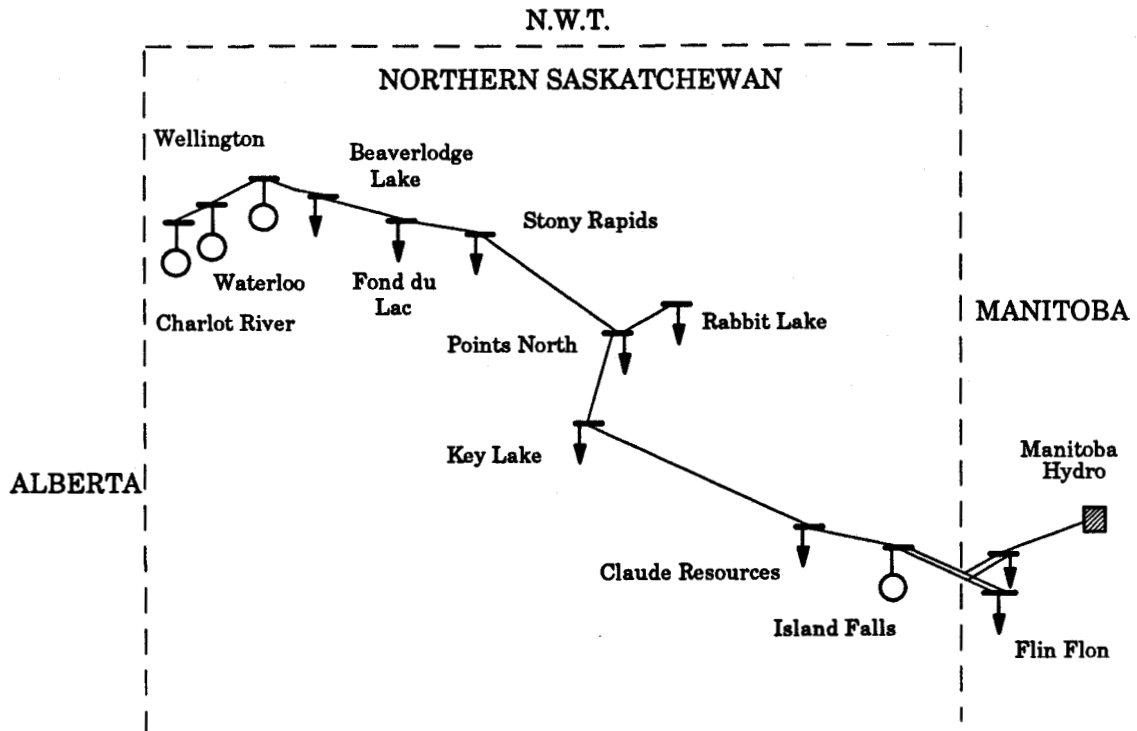


**Figure 4.1:** Geographic depiction of the Athabasca-Points North Power System.

**Table 4.1:** Load and generation distribution(MW).

Area	Load	Generation	Deficit
North	0.5	23	22.5
Center	34	0.0	-34
South	75	97	12

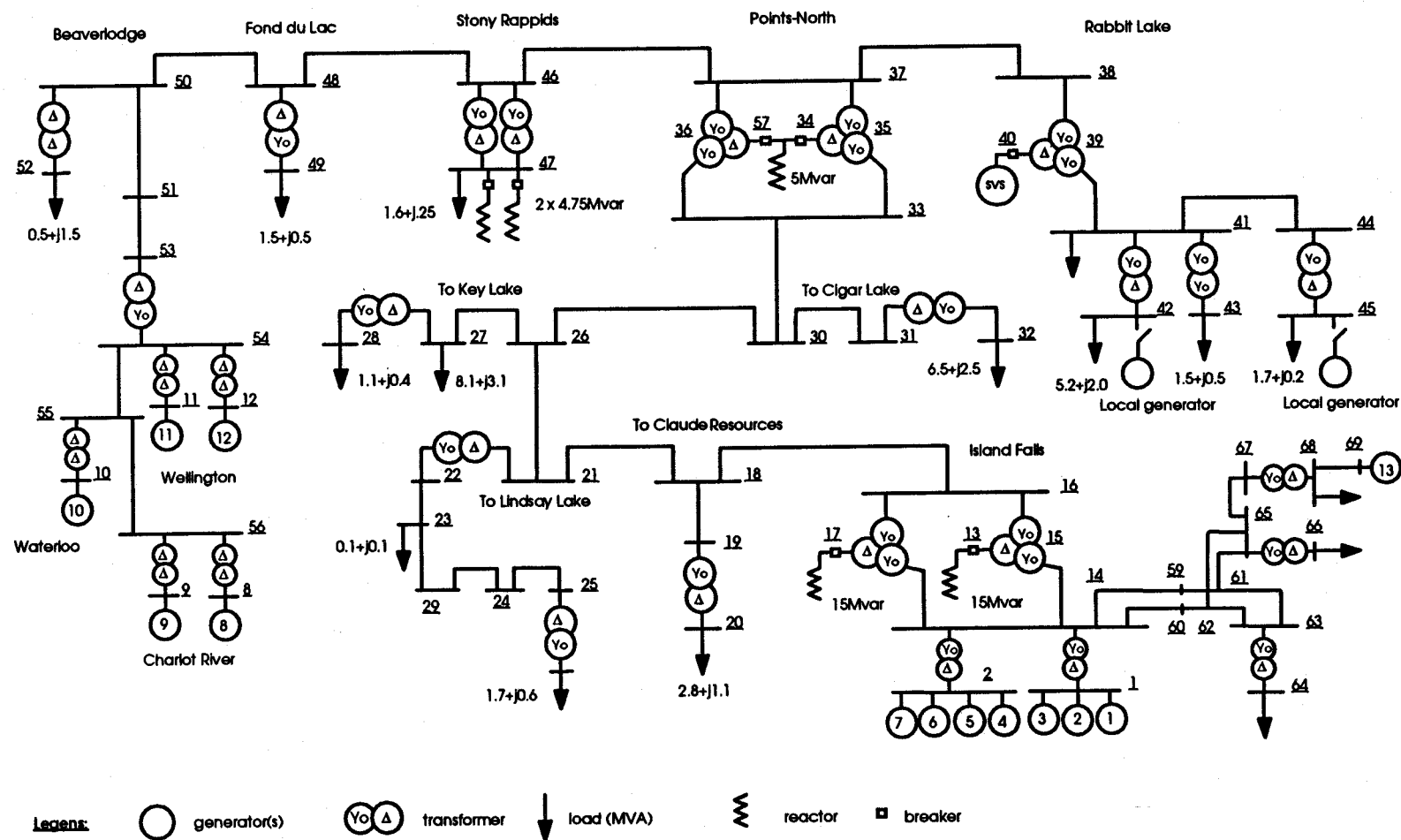


Figure 4.2: Single line diagram of the Athabasca-Points North System (APNS)

Generators #1 through #7 are equipped with bus fed static exciters and electrical power input PSSs. Generators #8 and #9 are equipped with bus fed static exciters and accelerating power input PSSs. Generators #10 to #12 are equipped with modified IEEE DC Type 2 rotating excitation.

### 4.3 Load Flow Study in Steady State

Presented in this section is a load flow study of the system under normal operating condition with off-peak demand. The fast decoupled load flow (FDLF) algorithm was employed to perform the study.

The system data used in the FDLF program is listed in Appendix A.1 in the data file named *pqlf.inp*. The following points should be noted in reading the data file *pqlf.inp*, the single-line diagram of Figure 4.2 and the load flow results given in Appendix A.2:

1. The Manitoba Hydro bus was assigned as the *slack* bus and its voltage magnitude was fixed at 1.05 per unit with a zero degree voltage angle. The voltage angles of all other buses in the system were referred to this *slack* bus. The numbering of the *slack* bus is arbitrary but in this system it was the last bus.
2. The SVC was treated as a voltage controlled bus, i.e., PV bus with injected active power being zero. The given value of the voltage magnitude will be dependent on the voltage regulation at that area of the system and the availability of reactive power the SVC can either generate or absorb. In this study, the voltage magnitude at this bus was fixed at 1.02 pu.

3. Floating buses do not require any data input. This was taken care of internally in FDLF.
4. All network parameters were referred to a 100.0 MVA base. Provision is, however, made to allow the use of a different system base MVA. All generations, loads and line powers are in nominal values (MW and MVA), though per unit values can also be used in this program. Voltage is always in per unit and voltage angle in degrees.

The detailed results of the load flow study are given in Appendix A.2. The following observations can be made from the study:

1. About seventy four percent of the total generation at Island Falls is transferred to Flin Flon. The power transfer over line 30-33 is about 1.2 MW.
2. The line charging (reactive) power accumulates along the transmission lines and flows towards Island Falls where two reactors are installed.
3. The voltage profile of the system can be summarized as follows: the voltage at the north-western area is about 1.04 per unit; the SVC at Rabbit Lake keeps the voltage in this area about 1.0 per unit; and the voltage at the southern area is also about at rated voltage of 1.0 per unit.

#### **4.4 Eigenvalue Analysis**

It is a common practice to employ eigenvalue analysis to study the nature of system modes of a power system [29,30]. A positive real part of an eigenvalue indicates a negatively damped mode; a zero real part indicates an

undamped mode; and a negative real part indicates a positively damped mode. A negatively damped or undamped mode needs to be controlled to ensure stable system operation.

It should be noted that the eigenanalysis conducted in this section and functional sensitivity studies conducted in the next section were under the assumption that no PSSs were in service. The purpose of the study was to identify the best sites for PSS installation.

#### 4.4.1 Computation of Swing Modes

Two operating conditions for eigenvalue analysis were considered: the normal operation and the operating condition where one of the double circuit lines was tripped. Table 4.2 summarizes the results, including the eigenvalues, frequencies of swing modes and their participating generators for both situations.

**Table 4.2: Eigenvalues of APNS.**

Mode No	One Line Tripped	f(Hz)	Normal Operation	f(Hz)	Participating Generators
	$\sigma, \omega$		$\sigma, \omega$		
1	0.216, 5.919	0.94	0.183, 6.102	0.97	8,9,10
2	0.246, 9.050	1.44	0.249, 9.710	1.55	1,2,3,4,5,6,7
3	0.010, 10.973	1.75	0.010, 10.895	1.73	8,9
4	-0.058, 11.298	1.80	-0.060, 11.219	1.79	12
5	-0.065, 11.840	1.88	-0.066, 11.759	1.87	11,12
6	0.157, 12.326	1.96	0.161, 12.225	1.95	7
7	-0.053, 12.380	1.97	-0.054, 12.300	1.96	10,11
8	0.094, 12.623	2.01	0.100, 12.535	2.00	1,2,3
9	0.105, 12.625	2.01	0.112, 12.536	2.00	2,3
10	0.104, 14.192	2.10	0.107, 14.106	2.09	1,2,3,4,5,6,7
11	0.079, 14.807	2.20	0.083, 14.684	2.18	4,5,6
12	0.094, 14.809	2.20	0.098, 14.687	2.18	5,6

It was found that the participating generators in each swing mode under both cases were unchanged while swing mode  $\lambda_1$  by which three remote generators oscillate, became more negatively damped with the line tripped out. One of the most negatively damped modes,  $\lambda_2$ , and one of the second most negatively damped modes,  $\lambda_{10}$ , are intertie modes, by which all the seven generators at Island Falls oscillate together against the infinite bus. The other modes are either negatively damped or poorly damped.

#### 4.4.2 Factors that Affect Damping

It is shown in the previous section that the damping of various swing modes without PSSs is quite poor. In order to achieve improvement in dynamic stability by additional excitation control, the effects of the existing automatic voltage regulators (AVR) on damping were examined. Figure 4.3 shows that the damping deteriorates when the excitation gains increase from 40% to 120%. Note that a mode that does not change with the AVR gains is not shown in the figures. Figure 4.3 also shows that modes  $\lambda_3$  and  $\lambda_4$  are barely sensitive to the changes of AVR gains while modes  $\lambda_1, \lambda_2, \lambda_6, \lambda_8$  to  $\lambda_{12}$  are sensitive. These sensitive modes involve generators #1 to #9 mainly on which PSSs are already installed.

The effects of speed governors on damping were found to be negligible as shown in Figure 4.4. This might be due to the large equivalent time constants ( $T_1 > 30s$ ) as used in the general model for hydro speed governing system and small generator capacity (18 MVA at Island Falls). The only exception is that swing mode  $\lambda_1$  is sensitive to changes of speed governors.

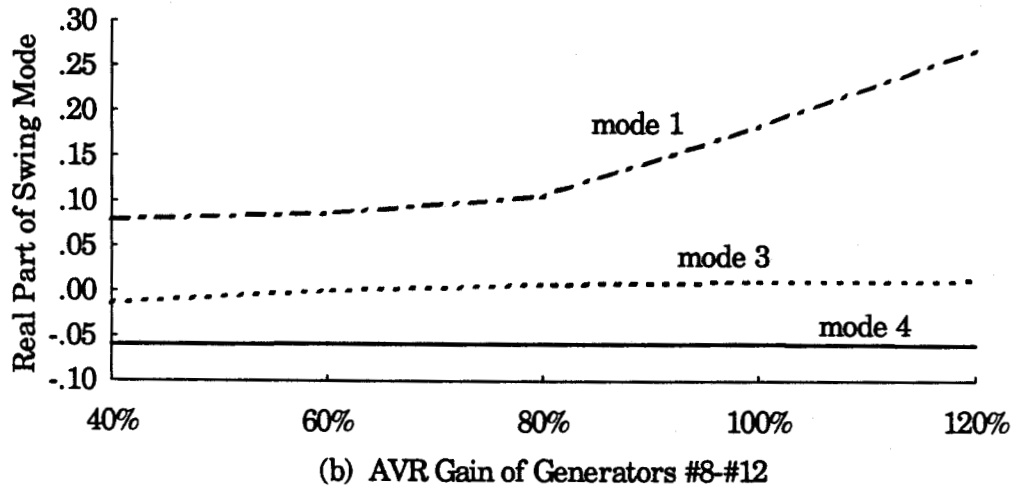
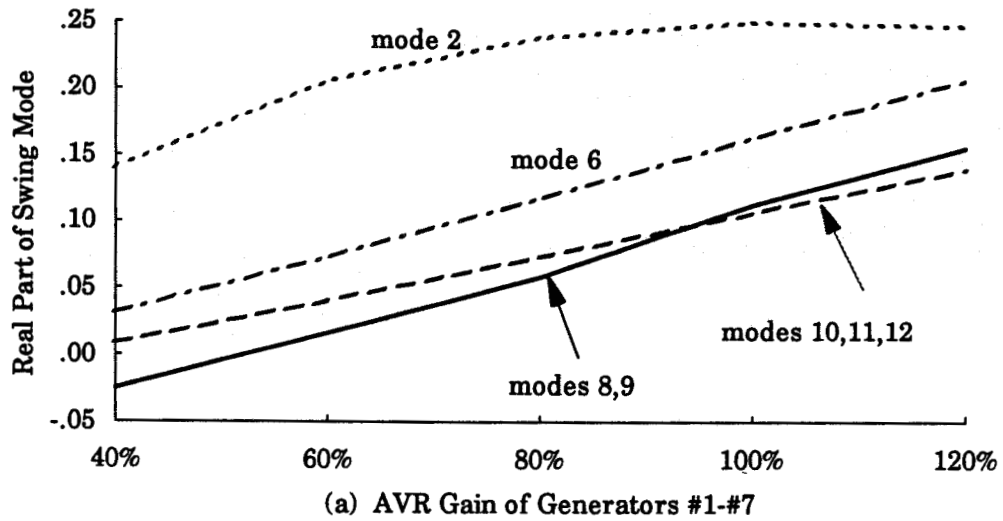


**Figure 4.3: Damping versus AVR gain**

## 4.5 Functional Sensitivity Studies

Functional sensitivity studies [31] were performed to find out what control devices affect the dynamics of the system the most. The analytical method is based on the unconventional sensitivity concept. Instead of computing the sensitivity in regard to a parameter, sensitivity in regard to a

transfer function of a control device was computed. In this manner, the overall effects of the device upon an index of interest, such as the damping of a particular swing mode, could be evaluated.

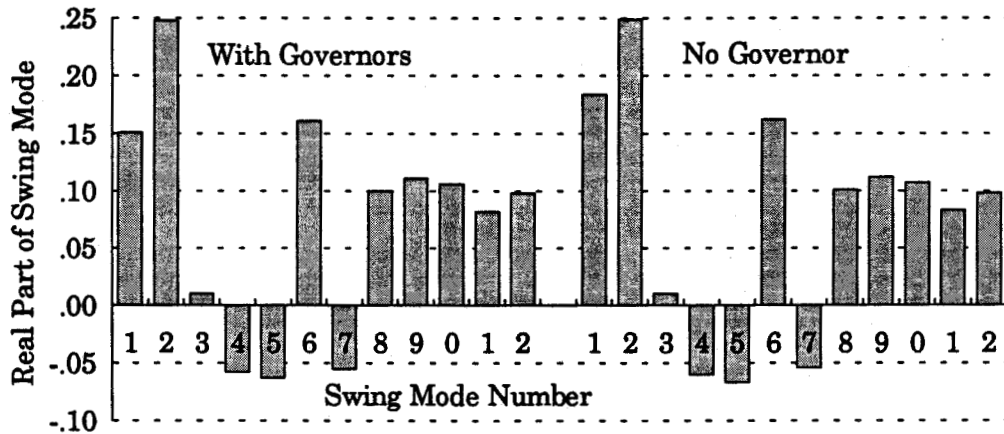


**Figure 4.4:** Damping affected by speed governor

The discussion of results follows this order: firstly, the effect of the AVR transfer functions is discussed; which identifies those swing modes that are sensitive to AVR devices; secondly, the effect of PSS transfer functions is presented, which is the basis for PSS design discussed in Chapter 6. As the effect of the speed governing and turbine system on dynamics is small, it is not discussed here.

The actual parameters of generators and excitation systems were used in computing the functional sensitivities. The objective was to find

$$\text{Sensitivity} = \frac{\partial \lambda}{\partial G(\lambda)} \Big|_{\lambda = \text{swing mode}} \quad (4.1)$$

where  $G(\lambda)$  is the transfer function of a device to be investigated. Tables 4.3 and 4.4 list the functional sensitivities of the swing modes with respect to AVR and PSS transfer functions (TF), respectively. These quantities are only valid near the vicinity of the current operating point and under the limitation that the changes of these transfer functions near the vicinity are not significantly large as compared to the changes of the system modes. However, they do provide quite accurate information for analyzing the effectiveness of existing controllers, such as AVRs, and for determining the most effective sites for PSS installation. It can be concluded from Table 4.3 that only swing modes  $\lambda_2, \lambda_6, \lambda_8$  to  $\lambda_{12}$  are sensitive to the AVR transfer function of generators #1 to #7. Swing mode  $\lambda_1$  is much more sensitive than swing modes  $\lambda_3$  and  $\lambda_4$  to the AVR transfer function of generators #10 to #12. This conclusion is also supported by the results displayed in Figure 4.3. Table 4.4 indicates how sensitive each swing mode is to various PSSs if they are installed at corresponding generators. The best PSS installation sites, as seen in the last row of Table 4.4, are decided based on the magnitude of the functional sensitivity. Usually each mode is coincident with more than one generator due to couplings among generators. To take these couplings into account, a coordinated PSS design procedure is proposed in Chapter 6 of this thesis.

It can be concluded that the results obtained and reported in this section are in agreement with the fact that the actual system is equipped with PSSs on generators #1 to #9 to provide positive damping to the various swing modes.

**Table 4.3: Swing mode sensitivity to AVR transfer function.**

Gen No	Swing Mode No											
	1	2	3	4	5	6	7	8	9	10	11	12
1	0	0	0	0	0	0.02	0	0.27	0	0.06	0	0
2	0	0	0	0	0	0.02	0	0.09	0.18	0.06	0	0
3	0	0	0	0	0	0.02	0	0.05	0.22	0.06	0	0
4	0	0	0	0	0	0	0	0	0	0.04	0.18	0
5	0	0	0	0	0	0	0	0	0	0.04	0.04	0.13
6	0	0	0	0	0	0	0	0	0	0.04	0.04	0.13
7	0	0.1	0	0	0	0.36	0	0	0	0.03	0	0
8	0	0	0.1	0.02	0	0	0	0	0	0	0	0
9	0	0	0.1	0.03	0	0	0	0	0	0	0	0
10	0.6	0	0	0	0.02	0	0.08	0	0	0	0	0
11	0.5	0	0	0	0.12	0	0.03	0	0	0	0	0
12	0.4	0	0	0.09	0.02	0	0	0	0	0	0	0

**Table 4.4: Swing mode sensitivity to PSS transfer function.**

Gen No	Swing mode No											
	1	2	3	4	5	6	7	8	9	10	11	12
1	0	0.03	0	0	0	0	0.02	0.15	0	0.03	0	0
2	0	0.03	0	0	0	0	0.02	0.05	0.11	0.03	0	0
3	0	0.03	0	0	0	0	0.02	0.03	0.13	0.03	0	0
4	0	0.02	0	0	0	0	0	0	0	0.03	0.08	0
5	0	0.02	0	0	0	0	0	0	0	0.03	0.02	0.07
6	0	0.02	0	0	0	0	0	0	0	0.03	0.02	0.07
7	0	0	0	0	0	0	0.1	0	0	0.01	0	0
8	0.05	0	0.15	0.02	0	0	0	0	0	0	0	0
9	0.05	0	0.15	0.02	0	0	0	0	0	0	0	0
10	0.04	0	0	0	0	0.03	0	0	0	0	0	0
11	0.03	0	0	0	0.05	0.02	0	0	0	0	0	0
12	0.03	0	0	0.04	0.02	0	0	0	0	0	0	0
PSS	10		8,9	12	11		7	1	2,3	0	4	5,6

## 4.6 Time Domain Simulation

Sustained low frequency oscillations are present and observed under small disturbances. For studying the response of the APNS under such a disturbance, it was assumed that a load increase of 1% of the total system capacity took place at Rabbit Lake. Figure 4.5 shows the resulting generator

rotor angle oscillations of generators #1 and #8 at Island Falls and Charlot River plants, respectively.

It can be seen from Figure 4.5 that generators #1 and #8 oscillate in opposition to each other. The reason is that as the electrical distance from generator #8 to the location of the disturbance is twice of that from generator #1, the terminal voltage at Island Falls drops more and generator #1 begins to accelerate. On the other hand, generator #8 begins to generate more power to balance the sudden increase of load. All other generators at Island Falls behave similar to generator #1 and the generators at the northern end behave similar to generator #8.

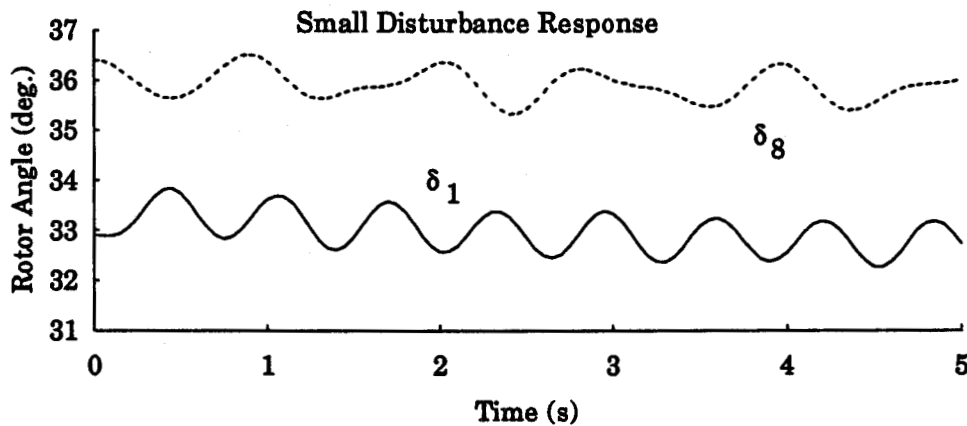


**Figure 4.5:** Rotor angle response to 1% load increase at Rabbit Lake.

## 4.7 Summary

In this chapter, an introduction is given to the problem of steady state stability, i.e., low frequency oscillation and damping. It is understood that the desired additional damping can be provided by the application of power

system stabilizers. Then, the description of the system studied in this thesis is given. A load flow study was performed for an off-peak condition. The steady state stability studies of the system were conducted by eigenvalue analysis and sensitivity study technique. The results of these studies are interpreted to obtain the best sites for installing power system stabilizers to provide positive damping. The time response of the system to a small disturbance is presented to demonstrate that more damping is desirable to improve the steady state stability of the system.

## **5. TRANSIENT STABILITY STUDIES OF THE ATHABASCA- POINTS NORTH POWER SYSTEM**

### **5.1 Introduction**

Transient stability of a power system is the stability of the system with respect to large disturbances, such as, short circuit, tripping of a transmission line or generating sets. The final operating condition may be quite different from the pre-disturbance operating condition due to alternations made to the configuration of the system. If there is a loss of synchronism of one or more generating sets, the system is transiently unstable.

Transient stability involves both the configuration of the system and its operating condition. It is, therefore, necessary to define the pre-disturbance operating condition and to completely specify the disturbance for studying the transient behavior of the system.

The investigations reported in this chapter were based on the system configuration of Figure 4.2 with all the existing controllers being present. However, load flow conditions may be changed for stability simulations under various situations. The purposes of these investigations were to:

1. evaluate the most severe disturbances the system could withstand;

2. determine the critical clearing times for different disturbances to be used as guide lines in designing protection schemes; and
3. define possible corrective measures to be applied in the system to prevent loss of synchronism.

In order to facilitate the analysis and presentation of simulated results of a stability study of a large power system, generators in the system can be grouped according to their coherency [32]. The dynamic behavior of the generators in a coherent group is assumed to be similar. The total coupling factors [33] can be utilized in this grouping process. Instead of analyzing all the generators in the system, a representative generator is selected from each coherent group and its dynamic behavior is studied.

This coherent grouping process is covered in more detail in Chapter 6. The results are quoted here for the convenience of presenting the simulation studies in this chapter. There are seven generators at Island Falls. Generators #1, #2, #3 and #7 were in group one. Generators #4, #5 and #6 were in group two. Generators #8 and #9 were in group three. Generators #10, #11 and #12 were in the last group. Generators in the last group do not have stabilizers and slight differences between their controllers also exist. Their rated capacities are also quite different, however, they behave in the very similar ways.

One or more representative generators from each group are selected each time when computed results are presented. It should be noted that the presented results are still identified by generator numbers, not by group numbers. It is not always necessary to have all the representatives being selected in a single result presentation.

## 5.2 Operating Procedure of APNS

As the APNS was interconnected from two smaller systems, i.e., the Athabasca System and the Points-North System, at the Points-North switching station, and due to the special arrangement of the circuit breakers in the system as seen from Figure 5.1, the stability of the system following a large disturbance depends on how much power is being transferred through the tie-line between the two systems, i.e., line 30-33 in Figure 4.2, and where the disturbance is located.

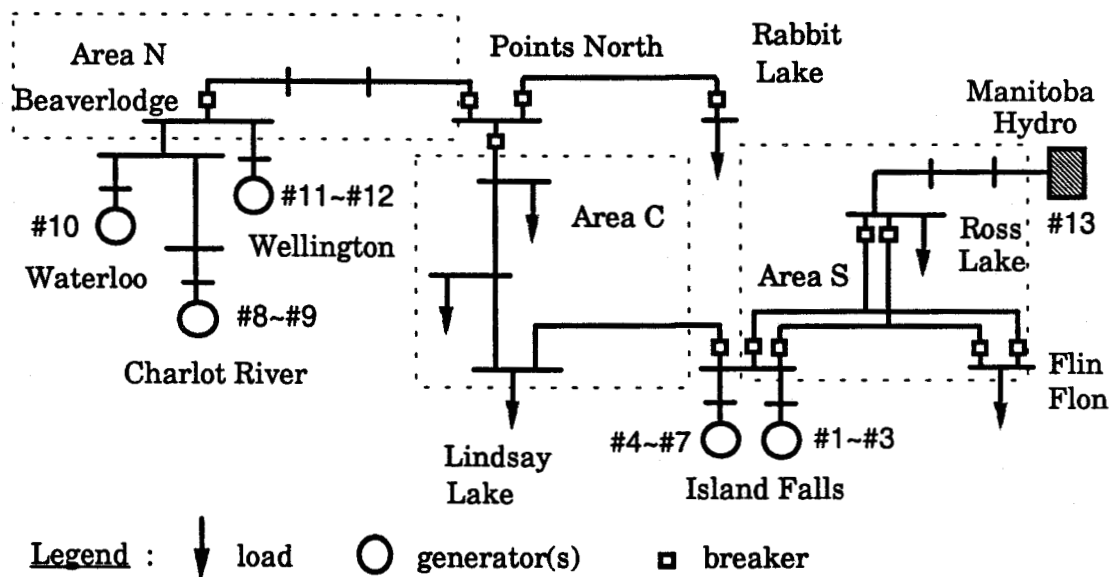


**Figure 5.1:** Simplified single line diagram of the APNS.

For instance, if a disturbance is located on the transmission line from Island Falls to Points-North, the circuit breakers at both ends of the line will trip to isolate it. In this case, if there is only a small power transfer over the

line 30-33, the Athabasca System and part of the Points-North System can be saved following the disturbance.

If a disturbance is located on the transmission line from Points-North to Beaverlodge, the five remote hydro generators in the Athabasca System will pull out of synchronism as the line trips out. On the other hand, the load at Rabbit Lake will be supplied from Island Falls plant.

A disturbance on one of the double circuit lines from Island Falls to Flin Flon will trip off that faulted line and bring the power transfer on the other line to the upper limit of its transfer capacity.

### **5.3 Parameters of Power Components and Controllers**

As explained in Chapter 3, parameters of power components and controllers are passed to the TSSP coordinator through data files in transient stability studies. These parameters include the following categories: machine data, excitation system data, speed governing and turbine system data and power system stabilizer data. For the APNS, these data were generously provided by the SaskPower. This section denotes some important points worth noting for easy reading of and referring to the system data provided in the form of data file in Appendices A, B and C. Detailed description of the data files is given in the TSSP users manual [3]. Please note that all the symbols used here are universal and self-explanatory. A complete list of these symbols can be found at the beginning of this thesis.

### 5.3.1 Machine Data

The required data for machine modeling are in a form commonly found in manufacture's data sheets. If a generator is modeled by a *two axis model with subtransient*, the following data records are entered.

*Generator #, Model #*

$M_{base}, H, r_a, x_t$

$x_d, \dot{x}_d, \ddot{x}_d, x_q, \ddot{x}_q$

$\tau_{do}, \tau_{do}', \tau_{qo}$

$D, S_{1.0}, S_{1.2}, -1 / \text{ or } D, A_G, B_G$

If the generator is modeled by an *one axis model with transient*, the data records entered are similar to the above. Those items with a double prime ("") are not entered. For an infinite bus modeled as a large generator, only the generator number, model number (#0) and a system capacity (100 MVA, for instance) are entered. At the end of each data record, a slash (/) is placed to end the record.

Saturation is approximated by an exponential function (see Appendix E). Alternatively, the two constants,  $A_G$  and  $B_G$ , can be used in the function or the saturation at terminal voltage 1.0 and 1.2 pu,  $S_{1.0}$  and  $S_{1.2}$ , respectively, can be used to compute the two constants by placing a '-1' option in the data record.

The format of data input for the three generator models discussed above was used in the studies reported in this thesis. Other machine models, i.e., *two axis model with transient only* and *one axis model*, are also available in the TSSP, as has been explained in Chapter 3.

### 5.3.2 Excitation System Data

For each excitation system model, a model number is assigned to identify it. The assigned numbers are shown in Table 3.1. The input data record follows a format similar to that in the machine data input. As an example, the data records for a modified DC type 2 excitation system are:

*Exciter #, Model #*  
 $K_A, K_E, K_F$   
 $T_C, T_B, T_A, T_E, T_F$   
 $V_{MIN}, V_{MAX}$   
 $A_E, B_E / \text{or } E_1, S_1, E_2, S_2, -1$

Saturation of an excitation system is treated in a fashion similar to that of a generator (see Appendix E).

### 5.3.3 Speed Governing and Turbine System Data

As has been explained in Chapter 2, all six steam turbine systems and their speed governor models recommended by IEEE [6] are available in TSSP. As they are not used in this study, they are not covered in detail here. The speed governor and turbine system for hydro generators can be simulated by two models, the detailed model and the simplified one. Both models were used in the studies reported in this thesis. As an example, the data records to be entered for the simplified model of a hydro generator's speed governing and turbine system is of the following format:

*Generator #, Model #*  
 $T_W, T_1, T_2, T_3$

$$K$$

$$P_{MIN}, P_{MAX}$$

### 5.3.4 Power System Stabilizer Data

The IEEE standard PSS model [5] and two other SaskPower PSS models identified as IEEEESN and IEEEEST are incorporated in TSSP and were used in the studies reported in this thesis. Presented below are the data records for IEEEEST PSS, where 1,2,3 or 4 are identifiers of the input signals: speed deviation, terminal voltage deviation, electrical power or accelerating power, respectively.  $A_1$  is the time constant of the filter of the PSS with power input. The function of the filter here is to block torsional interaction.

*Stabilizer #, Model #*

*1,2,3 or 4*

$A_1$

$T_1, T_2, T_3, T_4, T_5, T_6$

$K_S, P_{MIN}, P_{MAX}$

Data records for IEEEESN PSS and IEEE standard PSS are similar to those of IEEEEST PSS. Exact records to be entered for each of these models are given in [3]. Table 3.1 of Chapter 3 shows the available PSS models and their assigned identifying numbers used in TSSP data file.

## 5.4 Transient Stability Studies

As has been explained in Section 5.2, any fault that initiates trips on the transmission line from Island Falls to the northern end will separate the

system into two or more parts, while a fault on one of the double circuit lines will trip that circuit, leaving the integrity of the system intact. The overall system stability is dependent on the disturbance under study. Therefore, the investigations reported in this section were conducted according to the location of a fault. In order to facilitate reference, the system was divided into three geographical areas as shown in Figure 5.1. The northern area is abbreviated as Area N, the central area as Area C and the southern area as Area S.

If a fault is located in Area N, that area will be lost after the fault clearing. The objective is to examine whether Area C and Area S will be stable or not. If a fault is located in area C, the stabilities of Area N and Area S are investigated. If a fault is located in Area S, the integrity of the system will be intact and the overall stability is studied.

#### **5.4.1 Disturbances in Different Geographic Areas**

##### **1. Fault in Area N**

It was assumed that there was a three phase to ground (3LG) fault on the line from Points North to Stony Rapids (line 37-46 near bus 37 in Figure 4.2). The fault was cleared by opening the circuit breakers of the line after 6 cycles. As there was no autoreclosure, Area N was lost after fault clearing. All the rest of the system was supplied by Island Falls plant. Figure 5.2 shows that generators #8 and #10 were accelerating while generators #1 and #4 displayed small oscillations. Each generator represents the group it belongs to.

It can be concluded that groups 3 and 4 would pull out of synchronism and Area N would be lost. The generators at Island Falls would supply the loads in both Areas C and S.

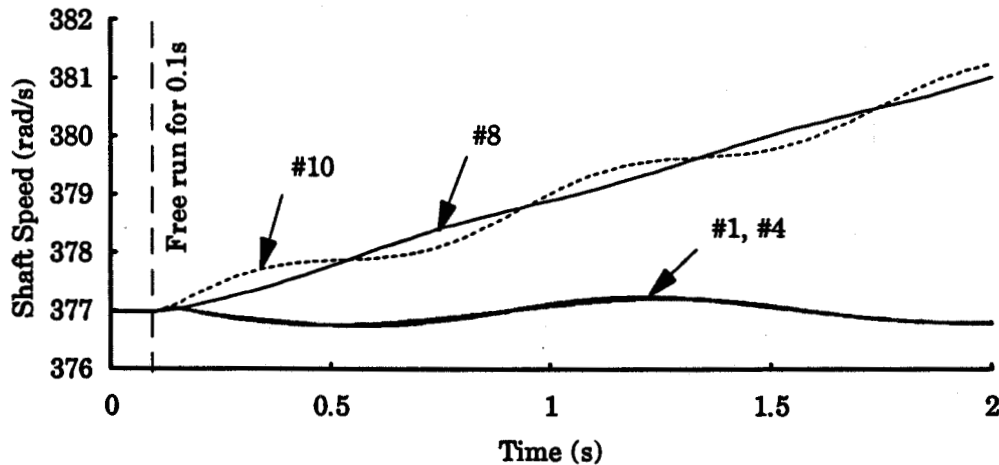


**Figure 5.2:** Machine shaft speed versus time. 3LG fault near Points North. Generators in Area N pull out of synchronism.

## 2. Fault in Area C

A fault on the main transmission line in Area C would separate the system into three parts. The center area would be lost. The stability of the other two areas would depend on the operating condition at the time of disturbance. It was assumed that there was a 3LG on the line from Island Falls substation to Lindsay Lake (line 18-21 nearby bus 18 in Figure 4.2) for a duration of 6 cycles. The fault was cleared by opening the line. Figure 5.3 shows the speed response of two typical generators. In fact, all the generators in groups 3 and 4 would behave the same way as generator #8 that was

decelerating and eventually would pull out of synchronism. The generators at Island Falls would oscillate severely. This was because the fault was close to the terminal of the generators at this plant.

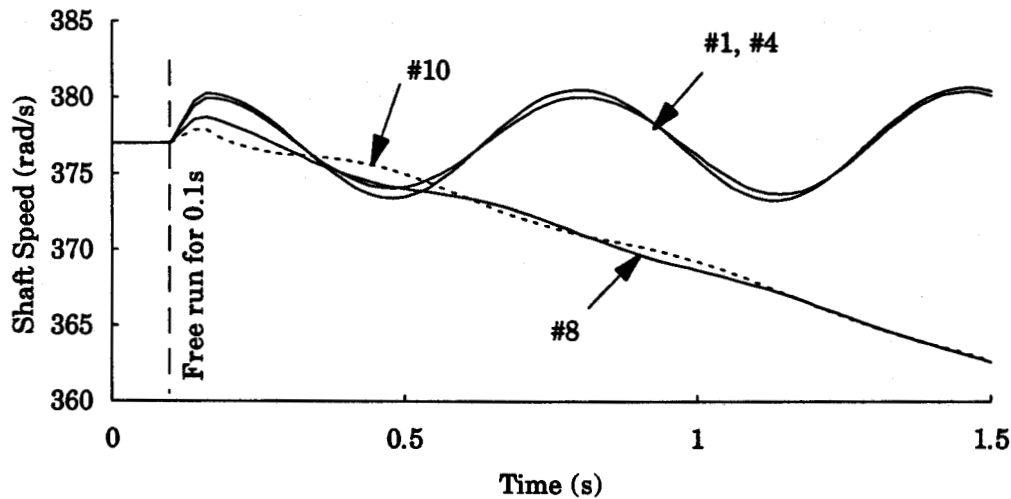


**Figure 5.3:** Machine shaft speed versus time. 3LG fault near Island Falls. Generators in Area N would pull out of synchronism.

### 3. Fault in Area S

Any fault in Area S is of the most concern. This is because eighty percent of the generated power at Island Falls is transferred through the double circuit line to Flin Flon of Manitoba Hydro. A fault that trips one of the double circuit lines would bring the power transfer of the other line to its maximum. A three phase autoreclosure device is available and is set to reclose after 10 seconds of dead line.

Case I: Suppose that there was a single phase to ground (SLG) fault on line 59-61 for a period of 6 cycles. It was cleared by opening the 3 phases of the faulted line. Reclosure was started in 10s after fault clearing. Figure 5.4 shows typical rotor angle oscillations. It can be concluded that the system would be oscillatorily stable. This oscillation may be due to lack of damping and the ineffectiveness of the PSSs at Island Falls. Figure 5.5 shows that the PSS outputs at Island Falls were trivial. A disturbance more serious than the SLG fault studied above would display similar but more severe oscillations.

Voltage responses resulting from the SLG fault are shown in Figures 5.6 and 5.7. As generators #1 to #9 were equipped with fast excitation systems (AVRs), the generator terminal voltage recovered quickly. The field voltage of generators #1 and #4 exhibited changes during the pre-fault period. This was because of the electrical power input PSSs that are always functioning as long as there is generated power output. This field voltage change under normal operation would cause fluctuation of the terminal voltage.

The mechanical power response of hydro generators is usually slow, as illustrated in Figure 5.8. Simulations show that for the SLG fault, the mechanical power is almost unchanged. Further analysis of the speed governing and turbine system is reported in Chapter 6. The electrical power was oscillating due to lacking of damping.

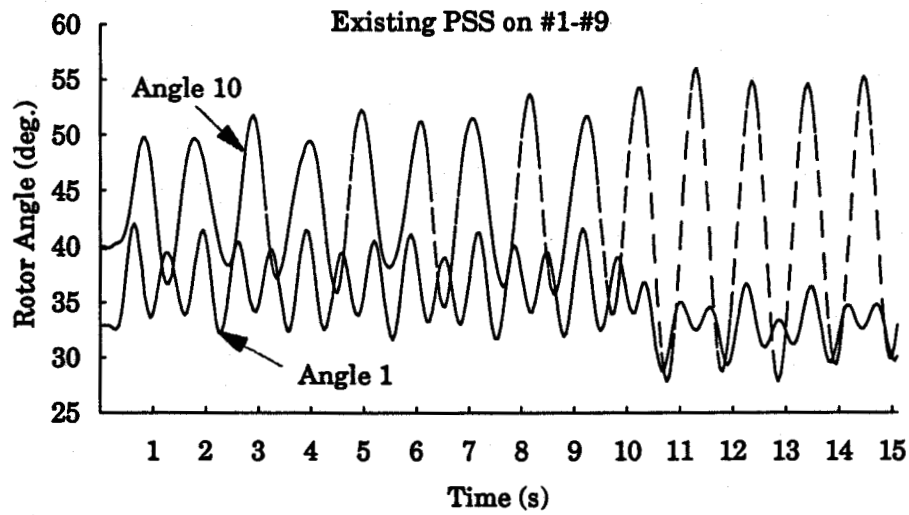


**Figure 5.4:** Rotor angle swings of generators #1 and #10 under the SLG fault. Reclosure in 10s of dead line.

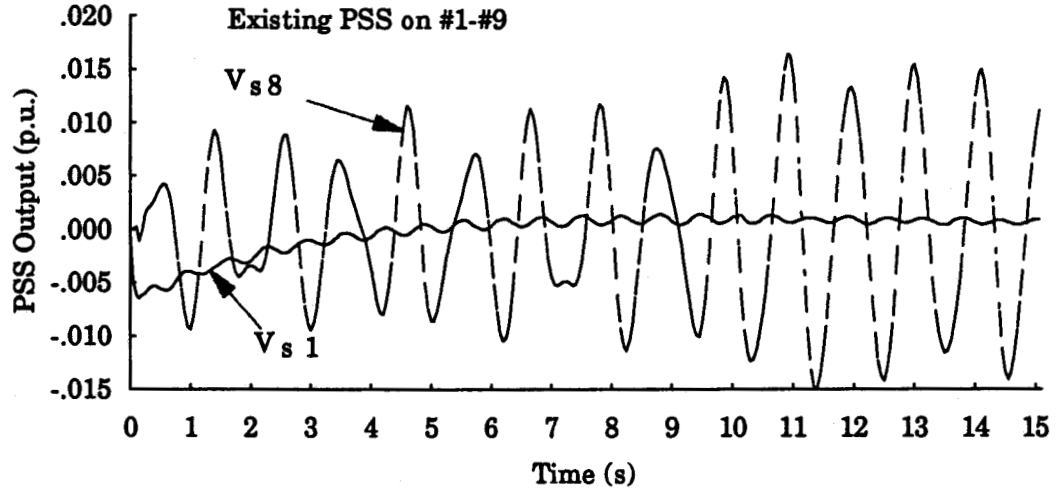


**Figure 5.5:** PSS output voltages of generators #1 and #8 under the SLG fault. Reclosure in 10s of dead line.

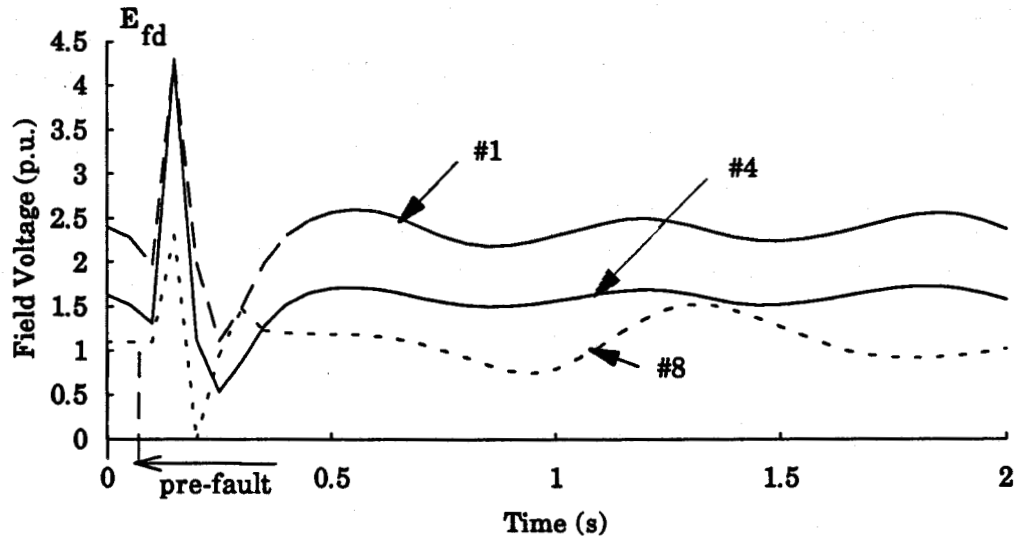


**Figure 5.6:** Field voltage versus time. SLG fault on the double circuit line.

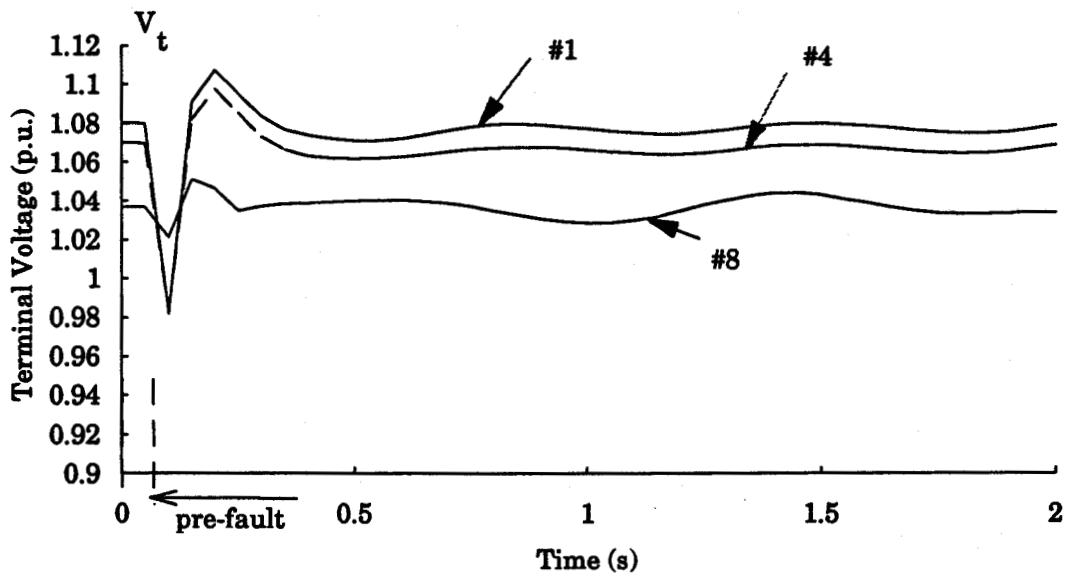


**Figure 5.7:** Terminal voltage versus time. SLG fault on the double circuit line.

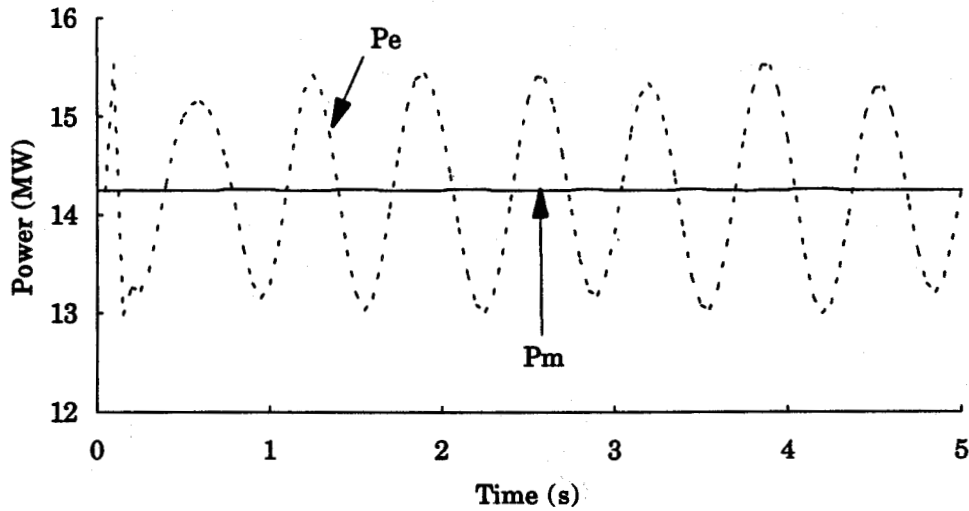


**Figure 5.8:** Mechanical and electrical power responses of generator #5 to the SLG fault.

Case II: Suppose that a three phase to ground (3LG) fault occurs on one of the double circuit lines. It is cleared after 6 cycles. Reclosure is initiated 10 seconds after clearing the fault. Figures 5.9(a) and 5.9(b) show the rotor angle oscillation of generators #1 and #10, respectively. Generator #1 represents the generators from the southern area while generator #10 represents the generators from the northern area. Comparing to Figure 5.4, we can conclude that the oscillations of the generators in the system are much more severe and that the fault has a larger impact on generator #1 at Island Falls as it is closer to the fault. The system is oscillatorily stable but it takes the oscillations a long time to settle down.

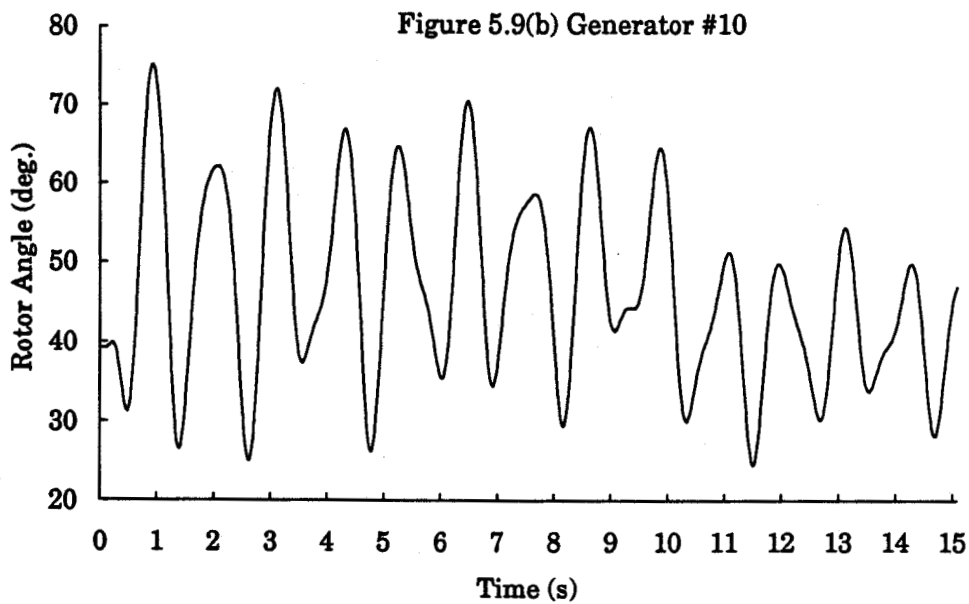
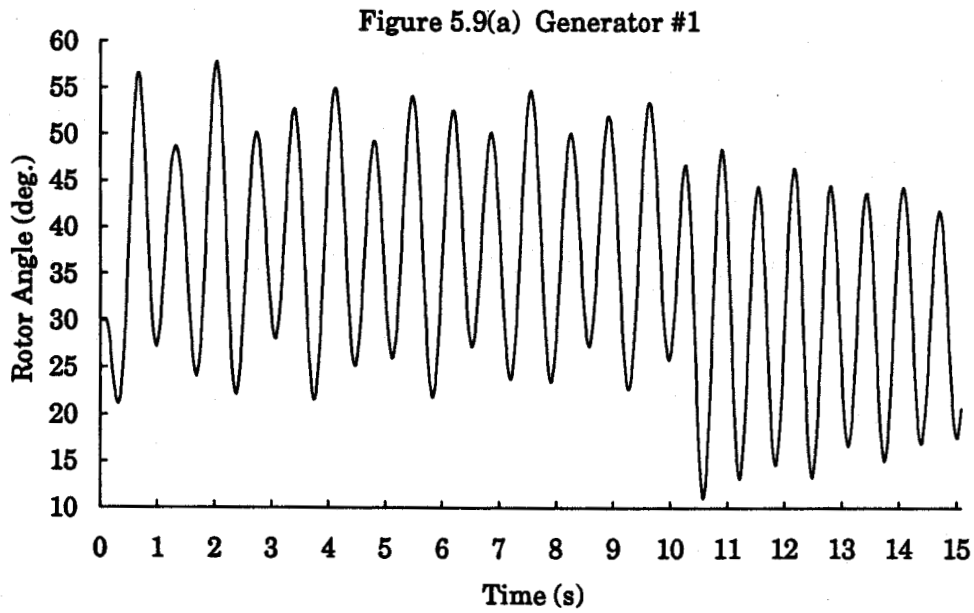


**Figure 5.9:** Rotor angle swings of generators #1 and #10 under the 3LG fault. Reclosure in 10s of dead line.

### 5.4.2 The Largest Load Area Is Lost

The main demand in the Athabasca System is located in the Rabbit Lake area. Suppose that there was a three phase to ground (3LG) fault on the line between Points North and Rabbit Lake near Points North ( line 37-38 near bus 37). The fault was cleared in 2.3s without reclosure. The following observations can be made from time domain simulations.

1. The study showed that when all the loads in this area were cut off after a fault on the line, the system would remain stable with a critical clearing time (CCT) being equal to 2.3 seconds and would be operating at another equilibrium point.
2. More power would be sent to Manitoba-Hydro system through the double circuit lines as shown Figure 5.10.

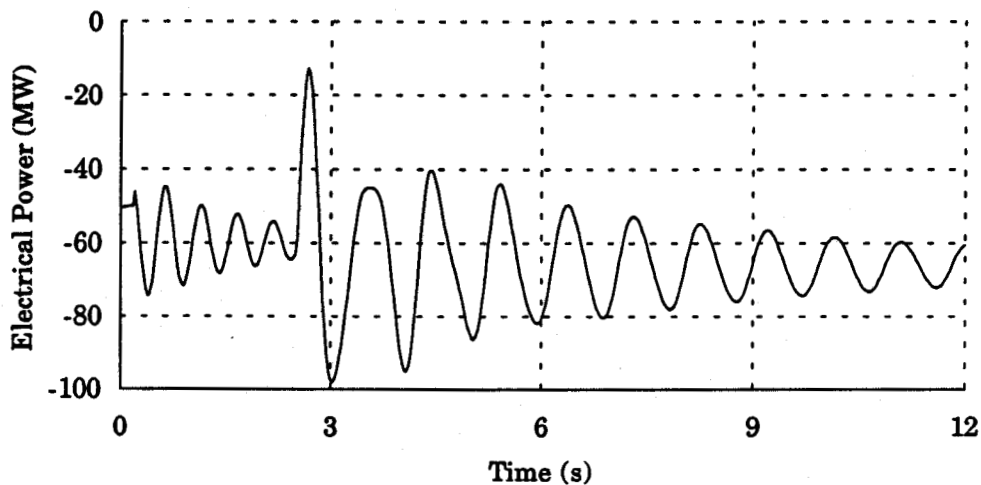


**Figure 5.10:** Transferred real power from Manitoba Hydro to this system. 3LG fault at bus 37 for 2.3s.

### 5.4.3 Balanced and Unbalanced Disturbances

#### 1. Effect of Autoreclosure on Stability under 3 $\phi$ Fault

Suppose that there was a three phase to ground fault (3LG) near Lindsay Lake on the line between Lindsay Lake and Key Lake ( line 21-26) for 6 cycles. Comparison was made between two situations where autoreclosure is either available or unavailable. Figure 5.11 shows the results obtained.

- 1). Figure 5.11 shows that the system would be unstable if no autoreclosure were initiated after the fault clearing by opening the line. It shows that the rotor angle of generator #8 would go to negative infinity. Generators #9 through #12 would behave in a similar fashion.
- 2). Autoreclosure might not be successful if it passed the dead time of 0.4 second. Simulation shows that the system would become unstable if the dead time were set to be 0.41 seconds.
- 3). If the critical clearing time (CCT) changes, the dead time would also change, but not significantly.

#### 2. Effect of Autoreclosure on Stability under 1 $\phi$ Fault

Case I: Suppose that there was a single phase to ground (SLG) fault on the line between Stony Rapids and Points-North near Points-North (line 37-46 near bus 37). The fault was cleared by opening the faulted phase of the line in 2 seconds. Two simulations were performed with and without reclosure, respectively, as shown in Figure 5.12.

the line in 2 seconds. Two simulations were performed with and without reclosure, respectively, as shown in Figure 5.12.

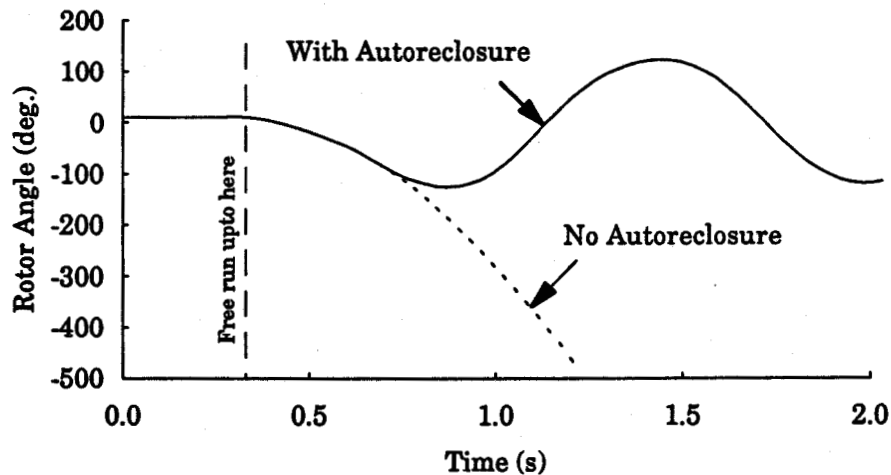


**Figure 5.11:** Rotor angle of generator #8. 3LG fault at bus 21 for 0.1s with and without autoreclosure.

- 1). The system would still be stable even the CCT is 2s. This indicated that the system could be operating for a longer time with only two phases connected between bus 46 and bus 37 without distorting the stability of the system.
- 2). Figure 5.12 also shows the situation where autoreclosure is initiated 0.4s after the fault clearing. It can be seen that autoreclosure could greatly quicken the stabilizing process of the system.

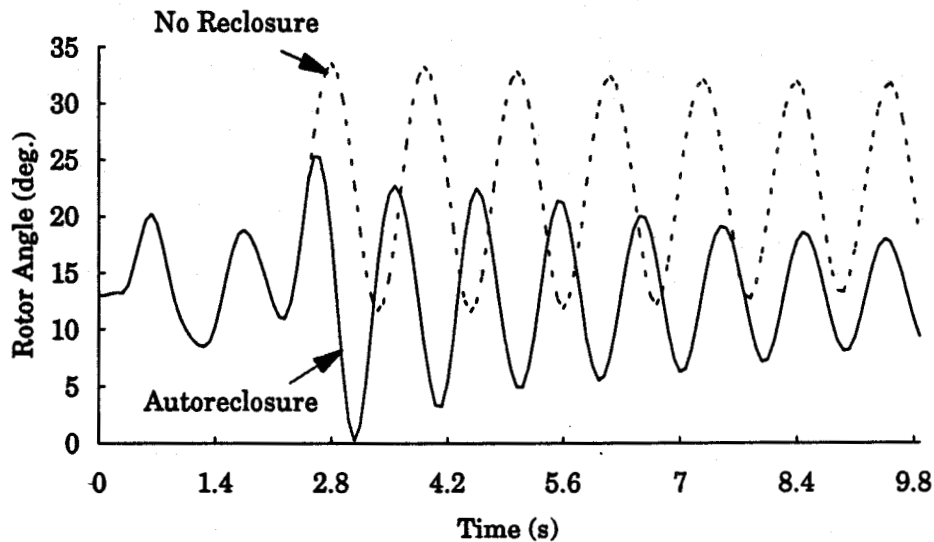


**Figure 5.12:** Rotor angle of generator #8. SLG fault at bus 37 for 2s with and without reclosure.

- 3). The system would be operating at a new equilibrium point if there were no autoreclosure to restore the system configuration after the fault. Single phase fault clearing by opening that phase is equivalent to increasing the impedance of the transmission line.

Case II: Suppose that a single phase to ground (SLG) fault appeared on the line from Lindsay Lake Tap to Key Lake Tap (line 21-26). The fault was cleared in 6 cycles (0.1s) by opening the faulted phase. Simulated results are presented in Figure 5.13.

- 1). The system would be oscillatory after the single phase fault was cleared in 1.0s without reclosure.

- 2). If reclosure was initiated 0.4s after the fault clearing, it would accelerate the restoration of system stability.

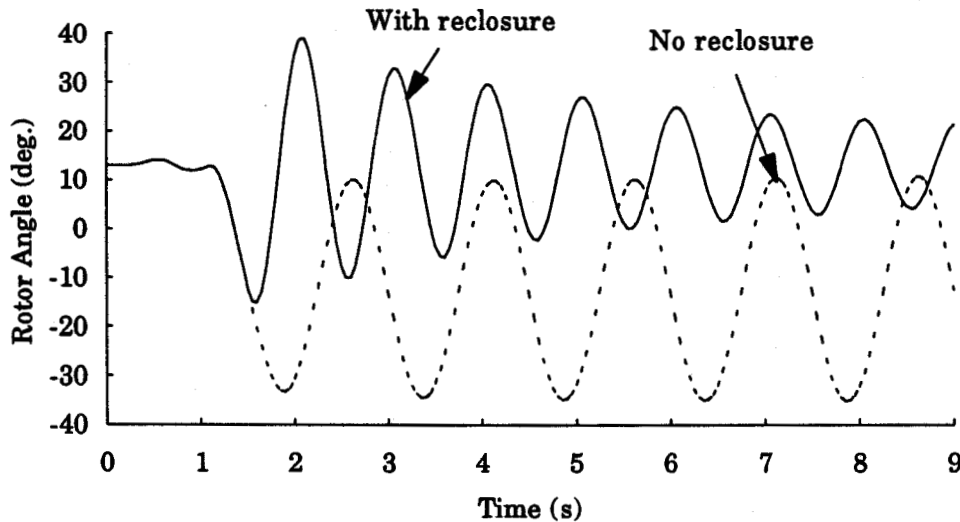


**Figure 5.13:** Rotor angle swing of generator #8. SLG fault at bus 21 with and without reclosure.

## 5.5 Summary

Presented in this chapter are the transient stability simulations of the Athabasca-Points North power system under different types of disturbances at different locations.

Three-phase-to-ground balanced faults represent the most severe disturbances and were investigated in greater detail. It was found that three phase faults on the main transmission lines from Island Falls to the northern end of the system would cause instability. Autoreclosure could prevent instability if it could be applied in a timely fashion.

Single-phase-to-ground faults have the highest frequency of happening in a practical power system. Simulations for this system have shown that no severe instability has been observed if the fault can be cleared by opening only that faulted phase in a time delay of normal protection, allowing two phases to be in service for a time period. Autoreclosure could greatly accelerate the process of stability restoration.

## **6. STABILIZATION OF THE APNS BY COORDINATED POWER SYSTEM STABILIZERS**

### **6.1 Introduction**

Control laws utilized to achieve stability enhancement can be divided into two classes: continuous and non-continuous. Continuous control methods are the primary controls, i.e., controls by speed governor, excitation system and power system stabilizer. They are very well understood and documented [27,28,29]. More detailed investigation of their applications in the APNS is reported in this chapter.

Non-continuous control methods are corrective remedies used to achieve stable operations without expensive network reinforcement. These corrective measures are called discrete supplementary controls. There are several such control schemes [34] and each can provide a particular control effect. For a specific application in a practical power system, not all of them can be employed. As far as the APNS is concerned, only hydro plants exist and they are far away from the load center. The total generation capacity is small and the operating voltage is not high. Reinforcement of the very long transmission lines is costly and is unrealistic. Load flow studies reported in Chapter 4 indicate that a large power imbalance exists in all the three geographically divided areas. Taking all these factors into account, the following two corrective measures may be considered as appropriate to be

employed in the APNS to improve its overall system stability: (a) generator tripping and (b) load shedding.

An appropriate application of these two methods must meet the practical requirement of the system operation and customers' demands. As this information is not available to the author at this moment, only continuous control methods were considered in the study reported in this thesis.

As shown in Chapter 4, the common practice to provide positive damping through excitation control is to use PSSs. Usually, the system modes must be known in PSS design. It is also generally true that the damping (real part) of a system mode is more sensitive to operating conditions than the frequency (imaginary part) of that mode. Reduction of these sensitivities of a mode increases the robustness of the PSS designed based on this mode. In this thesis, instead of using a specific frequency for a particular PSS design, an average frequency is derived for each coherent group of generators that oscillate together. The coherent generation groups can be identified by available methods [32]. Another parameter needed in tuning the PSS is a lead/lag time constant spread [25,26]. Nonlinear simulation is utilized to determine the optimum gain of each PSS. The last step is to coordinate the application of the designed PSSs. Input signals to all the PSSs in each coherent generation group are to be communicated with each other between two strongly coupled generators. The total coupling factors [33] computed from eigenanalysis are employed to take into account these interactions among generators.

## 6.2 Effect of Existing Primary Controls

The effect of the automatic voltage regulator (AVR) on dynamic stability has been discussed in Chapter 4 by eigenvalue analysis and computing parametric and functional sensitivities. There the effects of speed governors and power system stabilizers have been intentionally neglected as their effects are small. These observations are further illustrated in this section by time simulation under a specific disturbance.

### 6.2.1 AVR Effect

In order to illustrate the effect of the AVR, it was chosen to fix all other parameters of the available controllers in the system and change only the AVR gain and its time constant, respectively.

Time domain simulations for three situations were carried out. Specifically, they are:

- a). when the gain  $K_A$  of each AVR was set to be 0.001, i.e., the AVR is disabled;
- b). when the gain  $K_A$  of each AVR was set to be its existing value; and
- c). when the time constant  $T_A$  of the regulator of each AVR was set to be a large value, i.e., 10 seconds.

Figures 6.1 and 6.2 show typical responses of the rotor angle and terminal voltage of generator #8 for each of the three situations. The following observations can be made:

- 1). When the time constant of the AVR is large, the oscillation of the rotor angle is better damped, as per Figure 6.1.
- 2). When the AVRs are disabled by setting their gains very small, the terminal voltage can be quickly restored to normal value after the fault clearing, while the oscillation of the rotor angle is much more severe, especially the first swing, as per Figures 6.1 and 6.2. This is because that the field voltage of the machine does not increase and therefore the output electrical power can not be raised. Hence the net accelerating power is large.

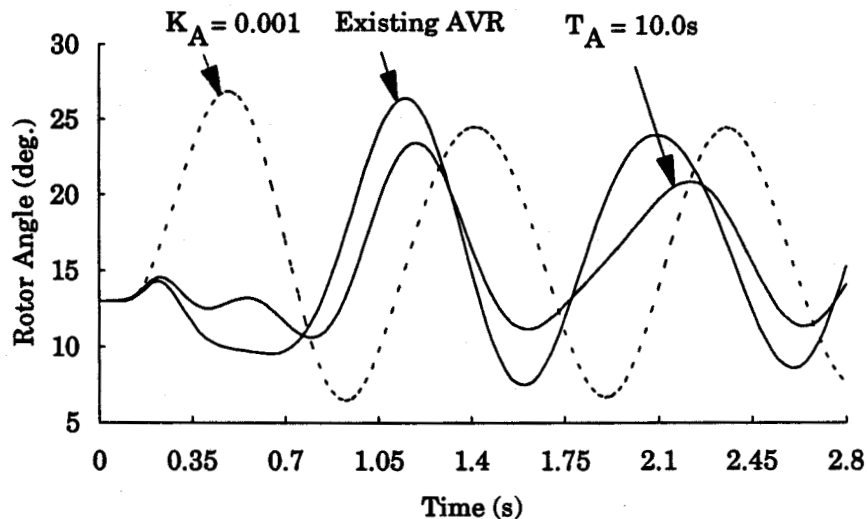


**Figure 6.1:** Rotor angle plotting of generator #8 under 3 $\phi$  fault at bus 30.

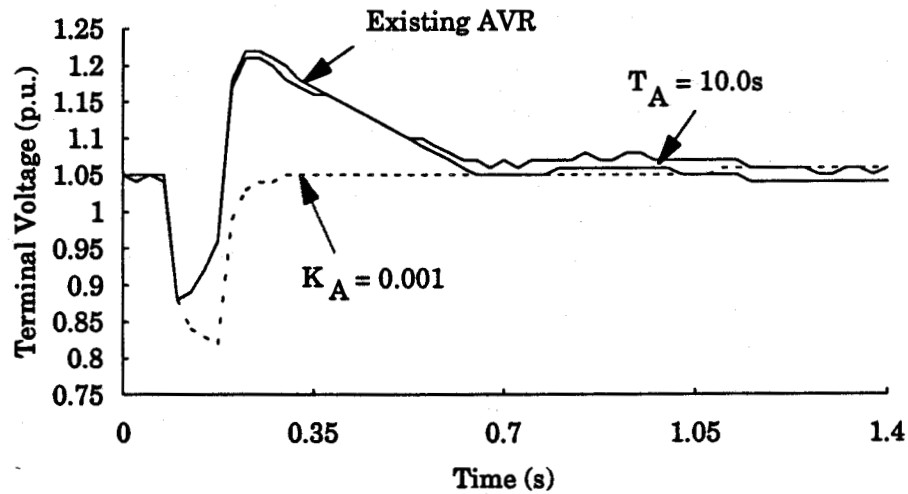


**Figure 6.2:** Terminal voltage plotting of generator #8 under 3 $\phi$  fault at bus 30.

### 6.2.2 Speed Governor Effect

As explained in Chapter 2, the speed governing and turbine system (SGTS) of a hydro generator can be simulated by either the accurate model or the approximate model.

In the APNS, the SGTS for generators #8 to #12 was simulated by the accurate model. The various parameters used in the model are in their normal ranges. The SGTS for generators #1 to #7 was simulated by the simplified model. The time constant  $T_1$  of generator #1 to #3 is 33.15 seconds and that of generators #4 to #7 is 51.2 seconds. Figure 6.3 illustrates the mechanical power responses of generator #1 when the time constant  $T_1$  changes from 33.15s to 3.315s. It can be seen that when the time constant  $T_1$  of generator #1 was set to 3.315s, one tenth of the existing value, the change of mechanical power was about nine times larger, as shown in Figure 6.3.

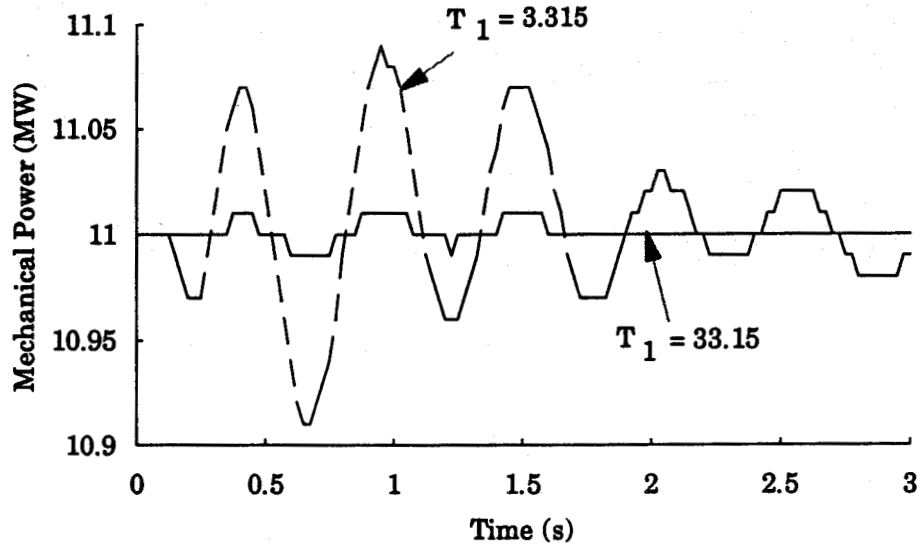


**Figure 6.3:** Mechanical power of generator #1 under 3 $\phi$  fault at bus 30.

### 6.2.3 PSS Effect

Generators #1 through #7 are equipped with PSSs which uses generated electrical power as input signal. The transfer function of the PSS has the form as given in (6.1):

$$G_{\text{pss}}(s) = K \left( \frac{1+sT_1}{1+sT_2} \right) \left( \frac{sT_3}{1+sT_4} \right) \left( \frac{sT_5}{1+sT_6} \right) \left( \frac{1}{1+sA_1} \right) \quad (6.1)$$

The values of the parameters in the transfer function are given in Table 2.1. The output of the PSS under disturbances is negligibly small, as shown in Figure 5.5 in Chapter 5. It is believed that utilization of more effective PSSs would be beneficial.

Generators #8 and #9 are equipped with PSS using accelerating power as input signal. The transfer function of the PSS has the form as given in (6.2):

$$G_{\text{pss}}(s) = K \left( \frac{1+sT_1}{1+sT_2} \right) \left( \frac{1+sT_3}{1+sT_4} \right) \left( \frac{sT_5}{1+sT_6} \right) \quad (6.2)$$

The actual parameters in the transfer function are also given in Table 2.1 of Chapter 2. Figure 6.4 illustrates the differences of rotor angle responses of generators #1 and #8 for a 3 $\phi$  fault at bus 30 with and without the existing PSSs in the system. It can be seen that the PSS on generator #8 has a slightly greater impact on oscillation than that on generator #1. On the other hand, the oscillation of generator #1 is less severe than that of generator #8, as the former is closer to the infinite busbar. It is possible to design more effective PSSs for the system to improve its overall stability. More discussion of this topic is presented in the following section.

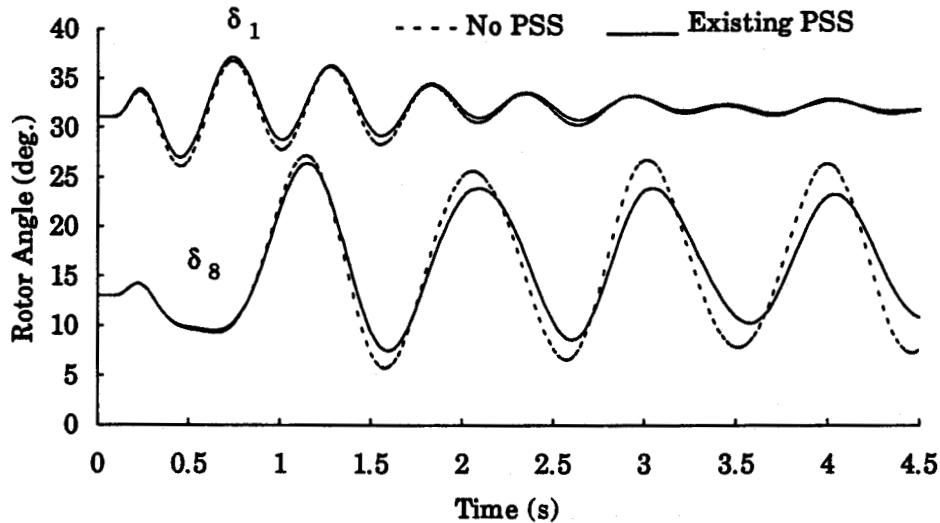


**Figure 6.4:** Rotor angle swing of generators #1 and #8 under 3  $\phi$  fault at bus 30. Effects of PSSs.

## 6.3 Coordinated PSS Design

As has been explained in Chapter 3, power system stabilizers (PSSs) have been widely utilized in excitation control to provide positive damping. In most conventional PSS applications, only local feedback control is used. A multivariable and/or optimal stabilizer can be designed theoretically but may not be implemented because of the difficulties in accurately obtaining required controlling inputs. Coordination in PSS design has been considered by either eigenanalysis [35], or frequency domain methods [36] or a hybrid of the two [37]. No matter what algorithm is employed in tuning the settings of a PSS, the more information dependent on operating conditions is used, the less robust the PSS will be to system changes.

A new coordinated PSS design procedure is proposed in this thesis. It is based on generation coherency, the total coupling factors and non-linear simulation.

### 6.3.1 Design Procedure

According to the previous analysis, the negatively damped modes  $\lambda_1, \lambda_2, \lambda_6, \lambda_8$  to  $\lambda_{12}$  mainly involve generators #1 to #10. In order to provide positive damping, these generators have been actually equipped with PSSs with the exception of generator #10. This chapter attempts to utilize different but very effective PSSs to further enhance the dynamic and transient stability of the system.

To design a PSS, it is essential to choose a proper input signal and then design a compensation circuit reasonably robust to different operating

conditions. Because of the interactions among generators, there seems to be no way to correspond each and every swing mode with one specific machine. A coordinated design and application procedure for PSSs was developed during the research reported in this thesis. The procedure is outlined below:

- Determine the coherent generation groups by an available technique [32].
- Find the average center frequency for each group of generators participating in various swing modes together.
- Choose a PSS input, say shaft speed.
- Let the system operate at full load and the strongest transmission for speed input type PSS tuning.
- Set a washout time constant.
- Set a lead/lag time constant spread for the compensation circuit of the PSS.
- Determine the time constants according to the center frequency and the spread.
- Change the PSS gain from 0 to infinity and compute the root loci or perform non-linear time simulations. When instability is met, the best gain value is chosen to be one third of the gain at instability [25].
- Evaluate the effectiveness of the settings by either eigenvalue analysis or time domain simulations. Change the spread if necessary and repeat the last three steps.

### 6.3.2 PSS Tuning

Extensive time simulations and calculations of coupling factors have shown that the following coherent generator groups can be identified: (#1,#2,#3,#7), (#4,#5,#6), (#8,#9) and (#10,#11,#12). The tuning of PSSs for generator group 1 is illustrated here. It is shown in Table 3.2 that the generators in group 1 participate in various swing modes at an average frequency of 1.9 Hz. The system is assumed to be operating at full load with the network intact. The time constant spread is set to be 8:1 and the deviation of the generator shaft speed with respect to the synchronous speed is chosen as the PSS input. The transfer function of a speed input PSS is given by:

$$G_{\text{pss}}(s) = K_s \left( \frac{sT_w}{1+sT_w} \right) \left( \frac{1+sT_1}{1+sT_2} \right) \left( \frac{1+sT_3}{1+sT_4} \right) \quad (6.3)$$

The initial lead/lag time constants,  $T_1, T_2, T_3$  and  $T_4$  are determined as follows [25]:

$$T_1 = T_3 = \sqrt{8} / 2\pi f_c = 0.237s \quad (6.4)$$

$$T_2 = T_4 = T_1 / 8 = 0.03s \quad (6.5)$$

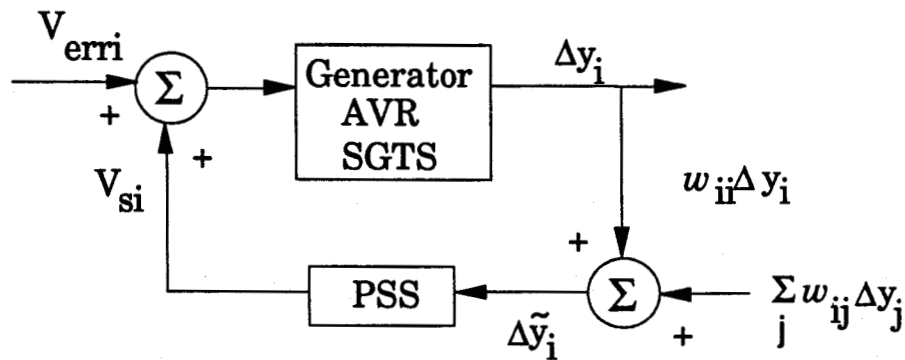
where  $f_c$  is the average (or central) oscillation frequency of generation group 1. The gain  $K_s$  is set to be equal to 5 and the washout time constant  $T_w$  is 10s. The final settings after adjustments are listed in Table 6.1. PSSs for other generation groups were also designed and their settings are also listed in Table 6.1.

**Table 6.1:** PSS settings of the 4 generation groups.

Group No	Ks	T1/T2	T3/T4	Tw
1	5	.2465/.0342	.2465/.0342	10
2	5	.2350/.0290	.2350/.0290	10
3	10	.2000/.0100	.1000/.0300	6
4	10	.2000/.0100	.1000/.0300	6

### 6.3.3 Communication of PSS Inputs

In order to increase the robustness of single input PSSs and to reflect the coupling among generators, the stabilizer inputs in each group will be communicated among its PSSs. As all the generators in a coherent group behave in a very similar fashion, their speed deviations with respect to the synchronous speed will be either positive or negative. These speed deviations can be summed up through the coupling factors to feed each PSS in that group as illustrated in Figure 6.5.

**Figure 6.5:** Realization of PSS coordination.

Fortunately, the generators in each group of the first three groups are in the same plant and the last group involves two plants seven kilometers away.

Therefore, only local communication is required, which can be realized without difficulty.

The input signal to the  $i$ -th PSS is given by:

$$\Delta \tilde{y}_i = w_{ii} \Delta y_i + \sum_{j \neq i} w_{ij} \Delta y_j = \sum_j w_{ij} \Delta y_j \quad (6.6)$$

where  $w_{ij}$  is the total coupling factor between generator  $i$  and generator  $j$  computed from eigenvalue analysis and reflects the extent of interaction between the two generators, and  $\Delta y_j$  is a measurable output of the  $j$ -th plant. For a speed input PSS,  $\Delta y_j$  is the speed deviation of generator  $j$ . The coupling factors calculated from eigenvalue analysis are listed in Table 6.2. Values less than  $10^{-2}$  are neglected.

**Table 6.2: Total coupling factors.**

Gen No	1	2	3	4	5	6	7	8	9	10	11	12
1	0.33	0.13	0.08	0.02	0.02	0.02	0.05	0	0	0	0	0
2	0.13	0.2	0.21	0.02	0.02	0.02	0.05	0	0	0	0	0
3	0.08	0.21	0.25	0.02	0.02	0.02	0.05	0	0	0	0	0
4	0.02	0.02	0.02	0.18	0.06	0.06	0.01	0	0	0	0	0
5	0.02	0.02	0.02	0.06	0.12	0.12	0.01	0	0	0	0	0
6	0.02	0.02	0.02	0.06	0.12	0.12	0.01	0	0	0	0	0
7	0.05	0.05	0.05	0.01	0.01	0.01	0.23	0	0	0	0	0
8	0	0	0	0	0	0	0	0.45	0.45	0.09	0.22	0.44
9	0	0	0	0	0	0	0	0.45	0.45	0.09	0.22	0.43
10	0	0	0	0	0	0	0	0.09	0.09	0.33	0.67	0.26
11	0	0	0	0	0	0	0	0.22	0.22	0.67	3.85	2.07
12	0	0	0	0	0	0	0	0.44	0.43	0.26	2.07	3.43

## **6.4 Improvement of System Stability by New PSSs**

It is expected that the new PSSs should be able to provide positive damping to various swing modes once they are installed in the system. Eigenvalue analysis and time simulations were performed in this section with the new PSSs in service.

### **6.4.1 New Eigenvalues**

Eigenvalue analysis of the system with these newly designed PSSs in service was performed and the results are listed in Table 6.3. It can be seen in Table 6.3 that the above designed PSSs are very effective in providing positive damping to almost all swing modes when they are installed on generators #1 to #7. It can also be seen that swing modes  $\lambda_1$  and  $\lambda_9$  are still slightly negatively damped. When new PSSs are also installed on generators #8 and #9, these swing modes will also become positively damped.

### **6.4.2 Time Simulation of the Small Disturbance**

The small disturbance previously studied in Section 4.6 was simulated with new PSSs on generators #1 - #9 without coordination. Figure 6.6 illustrates the rotor angle swing of generators #1 and #8. The oscillations are damped out in 5 seconds. This is a significant improvement as compared to the situation presented in Figure 4.5 where the existing PSSs were in service.

**Table 6.3: Eigenvalues after installation of new PSS on #1-#7.**

Swing No	$\sigma$	$\omega$	freq. (Hz)
1	0.060	5.919	0.90
2	-2.727	6.748	1.16
3	-2.853	6.851	1.18
4	-0.686	7.233	1.15
5	-2.836	7.514	1.28
6	-4.215	8.505	1.44
7	-2.950	8.942	1.5
8	-4.395	9.412	1.59
9	0.010	10.865	1.74
10	-0.042	11.107	1.75
11	-0.067	11.728	1.88
12	-0.054	12.268	1.95

### 6.4.3 Time Simulation of a Large Disturbance

As a demonstration of the function of the new PSSs when installed in the system and a verification of their effectiveness, a single phase to ground (SLG) fault on the double circuit line 59-61 near to bus 61 for 6 cycles was simulated. It was cleared by opening all the three phases of the faulted line. Figure 6.7 shows the rotor angle swings of generator #1 with the existing PSSs on generators #1 to #9 and new PSSs on generators #1 to #7, respectively. It is clearly shown that new PSSs can effectively damp down the oscillations and enhance system stability. Detailed comparison is provided in the next section.

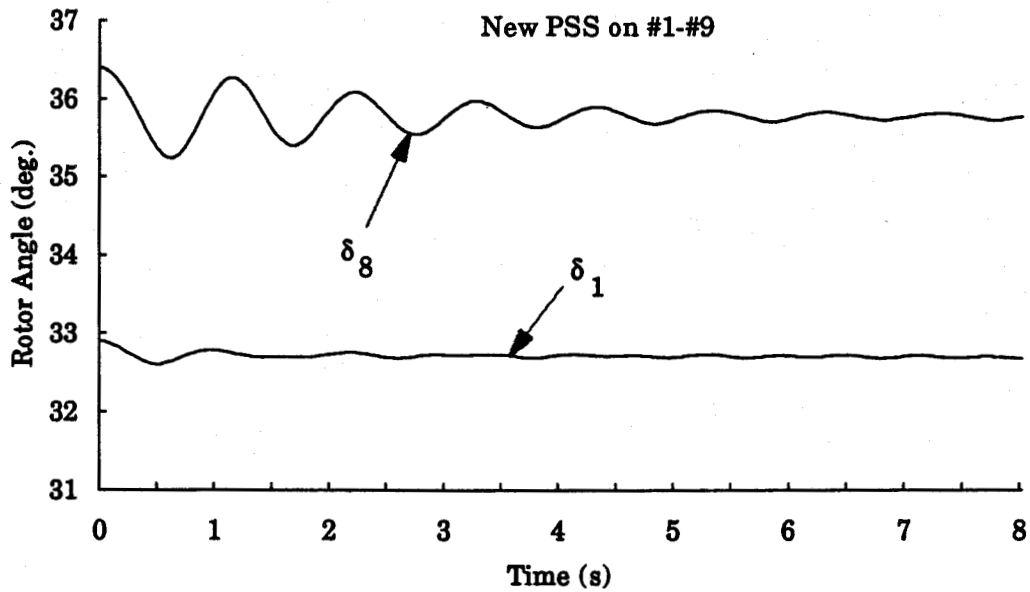


**Figure 6.6:** Rotor angle swing responding to a load increase of 1% the system capacity at Rabbit Lake.

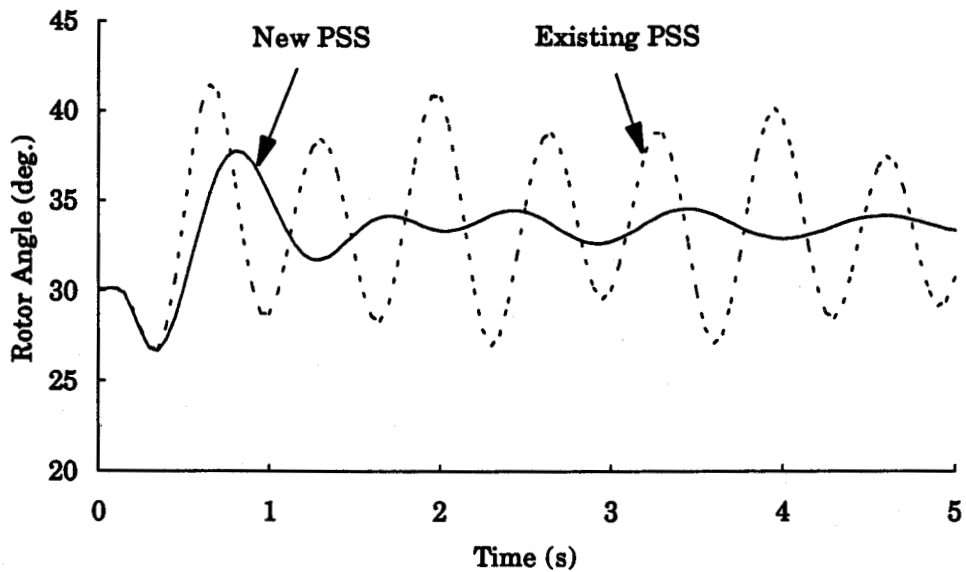


**Figure 6.7:** Rotor angle plotting of generator #1 versus time. Single phase fault near bus 61 for 6 cycles.

## 6.5 Transient Simulation Studies

Considering the actual difficulties in implementation of power system stabilizers at generators #10 to #12 because of their rotating excitation systems and in provision of extra communication means between these two plants, the application of the new PSSs was divided into two stages. Stage I: only generators #1 to #9 were equipped with new PSSs. Stage II: the remaining three generators were also equipped with PSSs. The two disturbances, i.e., the (SLG) fault and the 1% load increase at Rabbit Lake covered in Chapter 4, were employed for simulation studies. Other simulation tests are also included.

### 6.5.1 Existing PSSs

Simulations were conducted with and without the existing PSSs on machines #1 to #9 for the single phase to ground (SLG) fault condition. Figure 6.8(a) shows that the system was unstable if no PSS was installed in the system. When the existing PSSs were put into service, the system stability was improved significantly, as seen in Figure 6.8(b). Figure 6.8(c) displays the outputs of the existing PSSs.

### 6.5.2 New PSS on #1-#9

When the new PSSs are installed on generators #1 to #9, the sustained oscillations can be damped out much quicker in Figure 6.9(a), as compared with Figure 6.8(b). Further improvement in damping is also illustrated when coordination is incorporated in Figure 6.9(b). The outputs of new PSSs on generators #1 and #8 are given in Figure 6.9(c).

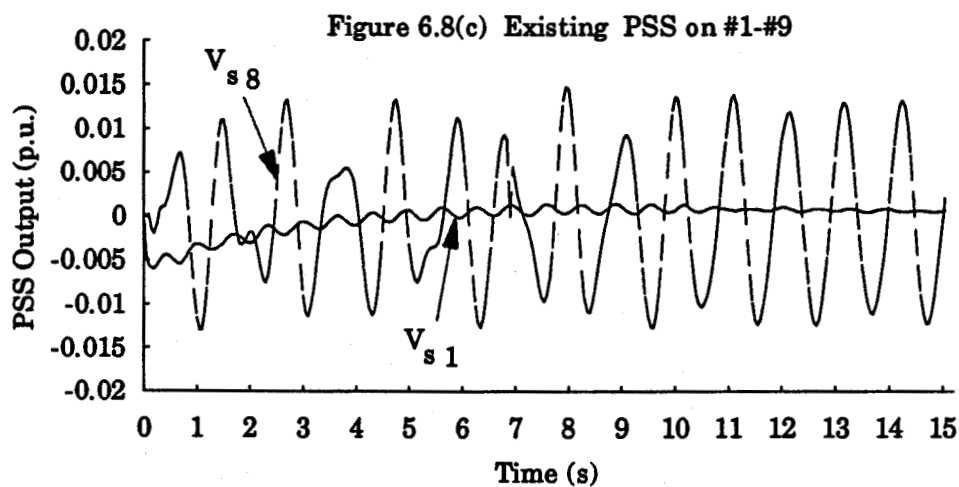
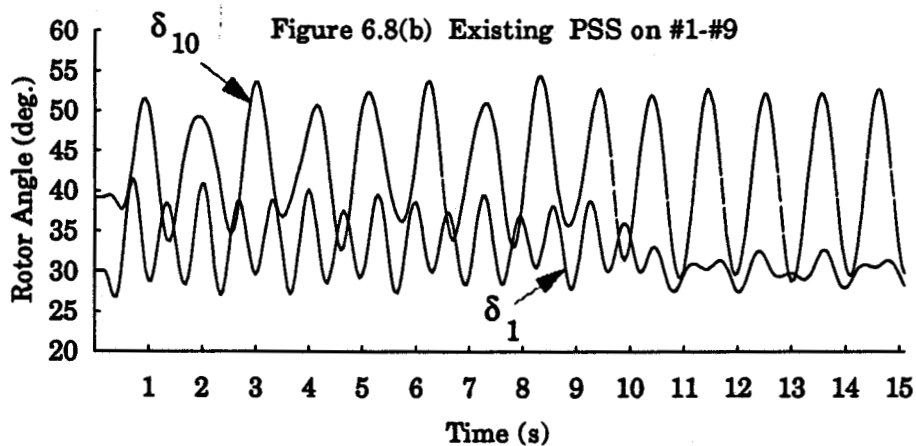
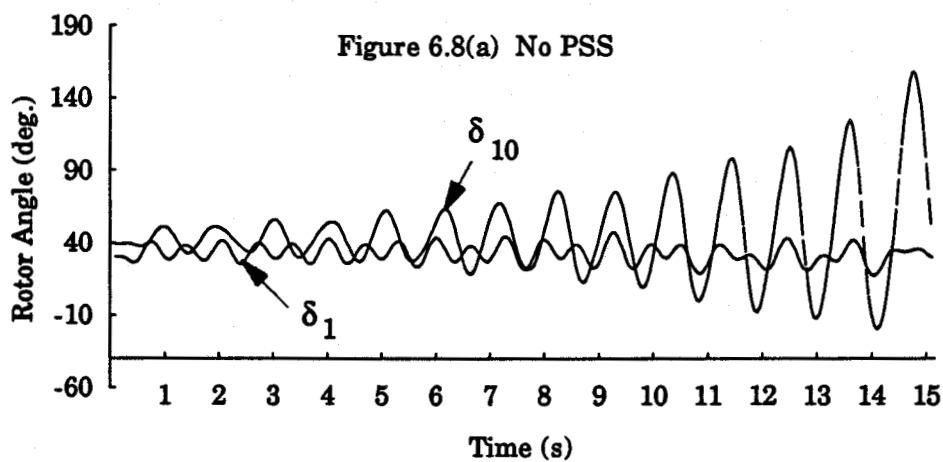


**Figure 6.8:** Time domain simulation of the SLG fault with and without the existing PSSs in service.

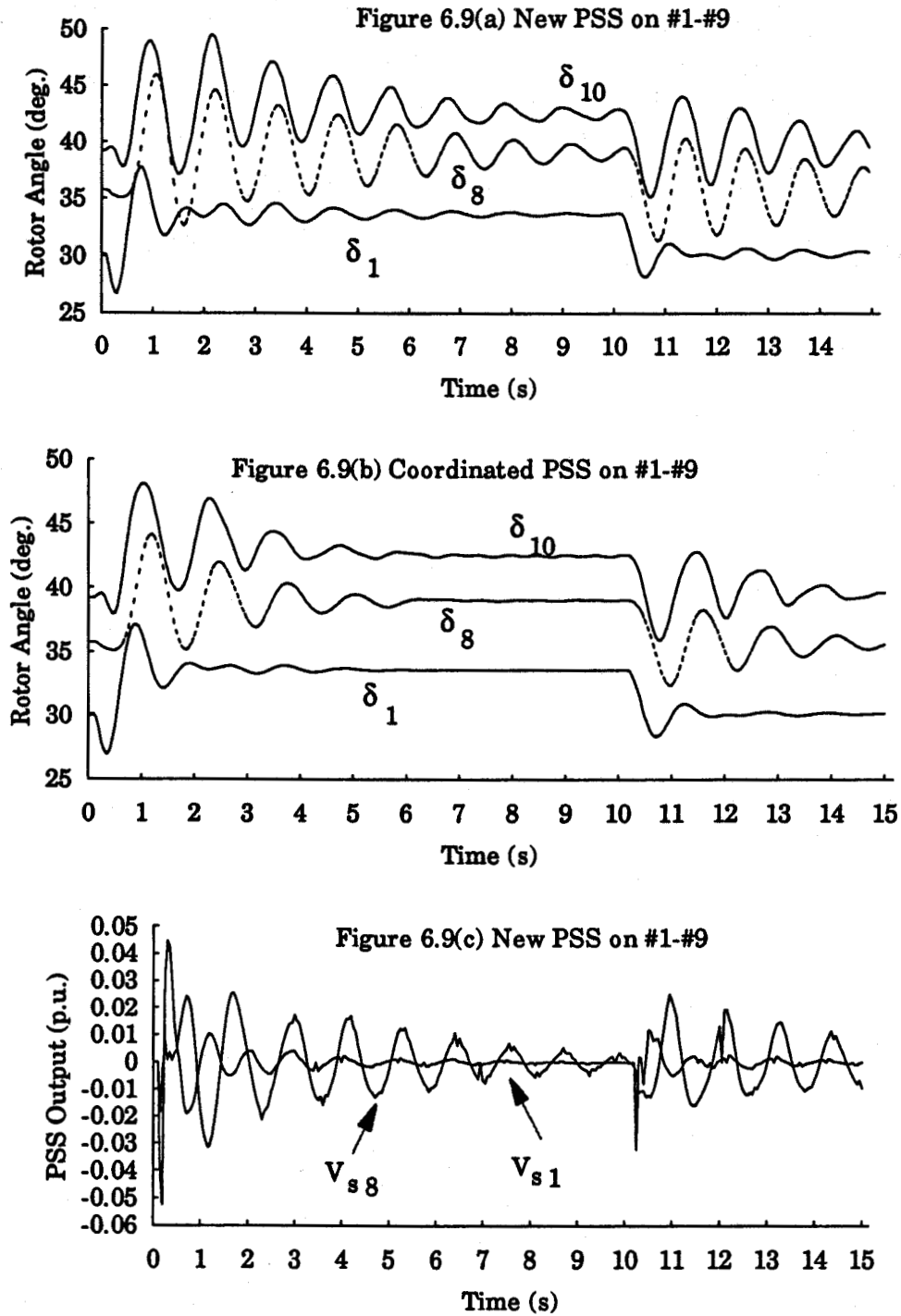


**Figure 6.9:** Time domain simulation of the SLG fault with new PSSs on generators #1 - #9 in service.

### 6.5.3 New PSSs on All Machines

If the three hydro generators of the last coherent generation group are also equipped with new PSSs, further enhancement in dynamic and transient stability can be expected. This is illustrated in Figure 6.10(a) and 6.10(b). The latter is with coordinated PSS application.

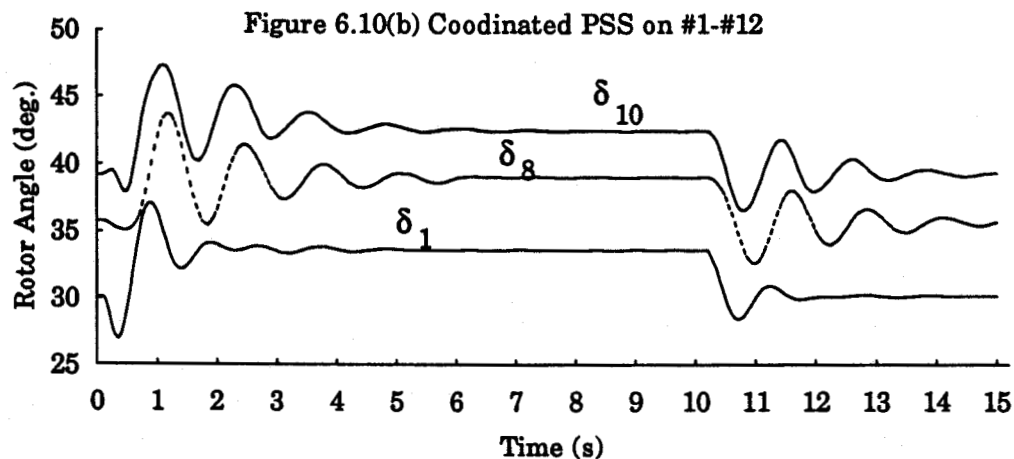
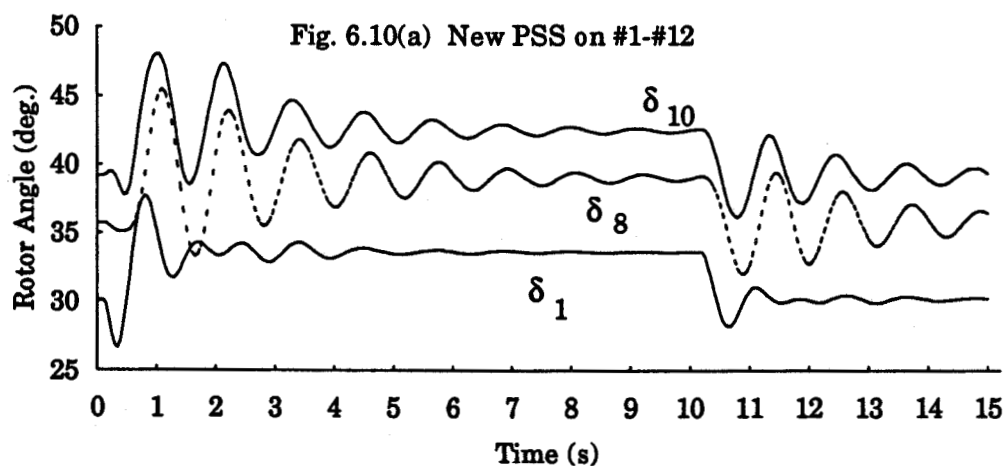


**Figure 6.10:** Time domain simulations of the SLG fault with new PSSs on all machines in service.

It can be observed that (i) the oscillations using coordinated PSSs take less than half of the time to settle down as compared to that with non-coordinated PSSs (compare Figures 6.9(a) with 6.9(b), 6.10(a) with 6.10(b)), and (ii) coordinated PSSs on generators #1 to #9 are more efficient than non-coordinated PSSs on all generators (compare Figures 6.9(b) with 6.10(a)).

#### 6.5.4 Other Tests

A number of other disturbances were simulated and a summary of the results obtained is presented in this section. All these tests were conducted with new PSSs only on generators #1 through #9. The objective was to make a valid comparison with the existing PSSs and to avoid the difficulties in installing new PSSs on the hydro generators #10-#12.

1. When there is one PSS failure in each of the three coherent groups, simulation of the SLG fault studied above shows that it took the system 12 seconds to completely settle down to a new equilibrium point without PSS coordination and about 7 seconds with PSS coordination.
2. A minimum of one new PSS for each of the three groups is needed to maintain stable operation of the system. This observation is in agreement with that of [25].
3. A three phase fault of the same duration as the SLG fault on the double circuit was simulated. It took the system 5 seconds longer than in the case of SLG fault to damp out the oscillations.

4. A three phase fault for a duration of 6 cycles on the line from Island Falls to Lindsay Lake will separate the system into three parts. The parts from Island Falls to the northern end of the system will be lost after a number of breaker trips. The objective of this simulation was to examine whether the Island Falls plant could be saved after the disturbance. Figure 6.11 shows the swing of speed difference of generator #1 with the existing PSSs and new PSSs in service, respectively.

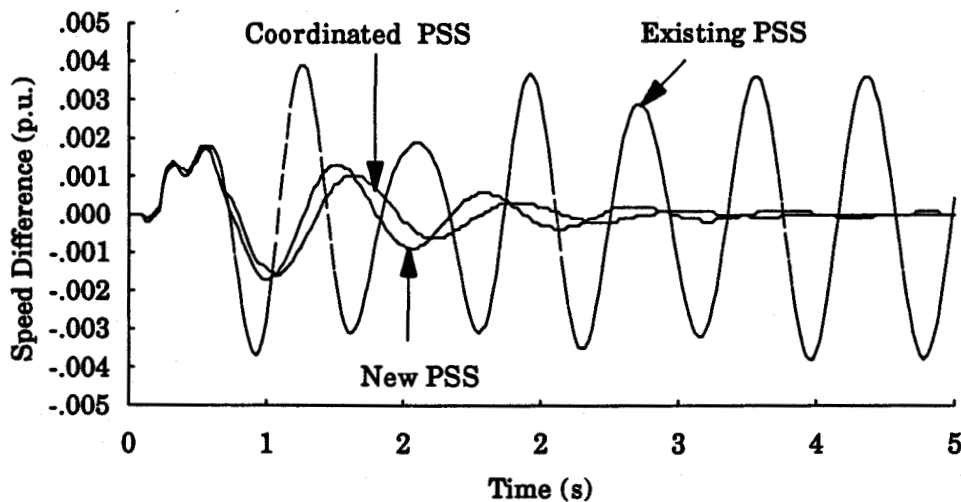


**Figure 6.11:** Responses of speed difference of generator #1 to 3LG fault for 6 cycles at bus 18.

5. Simulations of the SLG fault for a duration of 6 cycles under 50%, 75% and 100% loading were also performed with coordinated PSSs in service. Figure 6.12 displays the rotor angle swings of generator 1 under different loading. It can be concluded that though the new PSSs were tuned under full system loading, they perform very well under other system loading.

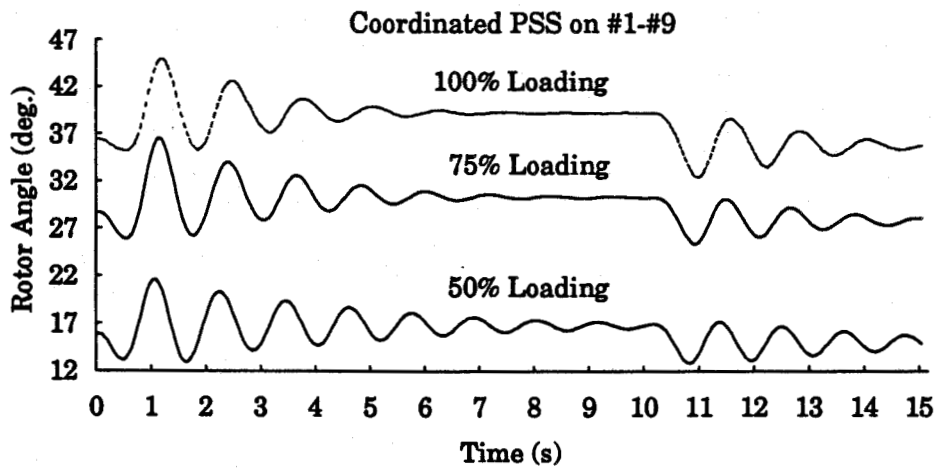


**Figure 6.12:** Rotor angle swing of generator #1. SLG fault for 6 cycles under different system loading.

## 6.6 Summary

This chapter presents the effects of the existing primary controls in the APNS. It is shown that the SGTS has little effect on damping and that the existing PSSs do not work as expected. Additional excitation control could be more effective. Secondly, a coordinated design and application procedure for new PSSs is described. New PSSs were designed and their performance is illustrated when they were applied to the system. Finally, a report is given of the results of a comprehensive investigation of the steady state and transient stability of the system.

## **7. CONCLUSIONS**

The work reported in this thesis is concerned with a comprehensive investigation of the steady state and transient stability of the Athabasca-Points North System (APNS) in northern Saskatchewan. This chapter presents a brief summary of the work reported in the thesis and important conclusions from the studies.

To carry out steady state and transient stability studies, the following preparation tasks were accomplished first:

1. the modeling of power components and the network; and
2. the development of a time domain simulation package.

The investigation of the system stability has been accomplished by:

3. eigenvalue analysis and functional sensitivity studies for steady state stability; and
4. time simulations for transient stability studies.

Then, the stabilization of the overall system stability has been realized by:

5. a coordinated PSS application.

The modeling of a power system for stability studies includes two categories, i.e., (i) the modeling of power components which must be

described by differential equations; and (ii) the modeling of the network and transformers which can be described by algebraic equations.

A synchronous machine is the most influential power component in stability studies. Its modeling should be sufficiently accurate and simple while the transient and subtransient phenomena must also be incorporated into the model. With all these requirements being considered, a fifth order model was utilized in this thesis and has been discussed in Chapter 2. It has been shown that other simpler models can also be obtained from this representation. Various load models have also been presented in Chapter 2.

Eigenvalue analysis and functional sensitivity studies were carried out to investigate the steady state stability of the system with no power system stabilizers (PSSs) in service. The purpose of this investigation was to identify the best sites for PSS installation. It was found that the system modes were either negatively or poorly damped when no PSS was in service. This is why the system is actually equipped with PSSs to provide positive damping. Detailed results have been presented in Chapter 4.

In order to perform stability studies of the APNS, a transient stability simulation package was developed. The description of the package has been given in Chapter 3 and the results from transient stability studies have been presented in Chapter 5.

The transient stability of the system depends largely on the disturbance and the operating condition at which the disturbance happens. Any fault that trips one or more sections of the transmission lines from Island Falls to the northern part of the system will separate the system into parts. Some parts may be saved while the rest will be lost. The situation of most concern is that

one of the double circuit lines from Island Falls to the Flin Flon is tripped out and the power transfer on the other line may reach its maximum capacity. In this case, low frequency oscillations were observed in time simulation.

As has been pointed out in Chapter 6, conventional PSSs are operating point dependant and are designed to damp out particular oscillation frequencies. When the operating condition changes, such a PSS may become inefficient. To overcome these shortcomings, a coordinated PSS design and application procedure was developed. The design algorithm is based on the concept that it is desirable to use less information that is operating condition dependent and to use more inherent properties of the system in tuning PSS settings. This idea is realized by utilizing the average natural oscillation frequency of a coherent generation group and a lead/lag time constant spread for PSS tuning. The spread reflects the strength of the system and the type of stabilizer input. The total coupling factors among strongly coupled generators are also used as weighting factors in communication of PSS inputs.

A number of disturbances were applied to the system and their time domain simulations conducted. Selected results have been presented in Chapter 6. The following conclusions have been drawn from the studies reported in this thesis.

1. It has been demonstrated that the system with the existing PSSs in service is stable under common outages.
2. It is beneficial to the system if more positive damping can be provided through excitation control.

3. The studies have shown that for a single phase to ground fault, it is possible to have two phases in operation for a short period of time, say a couple of hours, instead of tripping all three phases. The system will be still stable even if the faulted phase can be restored after a few hours. This operating procedure might be used, however, because most system disturbances are single phase faults.
4. Autoreclosure can prevent some instability from happening, especially when the disturbance is temporary. Single phase reclosure can greatly speed restoration of stability.
5. Application of the newly designed PSSs has exhibited promising results regarding their effectiveness to damp out oscillations and their robustness to different operating conditions and small or large disturbances.
6. A minimum of one new PSS must be installed in each coherent generation group of the first three groups to maintain stable operation and reasonably good damping.

As has been shown in the thesis, the newly designed PSSs are very effective in damping low frequency oscillations in computer simulation studies. It might be expected that if the proposed new PSSs could be implemented in the actual system, the overall stability of the system could be enhanced.

## REFERENCES

- [1] IEEE Task Force on Terms & Definitions, "Proposed Terms & Definitions for Power System Stability," *IEEE Trans. on Power Apparatus and System*, vol. PAS-101, No. 7, pp. 1894-1898, July 1982.
- [2] C. Barbier, L. Carpentier, F. Saccomanno, "Tentative Classification and Terminologies Relating to Stability Problems of Power Systems," *ELECTRA*, No. 56, 1978.
- [3] Z. Ao, *A Transient Stability Simulation Package (TSSP) — Users Manual*, Department of Electrical Engineering, University of Saskatchewan, Saskatoon, Canada, September 1993.
- [4] T. J. Hammons, D. J. Winning, "Comparisons of Synchronous-Machine Models in the Study of the Transient Behavior of Electrical Power Systems," *Proc. IEE*, Vol. 118, No. 10, pp. 1443-1458, October 1971.
- [5] IEEE Committee Report, "Excitation System Models for Power System Stability Studies," *IEEE Transactions on Power Apparatus and System*, Vol. PAS-100, pp. 494-507, February 1981.
- [6] IEEE Committee Report, "Dynamic Models for Steam and Hydro Turbines in Power System Studies," *IEEE Trans. on Power Apparatus and System*, Vol. PAS-92, pp. 1904-1915, November 1973.
- [7] R. H. Park, "Two-Reaction Theory of Synchronous Machines," *Trans. AIEE*, Part I: pp. 716-730, July 1929; Part II: pp. 352-355, June 1933.
- [8] P. M. Anderson, A. A. Fouad, *Power System Control and Stability*, The Iowa State University Press, Ames, Iowa, U.S.A., 1977.
- [9] E. V. Larson and D. A. Swann, "Applying Power System Stabilizers, Part I: General Concepts," *IEEE Trans. PAS*, vol. 100, pp. 3017-3024, 1981.
- [10] Nanjing Technology Institute, *Power System Analysis*, China Power Industrial Press, 1979.
- [11] D. S. Brereton, D. G. Lewis, C. C. Young, "Representation of Induction-Motor Loads During Power-System Stability Studies," *AIEE Transaction*, pp. 451-460, August 1957.

- [12] IEEE Task Force on Load Representation for Dynamic Performance, "Load Representation for Dynamic Performance Analysis," 92 WM 126-3 PWRD, pp. 1-11, 1992.
- [13] D. W. Olive, "Digital Simulation of Synchronous Machine Transients," *IEEE Trans. on Power Apparatus and System*, Vol. PAS-87, pp. 1669-1674, August 1968.
- [14] H. W. Dommel, N. Sato, "Fast Transient Stability Solutions," *IEEE Trans. on Power Apparatus and System*, Vol. PAS-91, pp. 1643-1650, July 1972.
- [15] R. B. I. Johnson, M. J. Short, B. J. Cory, "Improved Simulation Techniques for Power System Dynamics," *IEEE Trans. on Power Systems*, Vol. 3, No. 4, pp. 1691-1698, 1988.
- [16] The Math Works Inc., *PC-MATLAB Reference Manual*, Version 3.13, September 1987.
- [17] R. B. Anderson, *The Student Edition of MathCAD*, Version 2.0, Addison-Wesley Publishing Company, New York, 1989.
- [18] R. Bonert, "Interactive Simulation of Dynamic Systems on A Personal Computer to Support Teaching," *IEEE Trans. on Power Systems*, Vol. 4, No. 1, pp. 380-383, February 1989.
- [19] D. C. Yu, S. T. Chen and R. F. Bischke, "A PC-Oriented Interactive Graphic Simulation Package for Power System Study," *IEEE Trans. on Power Systems*, Vol. 4, No. 1, pp. 353-360, February 1989.
- [20] P. Buchner, M. H. Nehrir, "A Block-Oriented PC-Based Simulation Tool for Teaching and Research in Electric Drives and Power Systems," *IEEE Trans. on Power Systems*, Vol. 6, No. 3, pp. 1299-1304, august 1991.
- [21] Yuan-Yih Hsu, Sheng-Wehn Shyue and Chung-Ching Su, "Low frequency Oscillations in Longitudinal Power Systems: Experience with Dynamic Stability of Taiwan Power System," *IEEE Trans. on Power Systems*, vol. PWRS-2, No. 1, pp. 92-100, February, 1986.
- [22] V. Arcidiacono, E. Ferrai and F. Saccomanno, "Studies on Damping of Electromechanical Oscillations in Multimachine Systems with Longitudinal Structure," *IEEE Trans. PAS*, vol. 95, pp. 450-460, March/April, 1976.

- [23] A. Al-Said, N. Abu-Sheikhah, T. Hussein , R. Marconato and P. Scarpellini, "Dynamic Behaviour of Jordan Power System in Isolated Operation," *CIGRE Paper* 39-201, 1990.
- [24] R. L. Cresap and J. F. Hauer, "Emergence of a New Swing Mode in the Western Power System," *IEEE Trans. PAS*, vol. 100, pp. 2037-2043, 1981.
- [25] E. V. Larson and D. A. Swann, "Applying Power System Stabilizers, Part II: Performance Objectives and Tuning Concepts," *IEEE Trans. PAS*, vol. 100, pp. 3025-3033, 1981.
- [26] E. V. Larson and D. A. Swann, "Applying Power System Stabilizers, Part III: Practical Considerations," *IEEE Trans. PAS*, vol. 100, pp. 3033-3046, 1981.
- [27] M. Klein, G. J. Rogers and P. Kundur, "A Fundamental Study of Inter-Area Oscillations in Power Systems," *IEEE Trans. on Power Systems*, vol. PWR-6, No. 3, pp. 914-921, August 1991.
- [28] C. Corcordia and F. P. deMello, "Concepts of Synchronous Machine Stability as Affected by Excitation Control," *IEEE Trans. PAS*, Vol. 88, pp. 316-329, April 1969.
- [29] R. T. Byerly, R. J. Bennon and D. E. Sherman, "Eigenvalue Analysis of Synchronizing Power Flow Oscillations in Large Electric Power Systems," *IEEE Trans. PAS*, vol. 101, pp. 235-243, 1982.
- [30] D. Y. Wong, G. J. Rogers, B. Porreta and P. Kundur, "Eigenvalue Analysis of Very Large Power Systems," *IEEE Trans. on Power Systems*, vol. 3, No. 2, pp. 472-480, May 1988.
- [31] E. Z. Zhou, et al., "Theory and Method for Selection of Power System Stabilizer Location," *IEEE Trans. on Energy Conversion*, vol. 6, No.1, March 1991.
- [32] T. Hiyama, "Coherency-based Identification of Optimum Site for Stabilizer Applications," *IEE Proceedings*, vol. 130, Part C, pp. 71-74, 1983.
- [33] Dejan R. Ostojic, "Identification of Optimum Site for Power System Stabilizer Applications," *IEE Proceedings*, vol. 135, Part C, pp. 416-419, 1988.
- [34] IEEE Task Force, "A Description of Discrete Supplementary Controls for Stability," *IEEE Trans. PAS*, vol. 97, No. 1, pp. 149-157, 1978.

- [35] F. P. de Mello, P. J. Nollan, T. F. Laskowski, and J. M. Undrill, "Coordinated Application of Stabilizers in Multi-machine Power Systems," *IEEE Trans. PAS*, Vol. 99, pp. 892-901, 1980.
- [36] A. Doi, and S. Abe, "Coordinated Synthesis of Power System Stabilizers in Multimachine Power Systems," *IEEE Trans. PAS*, Vol. 103, pp. 1473-1479, 1984.
- [37] Dejan R. Ostojic, "Stabilization of Multimodal Electromechanical Oscillations by Coordinated Application of Power System Stabilizers," *IEEE Trans. on Power Systems*, vol. 6, No. 4, pp. 1439-1445, November 1991.
- [38] R. M. Mathur, *Static Compensators for Reactive Power Control*, Canadian Electrical Association Publication, 1984.

# APPENDIX A

## DATA FILE *pqlf.inp* AND LOAD FLOW RESULTS

### A.1 Data File *pqlf.inp*

```

! -----
!           SaskPower
!       Athabasca- Points North system
!       ( March, 1993 )
! -----
!       Data file for P-Q Decoupled LF studies
! -----
! => no of   |   max.   |   max. P, Q   |   ntwk   |   p.u. (0)   |
!   buses   | iterations | mismatch      | switch   | MVA (1)      |
! -----
!           69 ,    30    ,    0.0001    ,    0    ,    1    /
! -----
! => Positive(+), negative(-) sequence network data:
!   This block of data can be copied to or from the ntwk.inp file.
!   Attention should be paid to that the grounded
!   reactances of the generators used in ntwk.inp data file
!   are excluded here.
! -----
!   i,   j,   r(+),   r(-),   x(+),   x(-),   ratio/b/1.0/-1.0
! -----
!   1, -14, 0.0082, 0.0082, 0.2278, 0.2278, 1.0 /
!   2, -14, 0.0082, 0.0082, 0.2278, 0.2278, 1.0 /
!   3, -14, 0.0082, 0.0082, 0.2278, 0.2278, 1.0 /
!   4, -14, 0.0057, 0.0057, 0.1472, 0.1472, 1.0 /
!   5, -14, 0.0057, 0.0057, 0.1472, 0.1472, 1.0 /
!   6, -14, 0.0057, 0.0057, 0.1472, 0.1472, 1.0 /
!   7, -14, 0.0057, 0.0057, 0.1472, 0.1472, 1.0 /
!   8, -56, 0.0000, 0.0000, 1.1980, 1.1980, 1.0 /
!   9, -56, 0.0000, 0.0000, 1.1880, 1.1880, 1.0 /
!  10, -55, 0.0000, 0.0000, 0.7375, 0.7375, 1.0 /
!  11, -54, 0.0000, 0.0000, 2.1333, 2.1333, 1.0 /
!  12, -54, 0.0000, 0.0000, 2.1333, 2.1333, 1.0 /
!  14, 59, 0.1316, 0.1316, 0.2906, 0.2906, 0.0305 /
!  14, 60, 0.1316, 0.1316, 0.2906, 0.2906, 0.0305 /
!  59, 61, 0.0381, 0.0381, 0.0827, 0.0827, 0.0078 /
!  60, 62, 0.0381, 0.0381, 0.0827, 0.0827, 0.0078 /
!  61, 63, 0.0038, 0.0038, 0.0084, 0.0084, 0.0009 /
!  62, 63, 0.0038, 0.0038, 0.0084, 0.0084, 0.0009 /
!  64, -63, 0.0000, 0.0000, 0.1020, 0.1020, 0.9500 /
!  61, 65, 0.0015, 0.0015, 0.0047, 0.0047, 0.0005 /
!  62, 65, 0.0015, 0.0015, 0.0047, 0.0047, 0.0005 /

```

66,	-65,	0.0000,	0.0000,	0.1020,	0.1020,	0.961	/
65,	67,	0.0013,	0.0013,	0.0102,	0.0102,	0.001	/
68,	-67,	0.0000,	0.0000,	0.0898,	0.0898,	0.975	/
68,	69,	0.0151,	0.0151,	0.1240,	0.1240,	0.0800	/
14,	15,	0.0000,	0.0000,	-0.0583,	-0.0583,	0.0	/
15,	16,	0.0000,	0.0000,	0.1583,	0.1583,	0.0	/
15,	13,	0.0000,	0.0000,	1.6750,	1.6750,	0.0	/
14,	17,	0.0000,	0.0000,	-0.0583,	-0.0583,	0.0	/
17,	16,	0.0000,	0.0000,	0.1583,	0.1583,	0.0	/
17,	58,	0.0000,	0.0000,	1.6750,	1.6750,	0.0	/
16,	18,	0.0546,	0.0546,	0.2187,	0.2187,	0.0542	/
18,	21,	0.0258,	0.0258,	0.1031,	0.1031,	0.0255	/
18,	19,	0.0155,	0.0155,	0.0363,	0.0363,	0.0082	/
20,	-19,	0.0,	0.0,	2.3333,	2.3333,	0.9875	/
22,	-21,	0.0,	0.0,	1.7500,	1.7500,	0.975	/
22,	23,	0.6408,	0.6408,	1.2739,	1.2739,	0.0005	/
23,	29,	1.7934,	1.7934,	3.5677,	3.5677,	0.0014	/
29,	24,	0.5418,	0.5418,	0.7785,	0.7785,	0.0004	/
25,	-24,	0.0,	0.0,	3.3330,	3.3330,	1.0	/
21,	26,	0.1017,	0.1017,	0.4097,	0.4097,	0.1023	/
26,	27,	0.0162,	0.0162,	0.0380,	0.0380,	0.0086	/
28,	-27,	0.0,	0.0,	0.7000,	0.7000,	0.975	/
26,	30,	0.0683,	0.0683,	0.2742,	0.2742,	0.0681	/
30,	31,	0.0085,	0.0085,	0.0199,	0.0199,	0.0045	/
32,	-31,	0.0,	0.0,	1.0000,	1.0000,	0.9750	/
30,	33,	0.0239,	0.0239,	0.0956,	0.0956,	0.0236	/
33,	35,	0.0,	0.0,	-0.2767,	-0.2767,	0.0	/
35,	34,	0.0,	0.0,	2.4567,	2.4567,	0.0	/
35,	37,	0.0,	0.0,	0.5433,	0.5433,	0.0	/
33,	36,	0.0,	0.0,	-0.2767,	-0.2767,	0.0	/
36,	57,	0.0,	0.0,	2.4567,	2.4567,	0.0	/
36,	37,	0.0,	0.0,	0.5433,	0.5433,	0.0	/
37,	38,	0.0391,	0.0391,	0.0926,	0.0926,	0.0103	/
38,	39,	0.0,	0.0,	0.3700,	0.3700,	0.0	/
39,	40,	0.0,	0.0,	-0.0185,	-0.0185,	0.0	/
39,	41,	0.0,	0.0,	0.2220,	0.2220,	0.0	/
42,	-41,	0.0,	0.0,	0.8240,	0.8240,	1.0	/
43,	-41,	0.0,	0.0,	0.9050,	0.9050,	1.0	/
41,	44,	0.3248,	0.3248,	0.4189,	0.4189,	0.0005	/
45,	-44,	0.0,	0.0,	0.8290,	0.8290,	1.0	/
37,	46,	0.2676,	0.2676,	0.6341,	0.6341,	0.0702	/
47,	-46,	0.0,	0.0,	1.0600,	1.0600,	0.9500	/
47,	-46,	0.0,	0.0,	1.0600,	1.0600,	0.9500	/
46,	48,	0.1417,	0.1417,	0.3328,	0.3328,	0.0365	/
49,	-48,	0.0,	0.0,	2.7000,	2.7000,	0.9500	/
49,	-48,	0.0,	0.0,	2.7000,	2.7000,	0.9500	/

48,	50,	0.1319,	0.1319,	0.3096,	0.3096,	0.0339	/
52,	-50,	0.0,	0.0,	0.1000,	0.1000,	1.0	/
50,	51,	0.0427,	0.0427,	0.0626,	0.0626,	0.0060	/
51,	53,	0.0711,	0.0711,	0.1044,	0.1044,	0.0100	/
53,	-54,	0.0,	0.0,	0.4444,	0.4444,	1.0000	/
54,	55,	0.0364,	0.0364,	0.1373,	0.1373,	0.0004	/
55,	56,	0.0490,	0.0490,	0.1490,	0.1490,	0.0006	/
0/							

! -----  
! ⇒ Bus data input includes the following:

! The connecting point to Manitoba system is numbered as  
! the slack bus and has a fixed voltage magnitude of 1.05 per unit.  
! The SVC at Rabbit Lake is modeled here as a  
! PV controlled bus with a voltage magnitude of 1.02 per unit. The rest  
! are supposed to be PQ buses. Bus numbering is arbitrary and bus  
! classification is made according to the requirements of system  
! operations and the availability of generation sources.  
! -----

! bus	! bus	! generation	! load	! voltage	!
! no	! type	! PG QG   PL QL	! V(p.u.)	!	!

1,	1,	12,	4.,	0.0,	0.0,	1.0	/
2,	1,	12,	4.,	0.0,	0.0,	1.0	/
3,	1,	12,	4.,	0.0,	0.0,	1.0	/
4,	1,	14.25,	3.0,	0.0,	0.0,	1.0	/
5,	1,	14.25,	3.0,	0.0,	0.0,	1.0	/
6,	1,	14.25,	3.0,	0.0,	0.0,	1.0	/
7,	1,	14.25,	3.0,	0.0,	0.0,	1.0	/
8,	1,	4.0,	-1.0,	0.0,	0.0,	1.0	/
9,	1,	4.0,	-1.0,	0.0,	0.0,	1.0	/
10,	1,	10.0,	1.0,	0.0,	0.0,	1.0	/
11,	1,	2.0,	0.0,	0.0,	0.0,	1.0	/
12,	1,	2.0,	0.0,	0.0,	0.0,	1.0	/
69,	3,	0.0,	0.0,	0.0,	0.0,	1.05	/
58,	1,	0.0,	0.0,	0.0,	15.0,	1.0	/
13,	1,	0.0,	0.0,	0.0,	0.0,	1.0	/
20,	1,	0.0,	0.0,	2.8,	1.1,	1.0	/
23,	1,	0.0,	0.0,	0.3,	0.1,	1.0	/
25,	1,	0.0,	0.0,	1.7,	0.6,	1.0	/
28,	1,	0.0,	0.0,	9.2,	3.5,	1.0	/
32,	1,	0.0,	0.0,	6.5,	2.5,	1.0	/
52,	1,	0.0,	0.0,	0.5,	1.5,	1.0	/
57,	1,	0.0,	0.0,	0.0,	5.0,	1.0	/
40,	2,	0.0,	0.0,	0.0,	0.0,	1.02	/
41,	1,	0.0,	0.0,	8.5,	2.9,	1.0	/
42,	1,	0.0,	0.0,	5.2,	2.5,	1.0	/
43,	1,	0.0,	0.0,	1.5,	0.6,	1.0	/
45,	1,	0.0,	0.0,	1.7,	0.4,	1.0	/

47,	1,	0.0,	0.0,	1.6,	10.25,	1.0	/
49,	1,	0.0,	0.0,	1.5,	0.5,	1.0	/
66,	1,	0.0,	0.0,	15.0,	6.2,	1.0	/
64,	1,	0.0,	0.0,	75.0,	10.7,	1.0	/
0/							

!-----  
! End of data file

## A.2 Load Flow Results

BUS	TYPE	PG	QG	PL	QL	V	$\delta$
1	1	12	4	0	0	1.0757	8.1922
2	1	12	4	0	0	1.0757	8.1922
3	1	12	4	0	0	1.0757	8.1922
4	1	14.25	3	0	0	1.0669	8.3391
5	1	14.25	3	0	0	1.0669	8.3387
6	1	14.25	3	0	0	1.0669	8.3387
7	1	14.25	3	0	0	1.0669	8.3387
8	1	4	-1	0	0	1.0341	21.3393
9	1	4	-1	0	0	1.0342	21.3178
10	1	10	1	0	0	1.0511	21.9631
11	1	2	0	0	0	1.0423	19.0326
12	1	2	0	0	0	1.0423	19.0326
13	1	0	0	0	0	1.0437	4.4193
14	1	0	0	0	0	1.0502	4.0793
15	1	0	0	0	0	1.0437	4.4193
16	1	0	0	0	0	1.0614	3.5059
17	1	0	0	0	0	1.0632	4.4191
18	1	0	0	0	0	1.0670	0.7989
19	1	0	0	0	0	1.0663	0.7541
20	1	0	0	2.8	1.1	1.0537	-2.5376
21	1	0	0	0	0	1.0670	-0.2708
22	1	0	0	0	0	1.0814	-2.0553
23	1	0	0	0.3	0.1	1.0597	-3.1407
24	1	0	0	0	0	0.9907	-6.3738
25	1	0	0	1.7	0.6	0.9683	-9.7600
26	1	0	0	0	0	1.0473	-3.8237
27	1	0	0	0	0	1.0446	-3.9759
28	1	0	0	9.2	3.5	1.0461	-7.2699
29	1	0	0	0	0	1.0055	-5.8295
30	1	0	0	0	0	1.0255	-4.7249
31	1	0	0	0	0	1.0245	-4.7828
32	1	0	0	6.5	2.5	1.0244	-8.2450
33	1	0	0	0	0	1.0173	-4.6761
34	1	0	0	0	0	1.0150	-4.5869
35	1	0	0	0	0	1.0150	-4.5869
36	1	0	0	0	0	1.0459	-4.5869
37	1	0	0	0	0	1.0196	-4.7617
38	1	0	0	0	0	1.0147	-5.6715

39	1	0	0	0	0	1.0218	-9.1311
40	2	0	0	0	-9.86843	1.0200	-9.1311
41	1	0	0	8.5	2.9	1.0063	-11.2233
42	1	0	0	5.2	2.5	0.9845	-13.7021
43	1	0	0	1.5	0.6	1.0008	-11.9956
44	1	0	0	0	0	0.9991	-11.5552
45	1	0	0	1.7	0.4	0.9957	-12.3669
46	1	0	0	0	0	1.0069	2.3517
47	1	0	0	1.6	10.25	1.0058	1.8959
48	1	0	0	0	0	1.0266	5.9281
49	1	0	0	1.5	0.5	1.0742	4.9285
50	1	0	0	0	0	1.0414	9.6192
51	1	0	0	0	0	1.0479	10.4083
52	1	0	0	0.5	1.5	1.0407	9.6060
53	1	0	0	0	0	1.0583	11.7352
54	1	0	0	0	0	1.0431	16.7836
55	1	0	0	0	0	1.0464	18.1181
56	1	0	0	0	0	1.0467	18.8019
57	1	0	0	0	5	0.9111	-4.5865
58	1	0	0	0	15	0.7090	4.4256
59	1	0	0	0	0	0.9988	-1.1984
60	1	0	0	0	0	0.9988	-1.1984
61	1	0	0	0	0	0.9840	-2.7565
62	1	0	0	0	0	0.9840	-2.7565
63	1	0	0	0	0	0.9819	-2.9250
64	1	0	0	75	10.7	1.0201	-7.0858
65	1	0	0	0	0	0.9844	-2.7496
66	1	0	0	15	6.2	1.0180	-3.5904
67	1	0	0	0	0	0.9866	-2.6206
68	1	0	0	0	0	1.0283	-1.4453
69	3	23.8795	11.3296	0	0	1.0500	0.0000

## APPENDIX B

### DATA FILE *ntwk.inp*

```
!
!
! -----
!           SaskPower
!       Athabasca - Points North system
!       ( May 26, 1993 )
! -----
!       Data file for short circuit calculations
! -----
! ⇒ No of buses , no of faults and no of events:
!       nbus , nfault , nevent/
! -----
!       69 , 1 , 4/
! -----
! ⇒ Fault information input: ( time in seconds )
!       The sequence events of a disturbance are distributed on TIME-axis
!       as follows:
!       | pre-fault | fault period | post-fault | autoreclose |
! -----
! | | | db/s | start | end | | |
! | i | j | cir. | time | time | Zgnd | Zfault |
! -----
! -16, 18, 0, 0.00, 0.10, (0,0), (0,0) /
! -16, 18, 1, 0.20, 0.20, (0,0), (0,0) /
! -16, 18, 1, 0.20, 0.20, (0,0), (0,0) /
! -16, 18, 1, 20.20, 20.00, (0,0), (0,0) /
! -----
! ⇒ Fault type indicator input:
!       A fault is chosen by deleting the [ ! !!! ] at the beginning of a line.
!       If no fault, no [ ! !!! ] should be deleted.
! -----
! 3-phase-to-ground
! !!! 1-phase-to-ground
! !!! 2-phases-to-ground
! !!! phase-to-phase
! !!! 1-phase-open
! !!! 2-phases-open
! -----
! ⇒ Positive(+), negative(-) sequence network data:
!       See note in pqlf.inp data file.
!
```

i,	j,	r(+),	r(-),	x(+),	x(-),	ratio/b/1.0/-1.0	
1,	0,	0.0000,	0.0000,	2.6061,	2.6061,	1.0	/
2,	0,	0.0000,	0.0000,	2.6061,	2.6061,	1.0	/
3,	0,	0.0000,	0.0000,	2.6061,	2.6061,	1.0	/
4,	0,	0.0000,	0.0000,	1.4,	1.4,	1.0	/
5,	0,	0.0000,	0.0000,	1.4,	1.4,	1.0	/
6,	0,	0.0000,	0.0000,	1.4,	1.4,	1.0	/
7,	0,	0.0000,	0.0000,	1.6,	1.6,	1.0	/
8,	0,	0.0000,	0.0000,	2.2807,	2.2807,	1.0	/
9,	0,	0.0000,	0.0000,	2.2807,	2.2807,	1.0	/
10,	0,	0.0000,	0.0000,	1.3929,	1.3929,	1.0	/
11,	0,	0.0000,	0.0000,	9.0667,	9.0667,	1.0	/
12,	0,	0.0000,	0.0000,	9.0667,	9.0667,	1.0	/
69,	0,	0.0000,	0.0000,	0.0200,	0.0200,	1.0	/
! copy (+), (-) sequence network parameters from <i>pqlf.inp</i>							
! and paste them here.							
⇒ Zero(0) sequence network data:							
! 1) The non-grounded lines are:							
!     Yo/Yo connected three-winding transformer branches;							
!     Yo/Yo connected two-winding transformer branches;							
!     Transmission lines.							
! 2) The grounded lines are:							
!     generator grounding during a fault. They							
!     do not contribute to zero sequence currents in this							
!     system because of the generator-transformers are in							
!     Delta/Delta connection.							
! 3) Other kinds of grounded lines are:							
!     Yo/Delta two-winding transformers;							
!     tertiary windings of Yo/Yo/Delta							
!     connected three - winding transformers.							
i,	j,	r(0) ,	x(0),	b/1.0/-1.0			
14,	0,	0.0000,	0.1936,	1.0000/			
14,	0,	0.0000,	0.1252,	1.0000/			
14,	59,	0.2972,	1.1323,	0.0171/			
14,	60,	0.2972,	1.1323,	0.0171/			
59,	61,	0.0711,	0.3042,	0.0044/			
60,	62,	0.0711,	0.3042,	0.0044/			
61,	63,	0.0078,	0.0388,	0.0005/			
62,	63,	0.0078,	0.0388,	0.0005/			
63,	0,	0.0000,	0.1020,	1.0000/			
61,	65,	0.0370,	0.0169,	0.0000/			
62,	65,	0.0370,	0.0169,	0.0000/			

65,	67,	0.0073,	0.0339,	0.0000/
65,	0,	0.0000,	0.1700,	1.0000/
67,	0,	0.0000,	0.0200,	1.0000/
14,	15,	.00000,	-.05830,	.00000/
15,	16,	.00000,	.15830,	.00000/
14,	17,	.00000,	-.05830,	.00000/
17,	16,	.00000,	.15830,	.00000/
16,	18,	.18870,	.90970,	.03168/
18,	21,	.08950,	.42960,	.01488/
18,	19,	.03710,	.14670,	.00489/
22,	23,	1.28160,	2.92990,	.00050/
23,	29,	2.58680,	6.20570,	.00140/
29,	24,	1.08360,	1.79050,	.00040/
21,	26,	.34650,	1.69230,	.06000/
26,	27,	.03870,	.15320,	.00511/
26,	30,	.23550,	1.13890,	.03982/
30,	31,	.02030,	.08040,	.00268/
30,	33,	.08280,	.39740,	.01376/
33,	35,	.00000,	-.27670,	.00000/
35,	37,	.00000,	.54330,	.00000/
33,	36,	.00000,	-.27670,	.00000/
36,	37,	.00000,	.54330,	.00000/
37,	38,	.09540,	.38480,	.00670/
38,	39,	.00000,	.34800,	.00000/
39,	41,	.00000,	.22200,	.00000/
43,	41,	.00000,	.90500,	.00000/
41,	44,	.64960,	.96340,	.00050/
37,	46,	.62590,	2.52440,	.04390/
46,	48,	.34160,	1.34850,	.02280/
48,	50,	.31820,	1.25520,	.02120/
50,	51,	.06870,	.14730,	.00050/
51,	53,	.14730,	.31550,	.00780/
54,	55,	.07280,	.31570,	.00040/
55,	56,	.09800,	.34270,	.00060/
53,	0,	.00000,	.44440,	1.00000/
36,	0,	.00000,	2.45670,	1.00000/
35,	0,	.00000,	2.45670,	1.00000/
41,	0,	.00000,	.74200,	1.00000/
44,	0,	0.0,	0.8290,	1.0 /
46,	0,	.00000,	.95000,	1.00000/
46,	0,	.00000,	.95000,	1.00000/
39,	0,	.00000,	-.01850,	1.00000/
15,	0,	.00000,	1.67500,	1.00000/
17,	0,	.00000,	1.67500,	1.00000/
0/				

!-----

!  $\Rightarrow$ Input the bus numbers which are either in( 1 ) or not in( -1 )  
! the zero sequence network under the fault of concern.

!  
!

! The bus set which is in zero sequence network is chosen here.  
! Hence a '1' is input as the first record of data in this  
! data block. Transmission lines will be automatically  
! connected to these buses, including line charges. If the fault  
! location changes, it may be necessary to modify this list.

!

! This bus list is required for both 'during fault' period and  
! 'fault cleared' period.

!

1 / / during fault  
14, 15, 16, 17, 18, 21, 26, 27,  
30, 33, 35, 36, 37, 38, 39,  
41, 43, 44, 46, 48,  
50, 51, 53, 59, 60, 61, 62, 63, 65, 67 /

1 / / fault cleared  
14, 15, 16, 17, 18, 21, 26, 27,  
30, 33, 35, 36, 37, 38, 39,  
41, 43, 44, 46, 48,  
50, 51, 53, 59, 60, 61, 62, 63, 65, 67 /

!

! End of data file

!

!

## APPENDIX C

### DATA FILE *mach.inp*

```

!
! -----
!           SaskPower
!       Athabasca - Points North system
!       ( March , 1993 )
! -----
!       Data file for stability study
! -----
! => No of machines, time step, print interval
! -----
!           13      ,   0.002  ,   0.02  /
! -----
! => Machine #, model # and corresponding parameters
!       (for detail, please refer to the user's manual)
!       Data input examples:
! 1, 4/                               / generator #, Model #:
! 13.2 , 2.24 , 0.0 , 0.326           / Mbase, H, R, XI
! 1.05, 0.3818, 0.344, 0.741, 0.344 / Xd,Xdo',Xdo'',Xq,Xqo"
! 2.62, 0.0500, 0.060                 / Tdo', Tdo'' , Tqo"
! 0.00, 0.2470, 0.5612, -1            / damp,s(1.0),s(1.2),-1
!
! 11, 2/                               / generator #, Model #:
! 3.0, 2.7 , 0.0 , 0.0                / Mbase, H , R, XI
! 0.876, 0.272 , 0.5                  / Xd , Xdo', Xq
! 2.27                                / Tdo'
! 0.00, 0.179 , 0.43 , -1             / damp,s(1.0),s(1.2),-1
! 13, 0 /                             / infinite bus
! 100                                 / capacity of system
! -----
1, 4/
13.2 ,      2.24 ,      0.0 ,      0.326      /
1.05,      0.3818,      0.344,      0.741,      0.344 /
2.62,      0.0500,      0.06      /
0.00,      0.2470,      0.5612,      -1      /
2, 4/
13.2 ,      2.24 ,      0.0 ,      0.326      /
1.05,      0.3818,      0.344,      0.741,      0.344 /
2.62,      0.0500,      0.06      /
0.00,      0.2470,      0.5612,      -1      /
3, 4/
13.2 ,      2.24 ,      0.0 ,      0.326      /
1.05,      0.3818,      0.344,      0.741,      0.344 /

```

	2.62,	0.0500,	0.06		/
	0.00,	0.2470,	0.5612,	-1	/
4, 4/					
	18.0 ,	2.31 ,	0.0 ,	0.239	/
	.6003,	.2801,	.252 ,	0.4243,	0.252 /
	2.82,	0.0500,	0.06		/
	0.00,	0.1733,	0.5556,	-1	/
5, 4/					
	18.0 ,	2.31 ,	0.0 ,	0.239	/
	.6003,	.2801,	.252 ,	0.4243,	0.252 /
	2.82,	0.0500,	0.06		/
	0.00,	0.1733,	0.5556,	-1	/
6, 4/					
	18.0 ,	2.31 ,	0.0 ,	0.239	/
	.6003,	.2801,	.252 ,	0.4243,	0.252 /
	2.82,	0.0500,	0.06		/
	0.00,	0.1733,	0.5556,	-1	/
7, 4/					
	18.0 ,	2.19 ,	0.0 ,	0.272	/
	1.1,	0.5403,	0.286 ,	0.6003,	0.286 /
	2.82,	0.0500,	0.06		/
	0.00,	0.1951,	0.5854,	-1	/
8, 4/					
	5.70,	3.78 ,	0.0 ,	0.12	/
	0.57,	.1900,	.1300,	0.39,	0.13 /
	2.2 ,	0.0300,	0.03		/
	0.00,	0.0800,	0.3000,	-1	/
9, 4/					
	5.70,	3.78 ,	0.0 ,	0.12	/
	0.57,	.1900,	.1300,	0.39,	0.13 /
	2.2 ,	0.0300,	0.03		/
	0.00,	0.0800,	0.3000,	-1	/
10, 4/					
	11.2,	2.6 ,	0.0 ,	0.0939	/
	0.624,	0.218 ,	.156 ,	0.47,	0.156 /
	4.07,	0.0380,	0.038		/
	0.00,	0.1712,	0.546 ,	-1	/
11, 2/					
	3.0,	2.7 ,	0.0 ,	0	/
	0.876,	0.272 ,	0.5		/
	2.27				/
	0.00,	0.179 ,	0.43 ,	-1	/
12, 2/					
	3.0 ,	2.9 ,	0.0 ,	0	/
	0.91, 0	.272 ,	0.51		/
	2.89				/

```

0.0, 0    .200 ,    0.524 ,    -1    /
13, 0/
100.0    /

```

---

!⇒ Exciter model # and its parameters

! (for detail, please refer to the user's manual)

! Data input examples:

```

! 1 , 41/                                / exciter #, model #
! 56.0 , 1 , 1                            / Ke, neg. logic, busfed
! 0.0 , 1.0 , 1.0, 0.035                  / T1, Ta , Tb, Te
! -3.94, 3.94                             / Emin , Emax

```

```

! 10 , 14/                               / exciter #, model #
! 369.0, 1.000, 0.022                     / Ka, Ke, Kf
! 1.000, 0.226, 0.000 , 2.000, 1.0        / Tc, Tb, Ta, Te, Tf1
! -3.97, 4.960                             / Vrmin, Vrmax
! 1.830, 0.108, 2.3570, 0.506 , -1        / E1, S1, E2, S2, -1

```

```

! 13, 888 /                               / NO AVR

```

---

```

1 , 41/
56.0 ,    1 ,    1    /
0.0 ,    1.0 ,    1.0,    0.035    /
-3.94,    3.94    /
2 , 41/
61.0 ,    1 ,    1    /
0.0 ,    1.0 ,    1.0,    0.035    /
-3.94,    3.94    /
3 , 41/
61.0 ,    1 ,    1    /
0.0 ,    1.0 ,    1.0,    0.035    /
-3.94,    3.94    /
4 , 41/
45.0 ,    1 ,    1    /
0.0 ,    1.0 ,    1.0,    0.035    /
-3.94,    3.94    /
5 , 41/
54.0 ,    1 ,    1    /
0.0 ,    1.0 ,    1.0,    0.035    /
-3.94,    3.94    /
6 , 41/
55.0 ,    1 ,    1    /
0.0 ,    1.0 ,    1.0,    0.035    /
-3.94,    3.94    /
7 , 41/
57.0 ,    1 ,    1    /
0.0 ,    1.0 ,    1.0,    0.035    /

```

	-3.94,	3.94			/
8 , 42 /					
	167.0 ,	1 ,	1		/
	0.0 ,	1.0 ,	1.0,	0.02	/
	0.0 ,	10.3	2.5		/
9 , 42 /					
	167.0 ,	1 ,	1		/
	0.0 ,	1.0 ,	1.0,	0.02	/
	0.0 ,	10.3	2.5		/
10 , 14 /					
	369.0,	1.000,	0.022		/
	1.000,	0.226,	0.000 ,	2.000, 1.000	/
	-3.97,	4.96			/
	1.830,	0.108,	2.3570,	0.506 , -1	/
11 , 14 /					
	433.0,	1.000,	0.023		/
	1.000,	0.226,	0.000 ,	2.000, 1.000	/
	-4.68,	5.85			/
	2.15 ,	0.680,	2.750 ,	1.130, -1	/
12 , 14 /					
	417.0,	1.000,	0.023		/
	1.000,	0.226,	0.000 ,	1.840, 1.000	/
	-4.44,	5.55			/
	2.290,	0.520,	3.000 ,	0.85 , -1	/
13 , 888 /					

---

! => Turbine governor model # and its parameters  
 ! (for detail, please refer to the user's manual)  
 ! Data input example:  
 ! 1 , 222 / /generator #, governor model #  
 ! 0.620, 0.320, 3.290, 33.150 /Tw, T1, T2, T3  
 ! 20.0 / K  
 ! 0.00 , 1.05 / Gmin, Gmax  
 !  
 ! 8 , 221 / /generator #, governor model #  
 ! 1.05, 0.05, 0.24, 4.2 /Tw, Tp, Tg, Tr  
 ! 0.03, 0.55 /perm-R, temp-r  
 ! -0.16, 0.16, 0.00, 1.0 /G min, G max, Gmin, Gmax  
 !  
 ! 13 , 888/ / No governor here

---

1 , 222 /					
	0.620,	0.320,	3.290,	33.15	/
	20				/
	0.00 ,	1.05			/
2 , 222 /					
	0.620,	0.320,	3.290,	33.15	/
	20				/

	0.00 ,	1.05		/
3 , 222 /	0.620,	0.320,	3.290,	33.15
	20			/
	0.00 ,	1.05		/
4 , 222 /	0.660,	51.20,	4.80,	0.5
	20			/
	0.00 ,	1.05		/
5 , 222 /	0.660,	51.20,	4.80,	0.5
	20			/
	0.00 ,	1.05		/
6 , 222 /	0.660,	51.20,	4.80,	0.5
	20			/
	0.00 ,	1.05		/
7 , 222 /	0.660,	51.20,	4.80,	0.5
	20			/
	0.00 ,	1.05		/
8 , 221 /	1.05,	0.05,	0.24,	4.2
	0.03,	0.55		/
	-0.16,	0.16,	0.00,	1
9 , 221 /	1.05,	0.05,	0.24,	4.2
	0.03,	0.55		/
	-0.16,	0.16,	0.00,	1
10 , 221 /	0.87,	0.05,	0.12,	7
	0.03,	0.48		/
	-0.333,	.333,	0.00,	1
11 , 221 /	1.5,	0.05,	0.4 ,	5.5
	0.03,	0.55		/
	-0.10,	0.10,	0.00,	1
12 , 221 /	1.5,	0.05,	0.4 ,	5.5
	0.03,	0.55		/
	-0.10,	0.10,	0.00,	1
13 , 888/				

---

! ⇒ Power system stabilizer model # and its parameters  
 ! (for detail, please refer to the user's manual)  
 ! Data input example:  
 ! 1, 311 /                      / Gen #, PSS model #

```

! 3 / /input 3: elec. power
! 0.014 /Ta1
! 0.000, 0.025, 4.4, 4.4, 5.0, 5.0 / T1,T2 ,T3, T4, T5,T6
! -0.05, -0.100, 0.100 / Ks ,Vsmin , Vsmax
!

```

---

```

1,311 /
3 /
0.014 /
0.000, 0.025, 4.4, 4.4, 5.0, 5.0 /
-0.05, -0.100, 0.1 /
2,311 /
3 /
0.014 /
0.000, 0.025, 4.4, 4.4, 5.0, 5.0 /
-0.05, -0.100, 0.1 /
3,311 /
3 /
0.014 /
0.000, 0.025, 4.4, 4.4, 5.0, 5.0 /
-0.05, -0.100, 0.1 /
4,311 /
3 /
0.014 /
0.000, 0.025, 4.4, 4.4, 5.0, 5.0 /
-0.05, -0.100, 0.1 /
5,311 /
3 /
0.014 /
0.000, 0.025, 4.4, 4.4, 5.0, 5.0 /
-0.05, -0.100, 0.1 /
6,311 /
3 /
0.014 /
0.000, 0.025, 4.4, 4.4, 5.0, 5.0 /
-0.05, -0.100, 0.1 /
7,888 /
8,312 /
4 /
0.000 /
0.400, 1.0, 0.08, 0.5, 2.0, 2.0 /
10.00, -0.200, 0.2 /
9,312 /
4 /
0.000 /
0.400, 1.0, 0.08, 0.5, 2.0, 2.0 /
10.00, -0.200, 0.2 /

```

10, 888/

11, 888/

12, 888/

13, 888/

!

!

!

End of data file

## APPENDIX D

### A FIFTH ORDER MACHINE MODEL

#### D.1 Generator model

Assuming that positive stator currents  $i_d$  and  $i_q$  are generated currents, positive rotor currents  $i_f$ ,  $i_D$ , and  $i_Q$  flow into the machine, where  $d$ ,  $q$ ,  $f$ ,  $D$  and  $Q$  denote the direct-axis winding, quadrature-axis winding, the field winding, the direct-axis and quadrature-axis damper windings, respectively. The voltage equations of the various windings are listed below when the transformer voltages are ignored:

$$v_d = -\dot{\phi}_q - r_a i_d \quad (D.1)$$

$$v_q = \dot{\phi}_d - r_a i_q \quad (D.2)$$

$$\dot{\phi}_f = v_f - r_f i_f \quad (D.3)$$

$$\dot{\phi}_D = -r_D i_D \quad (D.4)$$

$$\dot{\phi}_Q = -r_Q i_Q \quad (D.5)$$

where

$v$  = voltage

$r$  = resistance

$a$  = subscript denoting armature

$\phi$  = flux linkage of a winding

The flux linkage is determined by the following equation, accordingly:

$$\phi_d = -x_d i_d + x_{ad} i_f + x_{ad} i_D \quad (D.6)$$

$$\phi_f = -x_{ad} i_d + x_f i_f + x_{fD} i_D \quad (D.7)$$

$$\phi_D = -x_{ad} i_d + x_{fD} i_f + x_D i_D \quad (D.8)$$

$$\phi_q = -x_q i_q + x_{aq} i_Q \quad (D.9)$$

$$\phi_Q = -x_{aq} i_q + x_Q i_Q \quad (D.10)$$

where  $x_d, x_q, x_{fD}, x_D$  and  $x_Q$  are complete reactances,  $x_{ad}$  and  $x_{aq}$  are mutual reactances, and usually it is assumed that  $x_{fD} = x_{ad}$ .

Solving (D.6) - (D.8) for  $\phi_d$  expressed in terms of  $\phi_f, \phi_D$  and  $i_d$ , we have

$$\begin{aligned} \phi_d = & \frac{x_{ad}}{x_D x_f - x_{ad}^2} \{ (x_D - x_{ad}) \phi_f + (x_f - x_{ad}) \phi_D \} \\ & - \left\{ x_d - \frac{x_{ad}^2 (x_D + x_f - 2x_{ad})}{x_D x_f - x_{ad}^2} \right\} i_d \end{aligned} \quad (D.11)$$

Defining the q-axis subtransient voltage as

$$E_q'' = \frac{x_{ad}}{x_D x_f - x_{ad}^2} \{ (x_D - x_{ad}) \phi_f + (x_f - x_{ad}) \phi_D \} \quad (D.12)$$

and subtransient reactance as

$$x_d'' = \left\{ x_d - \frac{x_{ad}^2 (x_D + x_f - 2x_{ad})}{x_D x_f - x_{ad}^2} \right\} \quad (D.13)$$

Then the voltage equation on (A.2) can be rewritten as

$$v_q = E_q'' - x_d'' i_d - r_a i_q \quad (D.14)$$

Similarly, defining the d-axis subtransient voltage and reactance as, respectively:

$$E_d'' = -\frac{x_{aq}}{x_Q} \phi_Q \quad (D.15)$$

$$x_q'' = x_q - \frac{x_{aq}^2}{x_Q} \quad (D.16)$$

Then the voltage equation (D.1) on d-axis can be rewritten as

$$v_d = E_d'' + x_q'' i_q - r_a i_d \quad (D.17)$$

The differential equations related to the rotor windings are given below [4,10]:

$$\dot{E}_q = \frac{1}{\tau_{do}} \{ kE_{fd} - E_q - (x_d - x'_d) i_d \} \quad (D.18)$$

$$\dot{E}_{sum} = \frac{1}{\tau_{do}} \{ -E_{sum} - (x'_d - x''_d) i_d \} \quad (D.19)$$

$$\dot{E}_d = \frac{1}{\tau_{qo}} \{ -E_d + (x_q - x''_q) i_q \} \quad (D.20)$$

where  $E_{sum} = E''_q - E'_q$ . A block diagram for this model is shown in Figure 3.1.

The differential equation describing machine motion is given by

$$\dot{\omega} = \{ T_m - T_e - D(\omega - 1) \} / 2H \quad (D.21)$$

$$\dot{\delta} = \omega_o(\omega - 1) \quad (D.22)$$

where  $H$  is the machine inertia in second and  $\omega_o$  is the synchronous speed of the machine in radian per second.

## D.2 Saturated Reactances

It is assumed that leakage flux does not contribute in any way to the saturation of the machine, and that the leakage flux itself does not saturate either. Thus the reactances on the two axes can be given by

$$x_d = x_l + x_{ad} \quad (D.23)$$

$$x_q = x_l + x_{aq} \quad (D.24)$$

The saturated values of the reactances in the above two equations are given by

$$x_d^{(0)} = x_l + x_{ad}^{(0)} \quad (D.25)$$

$$x_q^{(0)} = x_l + x_{aq}^{(0)} \quad (D.26)$$

and

$$x_{ad} = kx_{ad}^{(0)} \quad (D.27)$$

$$x_{aq} = kx_{aq}^{(0)} \quad (D.28)$$

$$x_d = x_l + kx_{ad}^{(0)} = kx_d^{(0)} + (1 - k)x_l \quad (D.29)$$

$$\mathbf{x}_q = \mathbf{x}_\ell + k\mathbf{x}_{aq}^{(0)} = k\mathbf{x}_q^{(0)} + (1-k)\mathbf{x}_\ell \quad (\text{D.30})$$

$$\mathbf{x}_{ad} = \mathbf{x}_d - \mathbf{x}_\ell = k(\mathbf{x}_d^{(0)} - \mathbf{x}_\ell) \quad (\text{D.31})$$

### D.3 Time Constants

The single line diagrams of the excitation winding and the two damping windings on the rotor are used to derive the time constants. Figure D.1 represents the open circuit of the excitation winding, from which the transient time constant of it is given by

$$\tau'_{do} = \tau_f = \frac{(\mathbf{x}_{fl} + \mathbf{x}_{ad})}{r_f} \quad (\text{D.33})$$

Then the saturated time constant can be found from

$$\begin{aligned} \frac{\tau'_{do}}{\tau_{do}^{(0)}} &= \frac{\frac{(\mathbf{x}_{fl} + \mathbf{x}_{ad})}{r_f}}{\frac{(\mathbf{x}_{fl} + \mathbf{x}_{ad}^{(0)})}{r_f}} \\ &= \frac{\mathbf{x}_{fl} + k(\mathbf{x}_d^{(0)} - \mathbf{x}_\ell)}{\mathbf{x}_{fl} + (\mathbf{x}_d^{(0)} - \mathbf{x}_\ell)} \\ &= k + (1-k) \frac{(\mathbf{x}_d' - \mathbf{x}_\ell)}{(\mathbf{x}_d^{(0)} - \mathbf{x}_\ell)} \end{aligned} \quad (\text{D.34})$$

where (D.25) and (D.35)-(D.36) are used:

$$\mathbf{x}_{ff} = \mathbf{x}_{fl} + \mathbf{x}_{ad} \quad (\text{D.35})$$

$$\mathbf{x}_d' = \mathbf{x}_d - \frac{\mathbf{x}_{ad}^2}{\mathbf{x}_{ff}} \quad (\text{D.36})$$

It is assumed that  $x_{fl}$ , the leakage flux of the excitation winding, does not saturate either.

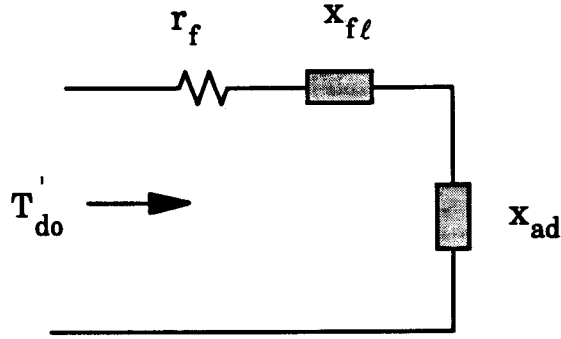


**Figure D.1:** Diagram for calculation of  $T'_{do}$

Figure D.2 represents the open circuit of the damper winding on d-axis, from which its subtransient time constant is calculated by

$$\tau''_{do} = \frac{(x_{D\ell} + x_{ad} || x_{\ell})}{r_D} \quad (D.37)$$

Then its saturated can be calculated by

$$\begin{aligned} \frac{\tau''_{do}}{\tau''_{do}(0)} &= \frac{x_{D\ell} + (x_{ad} || x_{\ell})}{x_{D\ell} + (x_{ad}^{(0)} || x_{\ell})} \\ &= k + (1 - k) \frac{(x_d'' - x_{\ell})}{(x_d^{(0)} - x_{\ell})} \end{aligned} \quad (D.38)$$

where  $||$  denotes parallel connection of reactances. The following (D.39) is used in derivation of (D.38):

$$\begin{aligned} x_d'' &= x_{\ell} + \frac{x_{D\ell} x_{\ell} x_{ad}^{(0)}}{x_{D\ell} (x_{ad}^{(0)} + x_{\ell}) + x_{ad} x_{\ell}} \\ &= x_{\ell} + x_{D\ell} || x_{\ell} || x_{ad}^{(0)} \end{aligned} \quad (D.39)$$

which is the equivalent reactance of Figure D.2 when the damper winding is short circuited and  $r_D$  is set to be zero.

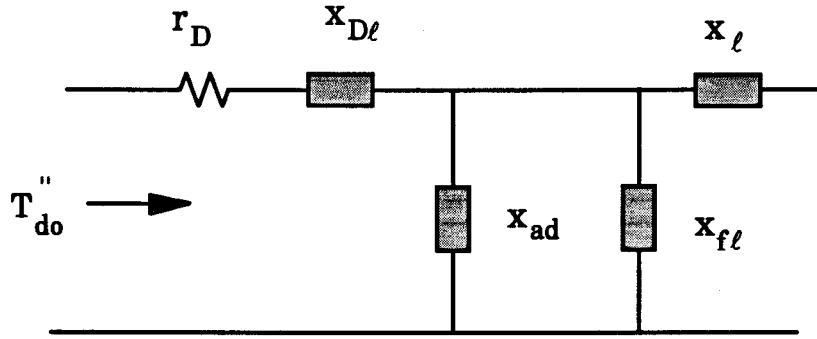


**Figure D.2:** Diagram for calculation of  $T''_{do}$

Figure D.3 represents the open circuit of the damper winding on q-axis, from which its subtransient time constant is calculated by

$$\tau''_{qo} = \frac{(x_{q\ell} + x_{aq})}{r_q} \quad (\text{D.40})$$

$$\frac{\tau''_{qo}}{\tau''_{qo(0)}} = k + (1 - k) \frac{(x''_q - x_{\ell})}{(x^{(0)}_q - x_{\ell})} \quad (\text{D.41})$$

The following (D.42) is used in derivation of (D.41):

$$x''_q = x_{\ell} + x_{q\ell} \parallel x^{(0)}_{aq} \quad (\text{D.42})$$

which is the equivalent reactance of Figure D.3 when the damper winding is short circuited and  $r_q$  is set to be zero.

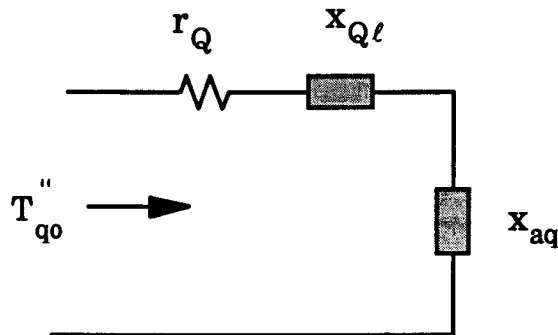


**Figure D.3:** Diagram for calculation of  $T''_{qo}$

## APPENDIX E

### SATURATION REPRESENTATION

#### E.1 Generation Saturation

A per unit saturation function  $S_G$  for a generator is defined in term of the open circuit terminal voltage versus field current characteristic as in Figure E.1.

$$S_G = A_G e^{B_G(V_t - 0.8)} \quad (\text{E.1})$$

where

$$A_G = S_{G1.0}^2 / 1.2 S_{G1.2} \quad (\text{E.2})$$

$$B_G = 5 \ln(1.2 S_{G1.2} / S_{G1.0}) \quad (\text{E.3})$$

0.8 = assumed saturation threshold

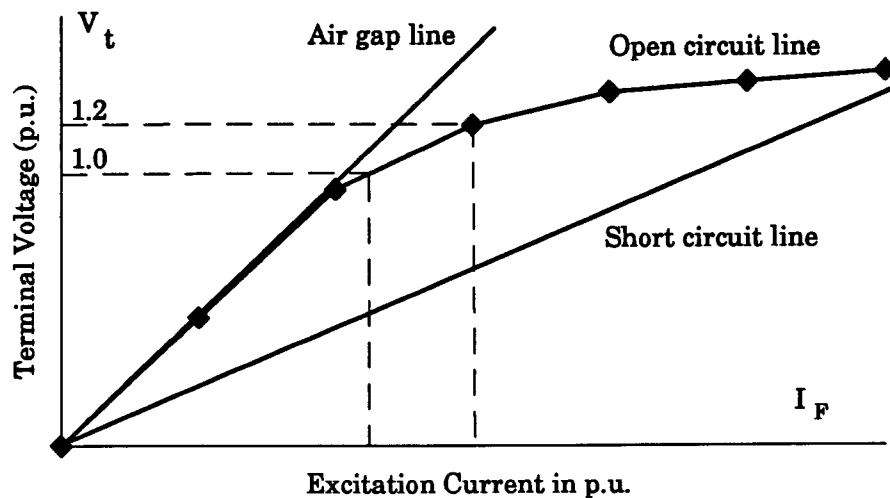


**Figure E.1:** Open circuit characteristic of synchronous generator

## E.2 Excitation Saturation

Assume that the saturation of an exciter can be approximately represented by an exponential function by fitting two points of the open circuit curve as shown in Figure E.2.

$$S_E = A_E e^{B_E E_{fd}} \quad (\text{E.4})$$

If two testing points  $(S_{E1}, E_{fd1})$  and  $(S_{E2}, E_{fd2})$  are known, the two fitting constants can be determined by

$$B_E = \ln\left(\frac{S_{E1}}{S_{E2}}\right) / (E_{fd1} - E_{fd2}) \quad (\text{E.5})$$

$$A_E = S_{E1} / e^{B_E E_{fd1}} \quad (\text{E.6})$$

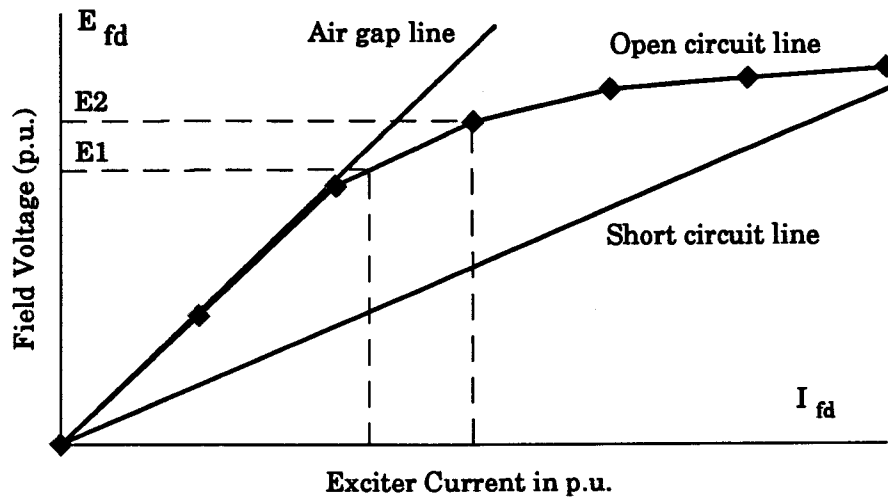


Figure E.2: Open circuit characteristic of exciter